Dissertation

Analysis of the role of RAF kinase inhibitor protein in the development of myeloid neoplasias

submitted by

Veronica CARAFFINI

for the Academic Degree of

Doctor of Philosophy

(PhD)

at the

Medical University of Graz

Department of Internal Medicine

under the Supervision of

Assoc.-Prof. Dr. Armin ZEBISCH

2019

Statutory Declaration

I hereby declare that this thesis is my own original work and that I have fully acknowledged by name all of those individuals and organisations that have contributed to the research for this thesis. Due acknowledgement has been made in the text to all other material used. Throughout this thesis and in all related publications I followed the “Standards of Good Scientific Practice and Ombuds Committee at the Medical University of Graz“.

Veronica Caraffini

Graz, July 2019

Disclosures

This thesis has been published in the following original papers:

- *Veronica Caraffini,[1] Olivia Geiger,[1] Angelika Rosenberger,[1] Stefan Hatzl,[1] Bianca Perfler,[1] Johannes L. Berg,[1] Clarice Lim,[2] Herbert Strobl,[2] Karl Kashofer,[3] Silvia Schauer,[3] Christine Beham-Schmid,[3] Gerald Hoefler,[3] Klaus Geissler,[4,5] Franz Quehenberger,[6] Walter Kolch,[7] Dimitris Athineos,[8] Karen Blyth,[8] Albert Wölfler,[1] Heinz Sill[1] and Armin Zebisch[1].*

  Loss of RAF kinase inhibitor protein is involved in myelomonocytic differentiation and aggravates *RAS*-driven myeloid leukemogenesis. Haematologica 2019; in press: doi: 10.3324/haematol.2018.209650

  [1]Division of Hematology, [2]Otto Loewi Research Center, Immunology and Pathophysiology, [3]Diagnostic and Research Institute of Pathology, Medical University of Graz, Graz, Austria; [4]5th Medical Department with Hematology, Oncology and Palliative Medicine, Hospital Hietzing, Vienna, Austria; [5]Sigmund Freud University, Vienna, Austria; [6]Institute of Medical Informatics, Statistics and Documentation, Medical University of Graz, Graz, Austria; [7]Systems Biology Ireland & Conway Institute, University College Dublin, Dublin, Ireland; [8]Cancer Research UK Beatson Institute, Glasgow, United Kingdom

- *Veronica Caraffini[1], Bianca Perfler[1], Johannes Lorenz Berg[1], Barbara Uhl[1], Silvia Schauer[2], Karl Kashofer[2], Nassim Ghaffari-Tabrizi-Wizsy[3], Herbert Strobl[3], Albert Wölfler[1], Gerald Hoefler[2], Heinz Sill[1], and Armin Zebisch[1].*

  Loss of RKIP is a frequent event in myeloid sarcoma and promotes leukemic tissue infiltration. Blood 2018;131(7):826–830

  [1]Division of Hematology, [2]Institute of Pathology, and [3]Institute of Pathophysiology and Immunology, Medical University of Graz, Graz, Austria

All co-authors declare that they have no conflicts of interest with the content of this thesis and have explicitly agreed to use their data in the thesis.

Doctoral candidate Veronica Caraffini received funding from the Austrian Science Fund (grant P26619-B19 to A. Zebisch) and was trained within the frame of the PhD Program Molecular Medicine of the Medical University of Graz.

“Nothing in life is to be feared,
it is only to be understood”

Marie Skłodowska-Curie

Acknowledgements

If I am writing the acknowledgments, it means that I am really at the end of this journey and I want to thank all the people that made it possible and amazing.

First, a huge thank you goes to my supervisor, Prof. Armin Zebisch. Thank you for choosing me for this PhD project, as you can see, I finished it! It would not have been possible without your guidance and help. Thank you for being an excellent guide, always present, and for helping me growing during this PhD experience. Above all, thank you for showing me not only how a scientist should work, but also what an excellent supervisor and mentor is.

I want to thank also the members of my thesis committee, Prof. Heinz Sill, Prof. Albert Wölfler and Prof. Gerald Hoefler. Thank you for the valuable comments during my presentations and your help through the project. Thank you also to all the collaborators that made this thesis and the two publications from it possible.

Thank you to the Medical University of Graz, in particular to the PhD program Molecular Medicine and to all the people that organize it and helped me whenever I had any question regarding the program.

Thanks to all the colleagues from the lab, to the ones that were there since the beginning and to the ones that joined later. Thank you for always being supportive and helpful. I could not have asked for better lab mates. I will miss spending time with you in the lab and especially our Escape Rooms! Thank you also to all the people at the division of Hematology, who always helped me when I needed it.

So important for my journey, thanks to all my friends. You are not only good friends, you became my family in Graz. Thanks for the support, we all went through some hard times… Thanks for the laughs, the trips, the parties, the happy memories… I will take them with me, wherever I will go. Thanks to Ila, I am so happy that I found not only the perfect flatmate but also such a good friend to share this journey with. Thanks to Ani, not only for the solid friendship but also for sharing the office since the first day, together with the good and the bad days, you were always there. Thanks Vitocic, Pias, Natasa, Mahmoud, Tommaso.

And thanks to my parents, for whom a switch to Italian is required. Grazie Mami e Papi per il vostro supporto a distanza. So che vorreste avermi più vicina a fare un

lavoro più redditizio… ma grazie per avermi sostenuto comunque nelle mie scelte. Le nostre chiamate via Skype sono sempre un bel momento e, ora che sono lontana, tornare a casa da voi è sempre un'emozione. Vi voglio bene.

Thanks also to all the other people with whom I shared moments outside the lab, especially the people I worked together with to organize the Doctoral Day and the Growing up in Science Graz events.

Table of contents

Abbreviations and Definitions

1,25D_3	1,25-Dihydroxyvitamin D_3
7-AAD	7-aminoactinomycin
AKT	alpha serine/threonine-protein kinase
AML	acute myeloid leukemia
BM	bone marrow
BSC	best supportive care
CAM	chorioallantoic membrane
cDNA	complementary DNA
CHIP	clonal hematopoiesis of indeterminate potential
CMML	chronic myelomonocytic leukemia
CR	complete remission
DMSO	dimethylsulfoxid
DNA	deoxyribonucleic acid
ELN	European Leukemia Net
ERK	extracellular signal-regulated kinase
FAB	French-American-British
FBS	fetal bovine serum
FFPE	formalin-fixed-paraffin-embedded
FL	Fms-related tyrosine kinase 3 ligand
GAP	GTPase-activating proteins
GDP	guanosine diphosphate
GEF	guanine nucleotide exchange factor
GEO	Gene Expression Omnibus
GFP	green fluorescent protein
GM-CSF	granulocyte-macrophage colony-stimulating factor
GTP	guanosine triphosphate

H&E	hematoxylin and eosin
HBSS	Hank's balanced salt solution
HRAS	Harvey rat sarcoma virus oncogene
HS	histiocytic sarcoma
HSCT	hematopoietic stem cell transplantation
HSPCs	hematopoietic stem and progenitor cells
KD	knockdown
KRAS	Kirsten rat sarcoma viral oncogene homolog
MAPK	mitogen-activated protein kinase
MDS	myelodysplastic syndrome
MEK	mitogen-activated protein kinase kinase
miRNA	microRNA
MN	myeloid neoplasia
MP	myeloproliferation
MPD	myeloproliferative disease
MPN	myeloproliferative neoplasia
MS	myeloid sarcoma
NCBI	National Center for Biotechnology Information
NF-kB	nuclear factor kappa-light-chain-enhancer of activated B cells
NGS	Next-Generation Sequencing
NRAS	neuroblastoma RAS viral oncogene homolog
OE	overexpression
OS	overall survival
PB	peripheral blood
PBS	phosphate buffered saline
PCR	polymerase chain reaction
PEBP	phosphatidylethanolamine binding protein

PI3K	phosphatidylinositol 3-kinase
pIpC	polyinosinic polycytidilic acid
qPCR	quantitative PCR
RAF	rapidly accelerated fibrosarcoma
RAS	rat sarcoma
RIN	RNA integrity number
RKIP	RAF kinase inhibitor protein
RNA	ribonucleic acid
RT	reverse transcription
sAML	secondary AML
SCF	stem cell factor
shRNA	short hairpin RNA
siRNA	small interfering RNA
SP	spleen
tAML	therapy related AML
TCGA	The Cancer Genome Atlas
TNFα	tumor necrosis factor alpha
WBC	white blood cells
WHO	World Health Organization

List of Figures

List of Tables

Zusammenfassung

RAF kinase inhibitor protein (RKIP) ist ein Inhibitor des *RAS-MAPK/ERK* Signaltransduktionspfades. RKIP ist ein Metastasen-Suppressorgen und ein somatischer Expressionsverlust wurde bei soliden Malignomen beschrieben. Ca. 20% aller PatientInnen mit akuter myeloischer Leukämie (AML) zeigen einen RKIP Verlust. Dieser korreliert dabei einerseits mit myelomonozytären AML Phänotypen, andererseits aber auch mit dem Auftreten von *RAS*-signaling Mutationen. In dieser Dissertation versuchten wir, das Wissen über RKIP in hämatologischen Neoplasien noch weiter zu vergrößern.

Zuerst analysierten wir RKIP im Myelosarkom (MS). MS ist ein AML-Subtyp, bei dem leukämische Blasten nicht-hämatopoetische Gewebe infiltrieren und dort solide Tumoren bilden. Da dieser Prozess der Metastasierung von soliden Tumoren ähnelt, hypothetisierten wir, dass RKIP Verlust an der Gewebsinfiltration von Leukämiezellen beteiligt ist. Durch eine Reihe von in-vitro und in-vivo Experimenten konnten wir zeigen, dass RKIP knockdown die Invasion und Migration von AML Zellen induziert. Mechanistisch zeigten wir, dass RKIP Verlust dabei über *RAS-MAPK/ERK* unabhängige Effektoren wirkt. Schlussendlich konnten wir noch klinische PatientInnenproben von AML untersuchen und zeigen, dass RKIP Verlust mit dem Auftreten eines MS korreliert. Darüber hinaus korrelierte RKIP Verlust auch mit *RAS*-signaling Mutationen, was ein weiterer Hinweis ist, dass diese beiden Aberrationen in der myeloischen Leukämogenese synergistisch zusammenarbeiten.

Dann untersuchten wir RKIP bei myelomonozytärer Differenzierung. Basierend auf der Korrelation zwischen RKIP Verlust und myelomonozytären AML Phänotypen, hypothetisierten wir, dass RKIP Verlust eine Rolle bei myelomonozytärer Differenzierung, und eventuell auch bei myelomonzytärer Leukämogenese spielt. Initial untersuchten wir die physiologische Hämatopoese und beobachteten, dass die RKIP Expression in myelomonozytär ausgereiften Zellen abnimmt. Durch in-vitro Experimente in $CD34^+$ hämatopoetischen Stamm- und Progenitorzellen (HSPZ) und HL-60 AML Zellen konnten wir auch eine funktionelle Relevanz von RKIP bei myelomonozytärer Differenzierung zeigen. Dies konnten wir in-vivo bestätigen: die GM-CSF induzierte Bildung von myelomonozytären Zellen war bei

Mäusen mit einer Deletion von *Rkip-/-* gesteigert. Um RKIP bei myelomonozytären Neoplasien zu studieren, fokussierten wir auf die chronisch myelomonozytäre Leukämie (CMML). Diese Erkrankung ist durch gesteigerte myelomonozytäre Proliferation, sowie durch das Vorkommen von *RAS*-signaling Mutationen charakterisiert. Das macht sie zu einem idealen Modell, um einerseits RKIP bei myelomonozytärer Leukämogenese zu studieren, andererseits aber auch um die Interaktion zwischen RKIP Verlust und *RAS*-signaling Mutationen zu analysieren. Dazu kreuzten wir *Rkip-/-* mit $Nras^{G12D}$ mutierten Mäusen. Das $Nras^{G12D}$ Modell entwickelt eine CMML, allerdings mit mildem Phänotyp. Die zusätzliche Deletion von *Rkip* führte zu einer Verstärkung dieser Erkrankung, was sowohl die Rolle von RKIP in myeloischer Leukämogenese, als auch den oben suspizierten funktionellen Synergismus von RKIP Verlust und *RAS*-signaling Mutationen bestätigt. Wie beim MS konnten wir auch diese Daten klinisch bestätigen. RKIP Verlust kam bei über 30% von primären CMML PatientInnenproben vor und ko-existierte mit *RAS*-signaling Mutationen.

Zusammenfassend zeigten wir, dass RKIP Expressionsverlust bei myeloischen Neoplasien vorkommt und für die myeloische Leukämogenese relevant ist. Erstens zeigten wir dabei, dass es mit dem Auftreten eines Myelosarkoms bei AML korreliert und die Gewebsinfiltration von Leukämiezellen verursacht. Zusätzlich zeigten wir, dass RKIP Verlust die myelomonozytäre Differenzierung und CMML Entstehung verstärkt. Dabei bestätigten wir auch, dass RKIP Verlust mit RAS-signaling Mutationen korreliert und mit diesen in der myeloischen Leukämogenese zusammenarbeitet.

Abstract

RAF kinase inhibitor protein (RKIP) is a negative regulator of the *RAS-MAPK/ERK* pathway. It is a well-known metastasis-suppressor in solid cancers and a somatic loss of RKIP has been described frequently in these entities. Around 20% of acute myeloid leukemia (AML) cases show a functionally relevant loss of RKIP, which correlates with *RAS* mutations and myelomonocytic AML phenotypes. In this thesis, we aimed at extending the knowledge about RKIP in hematologic neoplasias even further.

First, we clarified the role of RKIP in myeloid sarcoma (MS). MS is a subtype of AML, in which leukemic blasts form solid tumor masses in non-hematopoietic tissues. As this process resembles the development of metastases in solid tumors, we hypothesized that RKIP loss drives the tissue infiltration of leukemic cells. We could show that knockdown of RKIP promotes the invasion and migration of AML cells in-vitro. This could be confirmed in-vivo, where AML cells with RKIP knockdown invaded into, and formed tumor masses in the chorioallantoic membrane of chicken embryos. Mechanistically, we could show that RKIP loss induces the tissue infiltration of leukemic blasts via *RAS-MAPK/ERK* independent mechanisms and identified candidate effector genes via microarray analyses in RKIP knockdown cells. Finally, we could prove the clinical relevance of these findings by demonstrating that RKIP loss correlates with the presence of MS in primary AML patient specimens. We could additionally show that RKIP loss correlated with *RAS*-signaling mutations in MS using Next-Generation Sequencing (NGS). This suggests a functional synergism between these events in myeloid leukemogenesis.

Secondly, we studied the role of RKIP in myelomonocytic differentiation. Since the *RAS-MAPK/ERK* pathway plays a role in the myeloid lineage commitment of hematopoietic stem and progenitor cells (HSPCs), and as RKIP loss correlates with myelomonocytic AML phenotypes, we hypothesized that RKIP loss plays a role in myelomonocytic differentiation and in the development of myelomonocytic neoplasias. In physiologic hematopoiesis, we observed low RKIP levels in myeloid lineage cells. Then, we could prove a functional involvement of RKIP loss in myelomonocytic differentiation by modulating RKIP in $CD34^+$ HSPCs and HL-60

AML cells. These results could be confirmed in mice with a complete deletion of *Rkip* (*Rkip-/-*): GM-CSF induced formation of myelomonocytic cells was significantly increased in *Rkip-/-* animals. We then studied the role of RKIP in chronic myelomonocytic leukemia (CMML), which is characterized by increased myelomonocytic proliferation and frequent occurrence of *RAS*-signaling mutations. Therefore, it is an ideal model to study RKIP in myelomonocytic leukemogenesis and to investigate a potential interaction between RKIP loss and *RAS* mutations. We crossed *Rkip-/-* mice with animals carrying an inducible $Nras^{G12D}$ mutation. These mice develop a myeloproliferative disease resembling CMML (CMML-MPD). Additional deletion of *Rkip* caused a significant aggravation of CMML-MPD, proving the functional synergism between RKIP loss and *RAS*-signaling mutations in myeloid leukemogenesis. Mechanistically, we could show that loss of RKIP expression increases the activity of the *RAS-MAPK/ERK* signaling cascade within these leukemia models. Finally, we studied a cohort of primary CMML patient specimens. RKIP loss occurred in more than 30% of cases and again co-existed with *RAS*-signaling mutations.

Altogether, we show that loss of RKIP expression is a relevant event for myeloid leukemogenesis. Firstly, we demonstrate that it drives the tissue infiltration of myeloid blasts and thereby contributes to the development of MS. Then, we show that it contributes to myelomonocytic differentiation and the development of CMML. Finally, we corroborate the association between RKIP loss and *RAS*-signaling mutations and demonstrate a functional synergism between these events in myeloid leukemogenesis.

1. Introduction

1.1. Myeloid malignancies

Myeloid malignancies are aggressive hematopoietic malignancies comprising acute myeloid leukemia (AML), myeloproliferative neoplasias (MPN), myelodysplastic syndromes (MDS), as well as MDS/MPN overlap syndromes. The most frequent MDS/MPN overlap syndrome is chronic myelomonocytic leukemia (CMML). The work in my thesis focused on AML (in particular the subtype myeloid sarcoma) and CMML, therefore I will concentrate on these two entities within this introduction.

1.1.1. Acute myeloid leukemia and myeloid sarcoma

AML is an aggressive clonal disorder of the hematopoietic system. It is caused by malignant transformation of hematopoietic stem and progenitor cells (HSPCs). The malignant offspring is characterized by impaired differentiation and uncontrolled growth (1). These cells, called leukemic blasts, are generally found in the bone marrow (BM) and/or in the peripheral blood (PB). However, in some cases, leukemic blasts can invade extramedullary tissues and form solid tumor masses, a process that resembles metastasis formation in solid tumors (2–4). This subtype of AML is called myeloid sarcoma (MS).

1.1.1.1. Epidemiology, clinical presentation and diagnostic criteria

AML is the prevalent form of acute leukemias in adults. Although AML can occur at every age, it affects primarily the elder, with a greater incidence in subjects above 65 years. Consequently, the median age at AML diagnosis is over 70 years. The incidence rate of AML in individuals with less than 65 years is 1.8/100000 people per year. This number increases dramatically in older subjects, in which AML affects 17/100000 people per year (5).

The clinical manifestation of AML includes symptoms that are usually non-specific. In more detail, patients present with fatigue and weakness, due to anemia, bleeding, caused by thrombocytopenia, and impaired wound healing as well as infections, due to neutropenia. This is the result of the expansion of the leukemic blasts in the BM, which cause BM insufficiency and therefore the suppression of normal hematopoiesis.

A diagnosis of AML is performed by analysis of BM or PB and is confirmed when the percentage of blasts is above 20% (4).

Different types of AML are defined depending on when the neoplasia evolves:

- *de novo* AML, when it develops in previously healthy subjects;
- secondary AML (sAML), when AML evolves via transformation of another hematopoietic malignancy, in particular MDS, MPN and MDS/MPN, respectively (6);
- therapy-related AML (tAML), when AML develops after chemo- and/or radiotherapy for a primary malignancy (7).

The first classification of AML came from the French-American-British system (FAB) (8). The FAB subdivided AML into eight categories, depending on the morphology and maturation stage of the myeloid blasts. In more detail, the categories are defined as follows:

- M0: undifferentiated;
- M1: myeloblastic without maturation;
- M2: myeloblastic with maturation;
- M3: promyelocytic;
- M4: myelomonocytic;
- $M4_{EO}$: myelomonocytic with bone marrow eosinophilia;
- M5: monocytic;
- M6: erythroleukemia;
- M7: megakaryoblastic.

The current classification is the 2016 World Health Organization (WHO) classification. This system categorizes AML depending on recurrent cytogenetic aberrations, molecular abnormalities, immunophenotype, clinical manifestations and morphology (9). In more detail, AML is classified as follows (3,10):

- AML with recurrent genetic abnormalities:
    - AML with t(8;21)(q22;q22.1); *RUNX1-RUNX1T1*
    - AML with inv(16)(p13.1q22) or t(16;16)(p13.1;q22); *CBFB-MYH11*
    - Acute promyelocytic leukemia with *PML-RARA*
    - AML with t(9;11)(p21.3;q23.3); *MLLT3-KMT2A*
    - AML with t(6;9)(p23;q34.1); *DEK-NUP214*

        - AML with inv(3)(q21.3q26.2) or t(3;3)(q21.3;q26.2); *GATA2, MECOM*
        - AML (megakaryoblastic) with t(1;22)(p13.3;q13.3); *RBM15-MK*L1
        - Provisional entity: AML with *BCR-ABL1*
        - AML with mutated *NPM1*
        - AML with biallelic mutations of *CEBPA*
        - Provisional entity: AML with mutated *RUNX1*
    - AML with myelodysplasia-related changes
    - Therapy-related myeloid neoplasms
    - Acute myeloid leukemia, not otherwise specified:
        - AML with minimal differentiation
        - AML without maturation
        - AML with maturation
        - Acute myelomonocytic leukemia
        - Acute monoblastic/monocytic leukemia
        - Pure erythroid leukemia
        - Acute megakaryoblastic leukemia
        - Acute basophilic leukemia
        - Acute panmyelosis with myelofibrosis
    - Myeloid sarcoma
    - Myeloid proliferations related to Down syndrome
        - Transient abnormal myelopoiesis
        - Myeloid leukemia associated with Down syndrome.

In rare cases, AML can manifest as an extramedullary mass. This subtype of AML takes the name of MS. Since it is a relatively rare disease, literature about MS is mostly composed of case reports and retrospective studies. MS is defined by the WHO as a group of myeloid blasts, either mature or immature, which form a tumor mass in a tissue outside of the hematopoietic tissues (11).

MS can occur at any age and affect any site of the body. It is reported that the most commonly affected sites are lymph nodes, skin, soft tissues, bone, testes, gastrointestinal tract, and peritoneum (12–15). MS can develop at different stages of AML. In particular, MS can be concurrent with AML or it may manifest at relapse, for example in patients who received allogenic hematopoietic stem cell transplantation (HSCT) (16). In rare occasions, MS can also manifest without any

sign of leukemia or other hematologic neoplasm. This is defined as isolated MS and can precede the clinical disease by months or even years (17). Generally, isolated MS that is not treated develops into AML over 10-12 months. However, in some rare cases, the transformation has not occurred for over 16 years (18,19). MS has slight male predominance (male to female ratio of 1.2:1) and it was described in around 2.5–9.11% of AML patients (17). However, this percentage might be an underestimation of the real rate. This is mainly due to the difficulties of detecting MS, especially in cases of patients without a history of AML. For example, the use of ^{18}Fluoro-deoxy-Glucose Positron Emission Tomography / Computed Tomography to detect MS sites in patients with a clinical history of MS was able to detect additional, not previously detected, extramedullary manifestations in 6/10 of the patients analyzed (20). This highlights the need for improved detection systems, which are important especially for patients with isolated MS.

Symptoms of MS vary depending on the tissue it affects. In general, symptoms depend on the mass of the tumor and the dysfunction that it causes in the organ or tissue that is affected (21).

Diagnosis of MS can be performed by different methods, which include clinical evaluation, radiological analysis and tissue biopsy. The diagnosis is generally confirmed performing immunohistochemistry on the biopsy sample. In particular, an antibody panel can comprise myeloperoxidase, CD43, CD68, lysozyme, and CD117. These are the most common antigens expressed in MS, with myeloperoxidase expressed in 66 to 96% of MS patients. Other common markers include CD11c, CD13, and CD33 (16,22,23). The diagnosis of MS in patients with an already diagnosed AML can be easier as compared to patients with isolated MS. In these cases, it was recorded to have up to 75% rate of misdiagnosis, with MS being recognized as large cell lymphoma in the majority of the cases (24). The rate of misdiagnosis results reduced in recent studies, but is still high, ranging between 25 and 47% of cases (19,25).

MS presents as an infiltrate of myeloid cells, including myeloblasts, monoblasts and promyelocytes. The different degree of maturation of these cells defines the type of MS:

- Blastic MS, composed of myeloblasts with little maturation;
- Immature MS, which includes myeloblasts, promyelocytes, and eosinophilic myelocyte;
- Mature MS, composed of more mature cells, the promyelocytes, and eosinophils (22,26).

1.1.1.2. Prognosis, risk stratification and therapeutic strategies

Despite all therapeutic progress, AML still has a dismal outcome. The cure rate is only around 35-40% in cases below 60 years of age and around 5-15% in older patients (4,5,27,28). Risk stratification is important for taking treatment decisions in AML. An important element to take into account is the age of the patient and the presence of co-morbidities. Usually, older patients show a lower survival rate as compared to younger patients. But, in general, determining the co-morbidities plays an important role for deciding the treatment options in both groups (5,29). Other factors to take into account are the various molecular aberrations that are present in AML patients. The novel European Leukemia Net (ELN) classification divided AML in three risk groups, depending on these aberrations (4). In more detail, the risk groups are defined as follows:

- Favourable risk group, which includes patients with the following genetic abnormalities:
  - t(8;21)(q22;q22.1); *RUNX1-RUNX1T1*
  - inv(16)(p13.1q22) or t(16;16)(p13.1;q22); *CBFB-MYH11*
  - Mutated *NPM1* without *FLT3*-ITD or with *FLT3*-ITDlow
  - Biallelic mutated *CEBPA*
- Intermediate risk group, which includes patients with the following genetic abnormalities:
  - Mutated *NPM1* and *FLT3*-ITDhigh
  - Wild-type *NPM1* without *FLT3*-ITD or with *FLT3*-ITDlow (without adverse-risk genetic lesions)
  - t(9;11)(p21.3;q23.3); *MLLT3-KMT2A*
  - Cytogenetic abnormalities not classified as favorable or adverse
- Adverse risk group, which includes patients with the following genetic abnormalities:

- t(6;9)(p23;q34.1); *DEK-NUP214*
- t(v;11q23.3); *KMT2A* rearranged
- t(9;22)(q34.1;q11.2); *BCR-ABL1*
- inv(3)(q21.3q26.2) or t(3;3)(q21.3;q26.2); *GATA2,MECOM(EVI1)*
- -5 or del(5q); -7; -17/abn(17p)
- Complex karyotype, monosomal karyotype
- Wild-type *NPM1* and *FLT3*-ITDhigh
- Mutated *RUNX1*
- Mutated *ASXL1*
- Mutated *TP53*

The prognosis of AML patients belonging to the adverse risk group is the poorest in AML and they show extremely low rates of overall survival (OS) (30).

The therapeutic strategy for AML patients can be simplified in two approaches. On the one hand, patients in good health conditions are eligible for intensive therapies, which include high-dose chemotherapy and HSCT. On the other hand, patients that are older or unfit are treated with non-intensive regimens or given best supportive care (BSC) (28). In patients eligible for intensive therapeutic approaches, the first aim of AML treatment is to obtain complete remission (CR) by an induction therapy. CR is defined as the presence of less than 5% of leukemic blasts in the bone marrow together with absence of extramedullary manifestations. Once CR is obtained, post-induction treatment is administered in order to consolidate the CR. Otherwise, AML will relapse soon afterwards. Younger patients, below the age of 60, achieve CR in around 70-80% of cases (4,31). In the case of older patients, only 45 to 60% of the ones treated with intensive therapy achieve a CR (31). Induction therapy is generally composed of seven days of treatment with cytarabine and three days of treatment with an anthracycline, for example daunorubicin or idarubicin (7+3 scheme). Consolidation therapy normally includes chemotherapy with two to four cycles of intermediate/high dose of cytarabine and/or HSCT, depending on the risk type of the patient. While patients within the ELN favourable risk group are usually consolidated with chemotherapy only, patients within the intermediate and adverse risk groups cannot be cured with chemotherapy alone. These patients are

therefore consolidated with allogeneic HSCT (4,9,28). Non intensive therapies, dedicated to older patients incapable of tolerating intensive treatments, include the administration of hypomethylating agents (azacitidine, decitabine), low-dose cytarabine and/or BSC (5). In general the survival rates for older patients are much poorer, and these non-intensive therapies often only cause an extension in survival, but no cure (32).

Recently, targeted therapies have emerged and aim at improving the prognosis of AML patients. For example, sorafenib and midostaurin, which are multi-kinase inhibitors, were investigated in AML cases with FLT3 mutations. Particularly, midostaurin extended the overall survival of AML patients, when administered in combination with high-dose chemotherapy and achieved an EMA licensing recently (33). Another successful example is gemtuzumab ozogamizin, an anti-CD33 antibody, which is linked to a cytotoxic agent (34). By binding to the CD33 surface marker on AML blasts, the cytotoxic substance is delivered to these cells with a high specifity. Again, the results in clinical trials were positive, and the substance has been licensed for AML in combination with high-dose chemotherapy by the EMA recently. A wide range of other promising targeted therapies are in development, and are awaited to reach licensing soon.

Large studies dedicated to understand the prognosis of MS are lacking. This is due not only to the rarity of this disease but also to the differences in tumor location and genetics, timing of onset and treatment strategies. Moreover, the available studies show discordant data, with groups indicating a better outcome in patients with MS as compared to subjects with AML, others indicating the opposite and additional studies showing no difference in the disease outcome in presence or absence of MS. Studies performed in children showed that subjects with isolated MS had a better prognosis as compared to age-matched children with AML without signs of MS (35). This data is in agreement with other studies performed in adults. On the one hand, MS patients had increased overall survival after treatment with chemotherapy (36) and showed a 3-year higher survival rate as compared to AML patients (37). In particular, the best prognosis was for isolated MS affecting the pelvis, genitourinary organs, eyes, gonads and gastrointestinal mucosa. On the other hand, studies reported MS to be associated with poor prognosis and shorter overall survival (38,39). Additionally, other studies

showed a similar 5-year survival rate when comparing MS and AML patients without any evidence of MS (26,40). This discordance highlights the need for future studies, in order to gain more knowledge on MS and design an MS-tailored treatment approach.

MS is usually treated like all other subtypes of AML with high-dose chemotherapy and HSCT. This is also true for isolated MS. However, in case of isolated MS, the ideal consolidation treatment is currently unclear. This is mainly caused by the fact, that the paraffin-embedded MS biopsies do not allow a comprehensive risk stratification at diagnosis. In example, conventional karyotyping is impossible from these specimens. Recent studies employing Next-Generation Sequencing (NGS) and quantitative polymerase chain reaction (qPCR) worked on this topic, however, and managed to present algorithms, which enable risk stratification even without karyotyping (41,42).

1.1.1.3. Mutations and pathogenesis

A study conducted in more than 200 AML patients by The Cancer Genome Atlas (TCGA) revealed an average of 13 gene mutations per patient (43). Amongst the mutated genes, 23 had a proven involvement in the pathogenesis of AML. Amongst these genes are *FLT3*, *NPM1*, *DNMT3A*, *IDH2*, *IDH1*, *CEBPA*, *U2AF1, EZH2* and *RAS.* These results could be confirmed in a large cohort of more than 1500 AML patients. Importantly, more than 90% of AML patients carried at least one mutation within these recurrently mutated genes (44). The pathogenesis of AML is a multistep process. In the beginning, ageing HSPCs acquire one or more somatic mutations, a situation called clonal hematopoiesis of indeterminate potential (CHIP) (45–47). This is insufficient to cause a hematologic neoplasia, and indeed, these patients often fail to develop a malignancy during their lifetime. However, this clonal hematopoiesis might lead to an expansion of the mutated HSPCs and to the subsequent accumulation of additional mutations (48). This clonal evolution ultimately might result in the development of hematologic neoplasias, including AML (49). The model gets even more complex, as the developing clone can branch into different subclones at every time during AML development. This results in the typical picture of AML, where the disease does not only comprise one single clone, but rather exhibits a lot of different “main” and “subclones” (50).

Around 50% of MS patients present molecular aberrations (17). The most frequently affected gene is *NPM1* while the most common translocation is t(8; 21). Another common translocation, which is associated in particular with extramedullary manifestation in the abdomen, is inv(16). A various range of other abnormalities were detected in MS and these include t(9; 11), del(16q), t(8; 17), t(8; 16), and t(1; 11), as well as abnormalities affecting chromosome 4, 7, 8 and 11 (51–54).

Regarding the pathogenesis of MS, the exact mechanism by which leukemic blasts invade extra-hematopoietic tissues is not fully understood. Some studies indicate the existence of cytokine receptors as well as adhesion molecules, which control the invasion of leukemic blasts into specific tissue. Moreover, the deregulation of transcription factors, for example the ones involved in cellular adhesion, can contribute to the pathogenesis of MS (17).

1.1.2. Chronic myelomonocytic leukemia

CMML is a clonal malignancy of HSPCs. It presents overlapping features of MDS and MPN (55), therefore it is classified under the MDS/MPN neoplasms by the WHO (56).

1.1.2.1. Epidemiology, clinical presentation and diagnostic criteria

CMML mainly affects older people, with a median age at diagnosis ranging between 65 to 75 years, and a 2:1 male predominance (57,58). The exact incidence of this disease is unknown, but it is estimated to be around 0.3 cases per 100000 people per year in the USA (59). However, this estimation is most probably under representative of the true rate, since CMML is a rare disease and its classification has changed over the years.

CMML manifests in the patients with an excessive myelomonocytic proliferation and dysplasia of these cells in hematopoietic and sometimes also non-hematopoietic tissues. Particularly in the BM, this can lead to suppression of the remaining hematopoiesis, causing bone marrow insufficiency (60). This results in patients suffering from severe anemia, which in turn leads to fatigue, dyspnea and effort intolerance. Moreover, it can sometimes cause thrombocytopenia, leading to impaired blood coagulation, as well as ischemic organ damage. Leukocyte counts can be both, decreased or increased. Patients with a preponderance of the

myelodysplastic features are often leukopenic, those with a predominant myeloproliferation often present with leucocytosis. Importantly, even if the absolute number of leukocytes increases, CMML patients are at risk for infections, since the leukocytes are impaired in their function (58). Another manifestation of myelomonocytic proliferation in CMML is severe splenomegaly and, in some cases, myeloid cells can even infiltrate extra-hematopoietic tissues (61).

The diagnosis of CMML can be confirmed via PB and BM, as described in the WHO 2016 classification of myeloid neoplasms (3). In more detail, the diagnostic criteria for CMML are:

- persistent monocytosis in the PB (≥ $1x10^9$/L) and monocytes accounting for ≥ 10% of the white blood cells;
- not meeting the criteria of the WHO classification for chronic myeloid leukemia, primary myelofibrosis, polycythemia vera and essential trombocythemia;
- absence of platelet derived growth factor receptor (PDGFR) A, PDGFRB or fibroblast growth factor receptor-1 (FGFR-1) gene rearrangements as well as pericentriolar material-1/janus kinase-2 (PCM-1/JAK-2) fusion;
- blasts count (including myeloblasts, monoblasts and promonocytes) < 20% in PB or BM;
- dysplasia affecting one or more myeloid lineages; if myelodysplasia is minimal or absent, CMML can still be diagnosed when all the four previous requirements are met and there is presence of an acquired clonal cytogenetic or molecular genetic abnormality or when the monocytosis has persisted for at least three months and other causes of monocytosis have been excluded.

Whenever the percentage of immature myeloid blasts cells and/or promonocytes increases above 20% in the PB or BM, the diagnosis changes from CMML to AML. This transformation occurs with a 5-year risk which ranges between 18 and 63% (62).

CMML was classified by the FAB system as myelodysplastic (MDS-CMML) and myeloproliferative (MPN-CMML) depending on the white blood cell count (<13 × 10^9/L for MDS-CMML and > 13×10^9/L for MPN-CMML) (8). The WHO

classification divides CMML in three subtypes, depending on the amount of blasts: CMML-0 (< 2% blasts in the PB and/or < 5% in the BM) , CMML-1 (2-4% blasts in the PB and/or 5-9% in the BM) and CMML-2 (5-19% blasts in the PB and/or 10-19% blasts in the BM) (3,56).

1.1.2.2. Prognosis, risk stratification and therapeutic strategies

CMML patients show a highly variable clinical course. On the one hand, some patients fall in the low risk category, have a lower probability of AML transformation and therefore show a longer survival. On the other hand, some patients show a very aggressive form of CMML (63). This results in OS ranging from 5 to 97 months in the various risk groups of CMML (64,65). There are different risk stratification models for CMML, which were established in order to better predict the clinical course of different CMML patients. The most common models include the MD Anderson Prognostic Scoring System, the CMML-specific prognostic scoring system, the scoring system of the Groupe Francophone des Myelodysplasies and the Mayo scoring system (64–67). One of the latest models is the revised Molecular Mayo scoring system, which included as new risk factors the absolute monocyte count (>10x10^9/L), haemoglobin levels (<10 g/L), platelet count (<100x10^9/L), the presence of immature myeloid cells in the PB and mutations in ASXL-1 (with exclusion of missense mutations). According to this classification, CMML patients could be divided into four risk groups:

- high risk, including patients with three or more risk factors; the median OS is 16 months
- intermediate-2, including patients with two risk factor; the median OS is 31 months
- intermediate-1, including patients with one risk factor; the median OS is 59 months
- low risk, including patients with no risk factors; the median OS is 97 months (68).

Since CMML is a rare disease, designated clinical studies are difficult to establish and CMML is often treated following the guidelines for MDS and MPN, respectively. At the moment, the only curative option for CMML is HSCT (69). However, due to the elevated age and the presence of co-morbidities, many CMML patients are not eligible for HSCT. (70). A recently established therapeutic

option is the use of 5-azacitidine (71). This is a hypo-methylating agent that acts as an epigenetic modifier and has been shown to prolong survival in CMML patients. Importantly, this is a non-intensive therapy, so it is relatively well tolerated and can be used in older patients that are not eligible for transplantation. Other therapeutic options are currently studied and involve the targeting of specific pathways and new molecular markers. These are currently investigated in preclinical and clinical trials (72). Very old or unfit patients, who are not even able to tolerate 5-azacitidine, are treated using BSC. In BSC, only symptomatic treatment is employed. Some examples of treatment that fall in the category of BSC are the transfusion of erythrocytes, to treat anemia, of thrombocytes, in case of thrombocytopenia, and the administration of antimicrobial drugs, in case of infection (60). Other BSC treatments include the use of hematopoietic growth factors as well as the administration of hydroxyurea, a myelo-suppressive agent which helps in the control of leukocytosis (73,74). Particularly in patients with predominant myeloproliferation, hydroxyurea represents a successful therapeutic approach.

1.1.2.3. Mutations and pathogenesis

Cytogenetic aberrations are seen in around 30% of CMML patients, while gene mutations affect more than 90% of CMML cases (55).

The most frequent cytogenetic abnormalities in CMML include trisomy 8, complex karyotype, monosomy 7, deletion of 7q and alterations in chromosome 12p. Other aberrations found in CMML patients include trisomy 10, 19 and 21, deletions of 5q and 11q, as well as additions in 17p (55,63).

With the introduction of NGS, molecular abnormalities could be detected in more than 90% of CMML patients. These mutations affect:

- epigenetic regulator genes (*TET2, DNMT3A, IDH1* and *IDH2*);
- chromatin regulation and histone modification (*ASXL1, EZH2, UTX, EED* and *SUZ12*);
- the splicing machinery (*SF3B1, SRSF2, U2AF1* and *ZRSR2*);
- the cohesin complex (*STAG2, BCOR, SMC3, SMC1A* and *RAD21*);
- DNA damage response genes (*TP53* and *PHF6*);

- signal transduction and cellular/receptor tyrosine kinase pathways (*JAK2*, *SH2B3, KRAS, NRAS, CBL, FLT3* and *NPM1*).

Other mutations involve *RUNX1* and *SETBP1*.

Concerning the frequency, the most frequent genetic aberrations in CMML are found in *TET2* (~60%), *ASXL1* (~40%), *SRSF2* (~50%), *RUNX1* (~15%), *RAS* (~30%) and *CBL* (~15%) (55).

The development of CMML is caused by the accumulation of mutations in the HSPCs, which in this way gain a survival advantage and clonally expand. Before the onset of a malignant phenotype, these clones cause a CHIP. In this case, HSPCs do not show an abnormal phenotype, but harbour mutations, which are typical of hematologic malignancies. In some cases, CHIP can evolve into MDS, CMML and, eventually, AML (45). As described above for AML, the HSPCs of CHIP accumulate more mutations over time and branch into different subclones. Eventually, this causes the development of frank CMML. One such model was proposed for the evolution of CMML from HSPCs and its clonal architecture (75). This model indicates the presence of a first loss of function mutation in either *TET2* or *ASXL1* gene. Both these genes play an important role in epigenetic regulation. A second mutation will then affect *SRSF2*, or another member of the splice machinery system, as well as molecules involved in signaling, for example *RAS* or *JAK2*. These mutations induce a clonal expansion of the mutated HSPCs (75,76). Mutations affecting the *RAS* and *JAK/STAT* signaling pathway are also associated with hypersensitivity to granulocyte-macrophage colony-stimulating factor (GM-CSF), which enhances proliferation and cell survival and favours leukemic transformation (77). In particular, mutations affecting the *RAS* signaling pathway have a negative prognostic impact in CMML patients. This is because these mutations favour the progression of CMML from the myelodysplastic to the myeloproliferative variant (72,76).

1.2. The RAS oncogenes

1.2.1. Signaling and functions of the RAS family

The rat sarcoma (RAS) is a super gene family with more than 50 members, composed of low molecular weight G proteins. These molecules possess a guanine nucleotide-binding site and work as molecular switches that regulate

multiple cellular functions (78). For example, members of the RAS family play a role in regulating cell cycle and proliferation. Moreover, these molecules are involved in differentiation, rearrangements of the cytoskeleton, apoptosis and import of proteins inside the nucleus (79,80). The binding of guanosine triphosphate (GTP) activates the RAS proteins. This is favored by guanine nucleotide exchange factors (GEFs), which facilitate the formation of the RAS-GTP complex. The inactivation of the RAS proteins is caused by the hydrolysis of the RAS-GTP complex, when GTP is converted into the inactive state (guanosine diphosphate, GDP). This is caused by GTPase-activating proteins (GAPs), which transform the RAS-GTP complex into RAS-GDP (81). Activation of the *RAS* signaling happens via growth factors, cytokines or mitogen receptors (82) and causes the activation of various intracellular signaling cascades like the mitogen-activated protein kinase/extracellular signal-regulated kinase (MAPK/ERK) pathway or the phosphatidylinositol 3-kinase/alpha serine/threonine-protein kinase (PI3K/AKT) (83). Moreover, RAS proteins interact with various transcription factors and therefore also regulate the expression of target genes. From a clinical point of view, the most important members of the RAS group are Kirsten rat sarcoma viral oncogene homolog (KRAS), neuroblastoma RAS viral oncogene homolog (NRAS) and Harvey rat sarcoma virus oncogene (HRAS). These are highly homologous proteins of 21 kDa, that have in common the first 85 amino acids, which contain the binding site for the guanosine nucleotides (81).

1.2.2. RAS mutations in cancers

Oncogenic mutations affecting members of the RAS family are common in human cancers, being present in approximately 20 to 30% of cancer entities (81). Frequently mutated hotspots are present in codons 12, 13 and 61. All of these are located within the conserved G-protein domain. The presence of mutations in these hotspots prevents the hydrolysis of GTP and therefore causes a permanent activation of the signaling and the accumulation of RAS-GTP inside the cell (84). The constant activation and overstimulation of the RAS signaling caused by these mutations induces the transformation of the cells and initiates tumorigenesis, as it was observed in various animal models (85).

1.2.3. RAS mutations in myeloid malignancies

Mutations affecting RAS are frequently detected in myeloid neoplasias (MNs).

NRAS or KRAS mutations are detected in 10 to 20% of AML patients (42,44,86). This frequency is even increased in pediatric AML, in which the frequency is higher than 10% and 30% for KRAS and NRAS mutations, respectively (87). RAS mutations are frequently detected also in CMML, with more than 40% of CMML patients harboring one or more mutations affecting the *RAS* genes and/or the *RAS*-signaling pathway. RAS mutation have been proven to be functionally involved in the development of myeloid leukemogenesis (86,88). In more detail, mutations affecting RAS activate various signaling cascades, including MAPK/ERK and Pi3K/AKT, resulting in an increase of the proliferation and of the myelomonocytic lineage commitment of HSPCs. These are two seminal steps in the development of myeloid neoplasms (83). This was confirmed employing murine models with a somatically inducible *Nras* or *Kras* mutation. These models develop a CMML-like malignancy, which resembles the characteristics of human CMML (89–91).

1.2.3.1. Therapeutic options targeting RAS

Mutations affecting the *RAS*-signaling pathway, causing the constant activation of this cascade, can be abrogated employing specific inhibitors of this pathway. This can be used as a therapeutic strategy. Indeed, it showed promising results in murine models, in which inhibitors of the MAPK/ERK and Pi3K/AKT pathways abrogated MPN development in mice models harboring *Ras* mutations (92,93). Unfortunately, these results could not be repeated in clinical trials for human MNs. This might be caused by various factors, including the different genomic MNs landscape between murine models and human subjects and the absence of focus on patients who really showed dependence on the activation of the *RAS*-signaling. In order to select these patients, it is important to take into account that, in human leukemias, *RAS*-signaling mutations usually co-occur with other mutational and non-mutational aberrations. These aberrations can change the dependence on activated *RAS*-signaling in MNs, since these can influence the activating effects of *RAS* mutations. For example, our group has previously shown that a somatic, leukemia-specific loss of RAF kinase inhibitor protein (RKIP), a negative regulator of *RAS-MAPK/ERK* signaling, correlates with *RAS* mutations in AML and potentiates their oncogenic effects in-vitro (86). Other aberrations co-occurring with *RAS* mutations affect other signaling regulators, such as members of the

SPROUTY (SPRY) and *DUSP* families, as well as epigenetic modifiers, like *TET2* and *ASXL1* (94–97). Interestingly, these co-occurrences have been shown to amplify even further the activating effect of *RAS* mutations. Therefore, these represent interesting therapeutic targets. This is caused by the fact that these tumors show increased dependence on activated *RAS*-signaling and therefore are more sensitive to inhibition of this pathway. Delineating more of these interactions with mutated *RAS* will help in designing better clinical trials for MNs, taking into considerations patients with specific co-occurring aberrations.

1.3. RAF kinase inhibitor protein

1.3.1. The *RAS-MAPK/ERK* pathway

The *RAS-MAPK/ERK* signaling pathway is involved in transferring the signal from extracellular stimuli to the nucleus and cytoplasm. This highly conserved signaling cascade plays a role in the regulation of various fundamental cellular processes, for example proliferation, differentiation and cell cycle progression (79). In the hematopoietic cells, activation of the *RAS-MAPK/ERK* pathway happens by binding of growth factors or mitogens to cellular receptors, for example FLT3 or VEGF, causing their activation. Activation of the receptors favors the movement of the small GTPase protein RAS to the cellular membrane. Here, RAS protein is activated and therefore binds and successively activates the family of rapidly accelerated fibrosarcoma (RAF) serine/threonine kinases, which includes A-RAF, B-RAF and C- RAF (or RAF1). Active RAF has the power to phosphorylate and activate the dual specificity kinase MEK1/2. This, in turn, phosphorylates and activates ERK1/2. Activated ERK1/2 plays a role in regulating more than 160 effector proteins, for example transcription factors and cytoskeletal proteins (98). The correct function of this signaling cascade is finely regulated by several regulator proteins. These play a role not only in regulating the proper activation of the pathway but also in its inactivation after the signal has been transmitted.

The *RAS-MAPK/ERK* pathway plays a role not only in a physiological setting, but it is also of seminal importance for tumorigenesis. A permanent activation of the pathway, referred to as constitutive activation, is detectable in various human malignancies and is involved in malignant transformation. Constitutive activation of the pathway is caused by genetic aberrations affecting the member proteins of the pathway as well as the upstream activators and the regulators.

1.3.2. RKIP

RAF kinase inhibitor protein (RKIP), also known as phosphatidylethanolamine binding protein 1 (PEBP1), is a cytosolic protein ubiquitously expressed in all mammalian tissues (99). Originally, it was isolated from the brain of bovines and is a member of the PEBP superfamily, which includes almost 400 genes (99,100). The human RKIP gene comprises four exons and is located on chromosome 12q24.23. The human RKIP mRNA is 1343 base pairs long and encodes a protein, which is 187 amino acids and a molecular weight of 23kDa (101).

RKIP plays a role as a regulator of various intracellular signaling pathways. First, it was identified as an inhibitor of the *RAS-MAPK/ERK* pathway. In particular, it inhibits the interaction between C-RAF and MEK, preventing the phosphorylation of MEK, which is essential for signal propagation (102). Successively, it was shown that RKIP modulates also the nuclear factor kappa-light-chain-enhancer of activated B cells pathway (NF-kB) (103) as well as G-protein signaling (104).

1.3.2.1. RKIP in solid tumors

Complete or partial loss of RKIP protein has been observed in various human malignancies. A somatic loss of RKIP results in an increased activity of the *RAS-MAPK/ERK* and Nf-KB signalling cascades in affected tumors. Importantly, this phenomenon proved to be functionally involved in malignant transformation (99,105).

The role of RKIP in cancer was described for the first time in prostate cancer (106). It was observed that, comparing prostate cancer cell lines, RKIP levels were low in highly metastatic cells and higher in the cells with a low metastatic rate. Subsequent experiments proved the functional involvement of RKIP loss in the formation of metastasis both in-vitro and in-vivo. Therefore, RKIP is defined as a metastasis-suppressor gene (107,108). In detail, a metastasis-suppressor plays a role in inhibiting the dissemination of tumor cells and the formation of metastasis. Differently from tumor-suppressor genes, metastasis-suppressor do not affect the growth of the primary tumor (109). From a clinical point of view, it was observed that expression of RKIP is high in benign tumors, reduces in malignant cancers and is even lower, if not absent, in the metastatic site. After this first finding in prostate cancer, a role for RKIP as metastasis-suppressor was observed in various other cancers, including breast cancer (110), melanoma (111), colorectal

carcinoma (112) and hepatocellular carcinoma (113). The mechanism by which RKIP is deactivated or lost in tumor cells as these become more invasive is not well understood yet (109).

A part from its role as a metastasis-suppressor, loss of RKIP expression is implicated in causing radio- and chemotherapeutic resistance (101). In particular, it was observed in breast and prostate cancer cell lines that treatment with chemotherapeutic agents induced increased expression of RKIP, which in turn increased the predisposition of the cancer cells to apoptotic death (114,115). However, knockdown of RKIP in these cells conferred them protection against radio-and chemo-induced apoptosis.

RKIP loss is also associated with poor overall survival in most of the cancers (99,101). For example, a prognostic relationship between RKIP expression levels in the primary tumor and disease free survival could be demonstrated in colorectal cancer (112).

1.3.2.2. RKIP in hematologic malignancies

Previous studies from our group demonstrated the presence of a complete or partial loss of RKIP expression as a somatic event in patients predisposed to tAML by oncogenic CRAF germline mutations (116,117). In these individuals, RKIP loss is a leukemia-specific hit, which contributes to leukemogenesis by potentiating the malignant transformation driven by CRAF. In a follow up study, we discovered RKIP loss as one of the most frequent molecular aberrations occurring in myeloid leukemias. In particular, RKIP status was studied in more than 400 AML patients and RKIP loss was observed in around 20% of these subjects (86). We then screened for the reasons behind RKIP loss in AML. Initially, we checked for promoter methylation, mutations and/or copy number deletions, but failed to detect any abnormalities. Subsequently, we correlated RKIP expression to the expression of more than 600 miRNAs, and detected, that RKIP loss correlated with an increased expression of miR-23a. Functional experiments showed that miR-23a binds to the 3´-UTR of RKIP and causes its downregulation, thereby proving that RKIP loss is indeed caused by increased expression of these miRNA (118). When we studied the functional consequences of RKIP loss in AML, we could show in different myeloid cell lines in-vitro, that RKIP overexpression was able to reduce the growth of hematopoietic cells, by decreasing their proliferation

rate. Moreover, this caused also a reduction of the oncogenic potential of AML cell lines, as assessed by decreased colony formation (86). These data suggest a tumor-suppressor role of RKIP in AML, which is in stark contrast to solid cancers, where the metastasis-suppressor role seems to predominate. Whether RKIP loss plays a role for the development of MS in AML, a process resembling the formation of metastases in solid tumors, is currently unknown.

In AML, we could also show an inverse correlation between RKIP expression and *RAS* mutations. Moreover, colony formation in cells harbouring *RAS* mutations could be significantly inhibited by concomitant overexpression of RKIP. While these in-vitro data suggest that *RAS* mutations and RKIP loss synergise in myeloid leukemogenesis, proper leukemia-specific in-vitro and in-vivo models, which ultimately prove this assumption are missing so far.

Finally, we observed in clinical samples of AML, that RKIP loss correlated with myelomonocytic and monocytic AML phenotypes. While it is known, that activation of the *RAS-MAPK/ERK* pathway and/or *RAS* mutations can cause increased myelomonocytic lineage commitment of HSPCs, a functional involvement of RKIP within this process has not been studied so far.

2. Hypothesis and aim of the thesis

RKIP is a well-known metastasis-suppressor in a variety of solid cancers. MS, a subtype of AML, is characterized by leukemic blasts that invade extra-hematopoietic tissues and form tumor masses. Due to the analogies between metastasis formation in solid tumors and MS development, we hypothesized, that a loss of RKIP promotes the tissue infiltration of leukemic blasts and thereby contributes to the development of MS. To test this hypothesis, we employed a series of in-vitro and in-vivo experiments and studied RKIP expression in AML cases with and without the presence of MS.

RKIP is also a negative regulator of the *RAS/MAPK-ERK* pathway. This signaling cascade regulates many important events in the cell, including HSPCs differentiation. Hence, we hypothesized that loss of RKIP could play a role in myelomonocytic differentiation in physiologic conditions. The regulation of *RAS/MAPK-ERK* pathway is important also in cancer. Deregulation of this pathway is known to lead to leukemogenesis. In particular, constitutive activation of this pathway leads to increased myelomonocytic differentiation, which is known to be a pre-phase step in the development of MNs. Since it was shown previously that RKIP loss plays a role in myeloid leukemogenesis and that it is associated with myelomonocytic AML phenotypes, we hypothesized that RKIP loss could play a role in the development of MNs. In particular, we focused on investigating a possible role of RKIP in CMML.

3. Materials and methods

The experiments in this study were performed as described in the following section and are also illustrated in Caraffini et al. (119,120).

3.1. Primary samples

3.1.1. Primary patient samples

AML patient samples were collected at the Division of Hematology, Medical University of Graz, Graz, Austria. The presence of MS was assessed either by biopsy or by clinical evaluation, as previously described (121,122). CMML patient specimens were collected at the Division of Hematology, Medical University of Graz, Graz, Austria as well as in the Austrian Biodatabase for CMML. AML, MS and CMML were classified according to the 2016 revision to the WHO classification of myeloid neoplasms and acute leukemia (3). Subsequently, primary patient specimens were processed as follows.

3.1.1.1. Preparation of peripheral blood and bone marrow patient samples by Ficoll density gradient centrifugation

Freshly obtained PB and BM specimens were subjected to Ficoll density gradient centrifugation. In more detail, PB from patients was diluted with the same volume of phosphate buffered saline (PBS), carefully layered over Lymphoprep solution (LymphoprepTM, STEMCELL Technologies) and centrifuged at 2500 r.p.m. for 20 min at room temperature. After centrifugation, mononuclear cells and/or granulocytes were collected from the corresponding layer.

BM was treated by filling up to 50 ml a Falcon tube with lysing buffer, waiting about five minutes in order to obtain lysis and extract BM cells. Afterwards, cells were centrifuged at 1200 r.p.m. for 5 min at room temperature and the procedure was repeated a second time for complete lysis. The supernatant was then discarded and cells were washed twice with PBS. After counting, all the cells were immediately cryopreserved at -192°C in pellets of 3-5x10^7 cells using a freezing media containing RPMI 1640 (Sigma), 20% dimethyl sulphoxide (WAK-Chemie) and 10% human albumin (Octapharma). Cytospins were routinely performed for all the samples and stained using May-Grünwald Giemsa staining. Only specimens with more than 80% blasts or myelomonocytic cells were included in this study. In more detail, cytospin slides were placed in a slide holder and then immersed in

May-Grünwald Eosin-Methylenblau (Merck Millipore) for four minutes. The slide holder was then submerged for one minute in distilled water and then placed in diluted Giemsa Azur Eosin-Methylenblau stain (1.8 ml May-Grünwald Eosin-Methylenblau, Merck Millipore, with 50 ml of Giemsa-Buffer) for 20 minutes. The slides were then washed using water, until the excess stain came off, and air-dried.

3.1.1.2. Preparation of MS and bone marrow specimens by FFPE

Biopsies were obtained from the MS site of the patients and placed into 10% formalin solution (Sigma) for at least 24 hours. The same procedure was performed for BM aspirates. After this time, the specimens were distributed into embedding cassettes, one for each cassette, and paraffin-embedded. First, the cassettes were placed into an automated tissue processor machines (Leica Biosystems), which embeds the organs using a multi-step procedure. In detail, the machine treats the samples with 70% ethanol (two changes, one hour each), 80% ethanol (one change, one hour), 90% ethanol (one change, one hour) and 100% ethanol (three changes, 90 minutes each). Specimens are then treated with xylene (three changes, 90 minutes each) and then with paraffin wax (two changes, two hours each). Then, the samples are paraffin-embedded using the Tissue Tek-TEC embedding system (Sakura). The formalin-fixed paraffin-embedded (FFPE) specimens were then used for immunohistochemical staining and RNA extraction. In more detail, sections of 4 µm were cut using a microtome and mounted on slides. A staining for RKIP detection was then performed on these sections. For RNA extraction, TRIzol (Thermo Fisher Scientific) was used.

3.1.2. Preparation of primary cells from healthy donors

Samples from cord blood of healthy donors were collected during normal full-term deliveries. $CD34^+$ HSPCs were obtained from these specimens using a magnetic selection kit (EasySep™ Human CD34 Positive Selection Kit, STEMCELL Technologies), following the manufacturer´s protocol, and were immediately frozen in aliquots of $1x10^6$ cells, as previously described (123). After thawing, $CD34^+$ cells were maintained for two days in X-VIVO media (Lonza) supplemented with 1% P/S and 1% GlutaMax (both Thermo Fischer Scientific) as well as with 50 ng/ml TPO, SCF and FLT3L, respectively. After this time, the cells were immediately used for transduction and differentiation experiments.

$CD14^+$ monocytes, B-lymphocytes as well as granulocytes were collected from the PB of healthy donors, which was collected in heparin-coated tubes and processed immediately. In more detail, $CD14^+$ monocytes and B-lymphocytes were collected using selection kits (MACS, Miltenyi Biotec, and human B Lymphocyte enrichment set, BD biosciences, respectively) according to the manufacturer's instructions. For granulocytes, a Ficoll gradient was performed as described above (section "*3.1.1.1. Preparation of peripheral blood and bone marrow patient samples by Ficoll density gradient centrifugation*"). After centrifugation, the granulocytes were collected from the corresponding layer and lysed (1X Pharm Lyse, BD Biosciences, diluted with distilled water) to remove the remaining erythrocytes.

3.1.3. Detection of RKIP levels

RKIP protein expression was studied in FFPE patient specimens of MS, as well as in the corresponding leukemic BM samples, and also in FFPE patient specimens of AML, via immunohistochemistry. In all the primary CMML patient samples, RKIP protein expression was investigated via immunoblot while *RKIP* mRNA expression was investigated via qPCR. Levels of RKIP expression in healthy donors were studied by qPCR. The material available was not sufficient to perform the study of both, mRNA and protein levels of RKIP. However, it was previously shown that lower levels of *RKIP* mRNA expression correspond to lower levels of RKIP protein (86,117–119).

3.1.3.1. Immunohistochemistry for RKIP

To detect RKIP protein expression in MS and AML patient samples, immunohistochemistry using an antibody against RKIP (Merck Millipore) as well as a previously described semi quantitative scoring system were used. This scoring system accounts for both the amount and intensity of positively stained cells and allowed us to divide the patient samples in two groups, "RKIP loss" and "RKIP normal" (124). In more detail, four grades were used to score the staining intensity ranging from 0, indicating complete absence of staining, to 4, for a strong staining, with 1 and 2 indicating weak and moderate staining, respectively. Again four grades were employed to score the extent of positively stained cells: 0 indicating a completely negative staining, 1 for <10%, 2 for 10% to 50%, and 3 for tumors with 50% or greater cells staining positive. To obtain the final scores, the extent was multiplied by the intensity. Samples with a final score <4 were considered as

negative, indicating RKIP loss, and specimens with a final score ≥4 were considered as positive, indicating normal RKIP levels.

3.1.3.2. Immunoblot

Ice-cold RIPA-Buffer (Sigma), supplemented with protease and phosphatase inhibitor cocktails (Sigma and Thermo Fisher Scientific), was added to the cell pellets from CMML patient samples, in order to obtain cell lysis. Protein concentration was measured using the DC Protein Assay kit (BIO-RAD) following the manufacturer's protocol. Laemmli sample buffer (BIO-RAD), supplemented with β-mercapto-ethanol (Sigma), was added to the lysates and these were boiled for five minutes at 95° C to obtain protein denaturation. Successively, Mini-PROTEAN TGX gels for electrophoresis (Bio-Rad) were employed for the immunoblot and the Bio-Rad Trans Blot TurboBlotting System was used for transfer, as previously described (86). Polyvinylidene difluoride membranes (Bio-Rad) were incubated with anti-RKIP (Merck Millipore), anti–β-actin (Sigma) and anti-Vinculin (Abcam). Table 1 lists the information about the antibodies used. A ChemiDoc imaging system (BIO-RAD) was used to detect the bands and ImageJ was employed to compare the intensity of the bands (125). For the immunoblots, loss of RKIP was defined as previously described for AML (86). In more detail, patients were defined with RKIP loss when the expression of RKIP, compared to a calibrator set to 100%, was below 25%. This is because AML cell lines with minimal or non-detectable RKIP presence demonstrated RKIP expression levels below 5%. However, as the patient samples employed could contain up to 20% of non-leukemic cells, loss of RKIP was arbitrarily defined as an RKIP expression <25% when compared to the calibrator. NB4 AML cells were used as a calibrator, as they have been shown to harbor a normal RKIP expression previously (86).

Primary antibody	Blocking solution	Dilution	Staining solution	Time, temperature	Secondary antibody
anti-RKIP	5% Milk	1:2000	TBST	1 hour, 4°C	anti-rabbit
anti–β-actin	5% Milk	1:1000	TBST	1 hour, 4°C	anti-mouse
anti-Vinculin	5% Milk	1:1000	TBST	1 hour, 4°C	anti-rabbit

Secondary antibody	Dilution	Staining solution	Time, temperature
anti-rabbit	1:10000	5% BSA / TBST	1 hour, 4°C
anti-mouse	1:10000	5% BSA / TBST	1 hour, 4°C

Table 1. Antibodies for RKIP immunoblot. Detailed information about the antibodies used to detect RKIP protein levels via immunoblot are displayed.

3.1.3.3. RNA extraction, reverse transcription and qPCR

RNA was isolated using TRIzol (Thermo Fisher Scientific) from the paraffin embedded MS samples and BM specimens, as well as from the primary CMML samples, according to the manufacturer's instructions. RNA isolation from hematopoietic cells of healthy donors and from umbilical cord blood was performed using the miRNAeasy Micro Kit (Qiagen), following the manufacturer´s instruction. cDNA synthesis was performed with TaqMan Reverse Transcription (RT) Reagents (Applied Biosystems) starting from 400 ng of total RNA and random hexamers were used for RT of mRNA. qPCR for RKIP mRNA expression analysis was performed on an Applied Biosystems 7500 Real-Time PCR System (Applied Biosystems) using the SYBR Green method (Invitrogen) and the conditions listed below (Table 2). *B2M* and *GAPDH* were chosen as control genes while NB4 AML cells served as calibrator and the expression levels were evaluated employing the comparative ddCT method as previously described (86).

RKIP	**Time**	**Temperature**	
DNA polymerase activation	10 min	95°C	
Denaturation	15 sec	95°C	40 cycles
Annealing	1 min	60°C	
Extension	1 min	60°C	
Storage	hold	4°C	

	Primer sequences	
Gene	**Primer forward**	**Primer reverse**
RKIP	CTACACCTTGGTCCTGACAGA	GAGCCCACATAATCGGAGAGG
B2M	GAGTATGCCTGCCGTGTG	AATCCAAATGCGGCATCT
GAPDH	CAACAGCGACACCCACTCCT	CACCCTGTTGCTGTAGCCAAA

Table 2. Thermocycler steps for RKIP qPCR and relative primers.

3.1.4. Next-Generation Sequencing

NGS was performed on FFPE MS samples as well as CMML patient samples using an Ion Torrent Sequencing platform, as described previously (42,119,126,127). The NGS analysis comprised 39 genes recurrently mutated in myeloid neoplasms: *CEBPA* (full coding); *NPM1* (Exon 11); *FLT3* (Exon 14-

16,20,21); *ASXL1* (Exon 12); *BCOR* (full coding); *BRAF* (Hotspot Exon 15); *CALR* (Exon 9); *CBL* (Exon 8,9); *CSF3R* (Exon 14-17); *DDX41* (full coding); *DNMT3a* (full coding); *ETNK1* (Exon 3); *ETV6* (full coding); *EZH2* (Exon 16-19); *GATA2* (full coding); *IDH1* (Exon 4); *IDH2* (Exon 4); *JAK2* (Exon 13); *KIT* (Exons 8,10,11,17); *KRAS* (Exon 2,3); *MPL* (Exon 10); *NF1* (full coding); *NRAS* (Exon 2,3); *PHF6* (full coding); *PTPN11* (Exon 3,13); *RUNX1* (Exon 3-8); *SETBP1* (Hotspot Exon 4); *SF3B1* (Exon 14-16); *SF3B2* (full coding); *SFRP1* (full coding); *SRP72* (full coding); *SRSF2* (Hotspot Exon 1); *STAG2* (full coding); *STAT3* (Exon 20,21); *TET2* (Exon 3-11); *TP53* (full coding); *U2AF1* (Exon 2,7,9); *WT1* (Exon 7,9); *ZRSR2* (full coding). Mutation calling necessitated coverage of at least 1000x, a frequency in the 1000-genome project of <0.01% and a variant allele frequency (VAF) >10%.

3.1.4.1. Verification of RAS-mutations by Pyrosequencing

For MS samples, verification of the *RAS*-mutations obtained by NGS was performed by pyrosequencing, using the Therascreen RAS kits (Qiagen, Hilden, Germany) following the manufacturer´s instructions. In detail, DNA (20ng) was isolated from the MS FFPE samples and amplified using primer sets specific for the gene locus where NGS detected a mutation. Pyrosequencing was performed using luciferin reaction, after binding the PCR products to sepharose beads and immobilizing them on the pyrosequencing stamps. The Therascreen RAS RGQ software was used to capture and visualize the light traces and calculating the area under the respective peaks allowed to determine the mutant allele frequencies.

3.1.5. Database retrieval

The Gene Expression Omnibus (https://www.ncbi.nlm.nih.gov/geo/) was employed to download microarray expression data for *RKIP* expression in different murine hematopoietic cell compartments. Accession numbers: GSE27787 (128), GSE5677 (129), GSE27816 (130) and GSE20377 (131).

3.1.6. Transduction and in-vitro differentiation of human HSPCs

The effects of RKIP expression on myelomonocytic differentiation of healthy $CD34^+$ HSPCs were assessed in this experiment. Therefore, 293T packaging cells were transfected using CalPhos Mammalian Transfection Kit (Clontech) following the manufacturer's instructions. For RKIP knockdown, human $CD34^+$ HSPCs were

collected from six healthy donors and were lentivirally transduced with either RKIP shRNA or empty control (both psi-LVRU6GP; Genecopeia), respectively, both GFP-tagged. After transduction, knockdown of RKIP, as well as activation of the *RAS-MAPK/ERK* pathway, was assessed by immunoblot, as described above (section "3*.1.3.2. Immunoblot*"). In detail, membranes were incubated with anti-RKIP (Merck Millipore) and anti-Vinculin (Abcam) to check RKIP knockdown and with anti-ERK (Sigma) and anti-pERK (Cell Signaling) antibodies to assess *RAS*-pathway activation. The transduced cells were then treated with a mix of cytokines to induce differentiation. In particular, DC media (CellGenix) supplemented with GM-CSF, FLT3L, SCF and TNFa was used (132). After five days, cells were then used for flow cytometric analysis.

3.1.6.1. Flow cytometry

For flow cytometric analyses, LSRII and FACSCalibur machines (both BD Biosciences) were employed, $5x10^5$ events were recorded and data were analyzed using Kaluza software (Beckman Coulter). To assess differentiation of $CD34^+$ cells, with and without RKIP knockdown, the cells were stained using 1 µl CD11b-PECy7 (Biolegend), 1 µl CD14-PE (Thermo Fisher eBioscience) and 7-AAD. Briefly, cells were stained with the selected antibody panel for 15 minutes in the dark. Cells were then washed with PBS and centrifuged at 1500 r.p.m. for five minutes. After removing the supernatant, cells were resuspended in 150 µl PBS and 5 µl 7-AAD were added to the cell suspension. Only 7-AAD-negative cells were included in the analysis. First, a gate on GFP^+ cells was performed, then, the expression of the myelomonocytic surface markers CD11b and CD14 in the GFP^+ cells was assessed.

3.2. Cell lines

3.2.1. Cell lines and culture conditions

The cell lines used for all the experiments were obtained from the German National Resource Center for Biological Material (DSMZ, Braunschweig, Germany). Cells were maintained at 37°C/5% CO2 in DMEM for 293T HEK cells and RPMI-1640 for NB4, HL-60, THP-1 and U937, respectively. The medium was enriched with 10% heat-inactivated fetal bovine serum (FBS) (Thermo Fischer Scientific) and 1X Antibiotic-Antimycotic (Thermo Fischer Scientific, including 100U/ml penicillin, 100 mg/ml streptomycin and 0.25 mg/ml amphotericin B).

DMEM medium was further supplemented with 1X GlutaMAX (Thermo Fischer Scientific). Cells were always passaged for less than six months after resuscitation. Low passage stocks were frozen and were regularly screened by variable number of tandem repeat profiling (VNTR) for authenticity as previously described (118).

3.2.2. Transfection and transduction

293T packaging cells were transfected using CalPhos Mammalian Transfection Kit (Clontech) following the manufacturer's instructions. For RKIP knockdown, HL-60, THP-1 and U937 cells were lentivirally transduced with either RKIP shRNA or empty control (both psi-LVRU6GP; Genecopeia), respectively. Selection of stable clones for THP-1 and U937 cells was performed by adding to the media 1.5 µg/ml puromycin (Invitrogen), while 0.5 µg/ml puromycin were used for HL-60 cells. HL-60 cells used for differentiation experiments were transduced with siRNA (Qiagen) to express a transient RKIP knockdown. For RKIP overexpression, HL-60 were transduced with eGFP-C1-6xG-hRKIP or empty vector as previously described (86) while THP-1 and U937 cells with stable overexpression of pMSCV-FLAG-hRKIP or empty vector were established previously (86) and cultured with the addition of 0.3 µg/ml puromycin. Immunoblot, as described above (section "*3.1.3.2. Immunoblot*"), was used to verify the successful knockdown as well as overexpression of RKIP in all the cell lines after transduction. In particular, membranes were incubated using anti-RKIP (Merck Millipore), anti-GFP-RKIP (Cell Signaling), anti-FLAG (Sigma), anti–β-actin (Sigma) and anti-Vinculin (Abcam) antibodies. In order to study the activation of the *RAS*-MAPK/ERK pathway in transduced HL-60 cells, membranes were incubated using anti-ERK (Sigma) and anti-pERK (Cell Signaling) antibodies. The details regarding all the antibodies used are listed in Table 3.

Primary antibody	Blocking solution	Dilution	Staining solution	Time, temperature	Secondary antibody
anti-RKIP	5% Milk	1:2000	TBST	1 hour, 4°C	anti-rabbit
anti-GFP-RKIP	5% BSA	1:1000	5% BSA	overnight, 4°C	anti-rabbit
anti-FLAG	5% BSA	1:500	5% BSA	overnight, 4°C	NA
anti–β-actin	5% Milk	1:1000	TBST	1 hour, 4°C	anti-mouse
anti-Vinculin	5% Milk	1:1000	TBST	1 hour, 4°C	anti-rabbit
anti-ERK	5% BSA	1:1000	5% BSA	overnight, 4°C	anti-rabbit
anti-pERK	5% BSA	1:1000	5% BSA	overnight, 4°C	anti-rabbit

Secondary antibody	Dilution	Staining solution	Time, temperature
anti-rabbit	1:10000	5% BSA / TBST	1 hour, 4°C
anti-mouse	1:10000	5% BSA / TBST	1 hour, 4°C

Table 3. Antibodies for immunoblot. Detailed information about the antibodies used to detect RKIP protein levels as well as ERK and pERK via immunoblot are displayed.

3.2.3. Migration and invasion assays

These experiments were performed to assess the migration and invasion potential of myeloid cell lines after the modulation of RKIP expression. Migration experiments were performed using Transwell inserts having PET membranes with 3 µm pores (Corning). Using a twenty-four-well plate, one insert was placed into each well and the membrane was equilibrated by adding serum-free RPMI-1640 to the upper and lower compartment. After one hour at 37°C/5% CO2, 150 µl of serum-free RPMI-1640 were added to the upper compartment of the Transwell, while 600 µl of RPMI-1640 containing 10% FBS were placed in the lower compartment, functioning as chemoattractant. The stably transduced THP-1 and U937 cells were added to the upper chamber at a concentration of $1x10^6$ cells/ml and were allowed to migrate for 24 hours for RKIP overexpression and control, or 48 hours for RKIP downregulation and control. After the incubation time, cells that did not migrate through the PET membrane were removed by discarding the cell suspension in the upper compartment as well as by gently scrubbing the upper side of the membrane with a cotton swab. Subsequently, the membranes were fixed using Methanol, stained in Giemsa staining and then screened using an inverted microscope to count the cells that migrated. All the experiments were performed in triplicates and repeated at least three times.

THP-1 cells with and without RKIP knockdown were also used in migration experiments with the addition of 10µM of the MEK-inhibitor U0126 (Promega) or DMSO, respectively.

The same protocol used for the migration assay was employed for the invasion experiments, however, with few differences. In particular, Matrigel Invasion Chambers with 8 µm pores (Corning) were used as inserts and the membranes were equilibrated at 37°C/5% CO2 for 24 hours using serum-free RPMI-1640. Cells were then incubated for 24 hours to allow invasion.

3.2.4. mRNA microarray

These experiments were performed to assess, whether RKIP knockdown in myeloid cell lines causes a specific gene expression profile. Therefore, miRNeasy mini Kit (Qiagen), including DNAse treatment, was used to isolate 250 ng of total RNA from THP-1 cells with and without RKIP knockdown, following the manufacturer's instructions. The quality of RNA was checked using a Bioanalyzer BA2100 (Agilent; Foster City, CA) and only samples with a RNA integrity number (RIN) >8 were used for the analysis. Affymetrix Human Gene 2.0 ST mRNA Arrays (Affymetrix; Santa Clara, CA) was employed for whole transcriptome analysis, while for evaluation of the hybridization controls and pre-analysis Affymetrix Expression Console EC 1.3.1 was used, both according to the manufacturer's instructions. Data normalization and analysis were performed using Partek Genomic Suite v6.6 software (Partek Inc; St Louis, MO), as previously described (133). All microarray gene expression data have been deposited in the National Center for Biotechnology Information (NCBI)'s Gene Expression Omnibus (GEO) and are accessible through GEO accession number GSE103344.

3.2.5. In-vitro differentiation assay

In these experiments, we aimed to analyze, whether a modulation of RKIP expression in the immature HL-60 AML cell line has an effect on the myelomonocytic differentiation capacity of these cells. HL-60 cells were treated for 48 hours with 1,25-Dihydroxyvitamin D_3 ($1,25D_3$; Sigma) at a concentration of 100 nM, in order to measure the effects of $1,25D_3$-induced myelomonocytic differentiation on RKIP expression levels. To study the results of RKIP modulation on $1,25D_3$-induced differentiation, HL-60 cells were first transduced with RKIP downregulation and overexpression constructs, as described above (section "*3.2.2. Transfection and transduction*"). After 24 hours, the cells were treated with 10nM $1,25D_3$ and, after 48 hours, were screened by flow cytometry for the expression of CD11c. Flow cytometric analysis was performed as described above (section "3*.1.6.1. Flow cytometry*") using 1 µl of PE-CD11c (Beckman Coulter) and 7-AAD (BD Pharmingen) antibodies.

3.3. Animal models and in-vivo experiments

3.3.1. Ex-ovo CAM assay

The chorioallantoic membrane (CAM) assay was employed to test the effects of RKIP knockdown on the invasion and migration potential of myeloid cells in-vivo. Fertilized eggs of white Lohmann chicken from a local commercial hatchery were incubated at 37.6°C and 70% humidity (J. Hemel Breeding Machines, Germany) as previously described (134). After three days, the eggs were opened and the embryo was deposited in a sterile dish, covered with a lid and incubated for other seven days. After this time, $2x10^6$ THP-1 stable clones, either with or without knockdown of RKIP, were resuspended in 10 µl PBS and 10 µl growth factor reduced Matrigel (Corning). This mix was pipetted onto a petri dish covered with Parafilm and incubated at 37°C/5% CO2 for 45 minutes, until polymerization. Subsequently, these cell onplants were deposited on vascular branches of the CAM, into plastic rings, four for each embryo (Figure 1A-B). After seven days of incubation, the onplants as well as the surrounding CAM were excised, photographed (Figure 1C-D) and then fixed with 4% paraformaldehyde overnight. These samples were then embedded using paraffin and a microtome was employed to cut 5-µm-thick sections of the specimens, cutting sections of the whole onplant, which were subsequently stained with hematoxylin and eosin (H&E) staining. ImageJ (NIH, USA) was used for measuring the area of invading cells and/or solid tumors formed.

3.3.1.1. Hematoxylin and eosin staining

The slides were deposited in a 65°C incubator for 30 minutes to soak paraffin, which was then removed doing three washings with xylene, two minutes each. The samples were then hydrated using sequentially 100%, 96%, 70% and 50% ethanol (Merck-Millipore; diluted with distilled water) and leaving the slides into each solution for two minutes. Slides were rinsed with distilled water for two minutes. Samples were stained in hematoxylin solution (Sigma) for one minute and then washed with running hot tap water for two to three minutes. Eosin solution was then used to stain the slides for two minutes, which were then shortly washed with distilled water. As a last step, the specimens were dehydrated placing the slides into 50%, 70%, 96% and 100% ethanol, respectively, for two minutes each, and then placed into xylene for two minutes. In the end, a drop of Entellan mounting

solution (Merck-Millipore) was dispensed over the tissue and a coverslip was added.

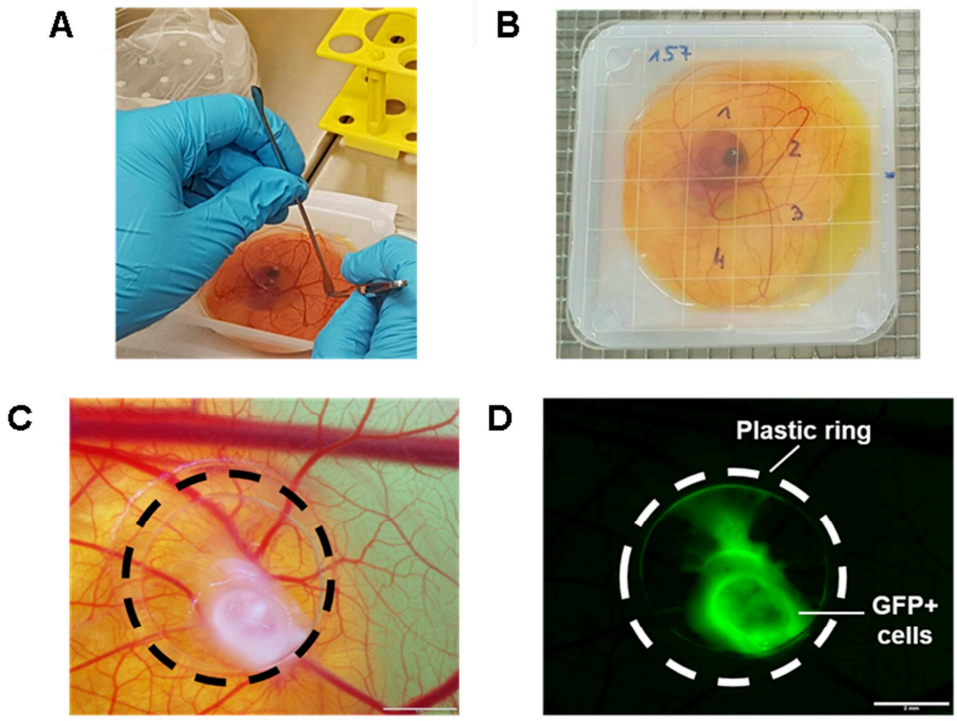

Figure 1. Ex-ovo CAM assay. (A-B) Cells were mixed with a Matrigel solution in order to polymerize and form onplants. Four plastic rings were placed on the CAM of each chicken embryo and the cellular onplants were carefully deposited into those. After seven days of incubation, the onplants were imaged (C), also using a fluorescence microscope (D), since the stably transduced THP-1 cells are GFP^+.

3.3.2. Mouse models, maintenance and genotyping

All the experiments involving mice were performed on a C57BL/6 strain background. Within this thesis, we used mice with a complete knockout of *Rkip*, as well as mice with an inducible mutation in *Nras* (see below for details). Mice were maintained in a specific pathogen-free environment, in the animal facility of the Medical University of Graz, in order to prevent the occurrence of infections. Two weeks after birth, all the mice pups were subjected to genotyping, in order to identify the genotype of the animals. For this purpose, either ear punches or tail tips from the mice were used, DNA was extracted from them and a PCR was

performed. For validation, the animals used in this project were subjected to repeated genotyping before carrying out any experiment. All experimental mice were assessed for their health status daily and, out of ethical reasons, mice were sacrificed by cervical dislocation after isofluorane anesthesia when they show signs of disease as previously described (disheveled appearance, hunching, abnormal gait, and pallor).

3.3.2.1. Mouse model with Rkip knockout

Mice with a complete deletion of the *Rkip* gene, hereby referred to as *Rkip*-/- mice, were provided by Professor John Sedivy (Brown University, RI, USA), together with control mice (in the text referred to as *Rkip*+/+ mice). *Rkip-/-* mice harbor a germline knockout of the RKIP gene and were developed using the gene/trap technology (135).

In order to test the complete deletion of *Rkip* gene in these mice, cells from BM and spleen (SP) were taken from 4-week-old *Rkip*-/- mice, as well as from control mice, and subjected to immunoblot (Figure 2). Immunoblot was performed as described previously (section "*3.1.3.2. Immunoblot*"), employing anti-RKIP (Merck Millipore) and anti–β-actin (Sigma) antibodies. *Rkip*+/+ mice served as a control to determine the successful knockdown of RKIP in the *Rkip*-/- mouse model.

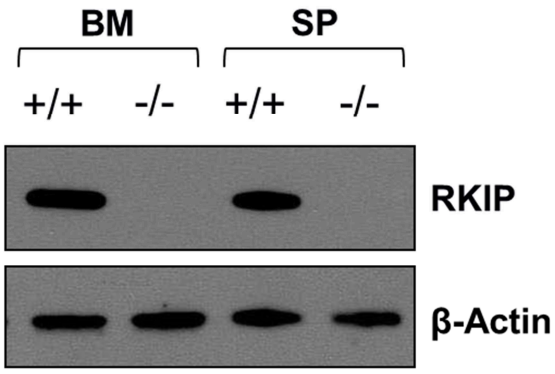

Figure 2. Immunoblot of *Rkip* mice. Immunoblot showing the complete deletion of Rkip in BM and SP of *Rkip-/-* mice. The figure is adapted from (120) with permission of *Haematologica*.

3.3.2.2. Nras-mutated murine model

In order to study the effects of *Rkip* loss in combination with *Ras* mutations in mice, we crossed our mouse model with *Rkip* deletion with a murine model harboring an inducible $Nras^{G12D}$ mutation. $Nras^{G12D}$ mice exhibit a G12D activating mutation in exon 2 of *Nras*, which is not transcribed since a loxP-flanked stop element is present in exon 1. LoxP sites can be recognized and excised by Cre-recombinase, which can be activated by interferon and polyinosinic polycytidilic acid (pIpC), respectively. By linking the Cre-recombinase with an Mx1-promoter, strong expression of Cre within the hematopoietic system can be achieved. Ultimately, *Mx1-Cre* and $Nras^{G12D}$ mice were bred together, which enables a pIpC induced activation of $Nras^{G12D}$ within the hematopoietic system. *Mx1-Cre* mice were supplied by Dr. Karen Blyth (Cancer Research UK Beatson Institute, Glasgow, UK) while *Nras-LSL*^{G12D} mice were purchased from The Jackson Laboratory (Bar Harbor, ME, USA; JAX stock #008304; hereafter referred to as *Nras*) (136).

3.3.2.3. Breeding strategy

Rkip-/- mice were crossed between themselves to maintain this strain, in order to avoid a heterozygous condition for *Rkip*.

Mx1-Cre and *Nras* animals were kept in a heterozygous situation. In order to obtain mice harboring *Mx1-Cre* as well as the $Nras^{G12D}$ mutation, in both the conditions with *Rkip* deletion (hereby referred as *Mx1-Cre/Nras/Rkip-/-*) and *Rkip* normal (thereafter referred as *Mx1-Cre/Nras/Rkip+/+*), as well as the control mice with $Nras^{G12D}$ mutation but lacking *Mx1-Cre* (hereby referred to as *Nras/Rkip+/+*), the breeding strategy depicted in Figure 3 was used.

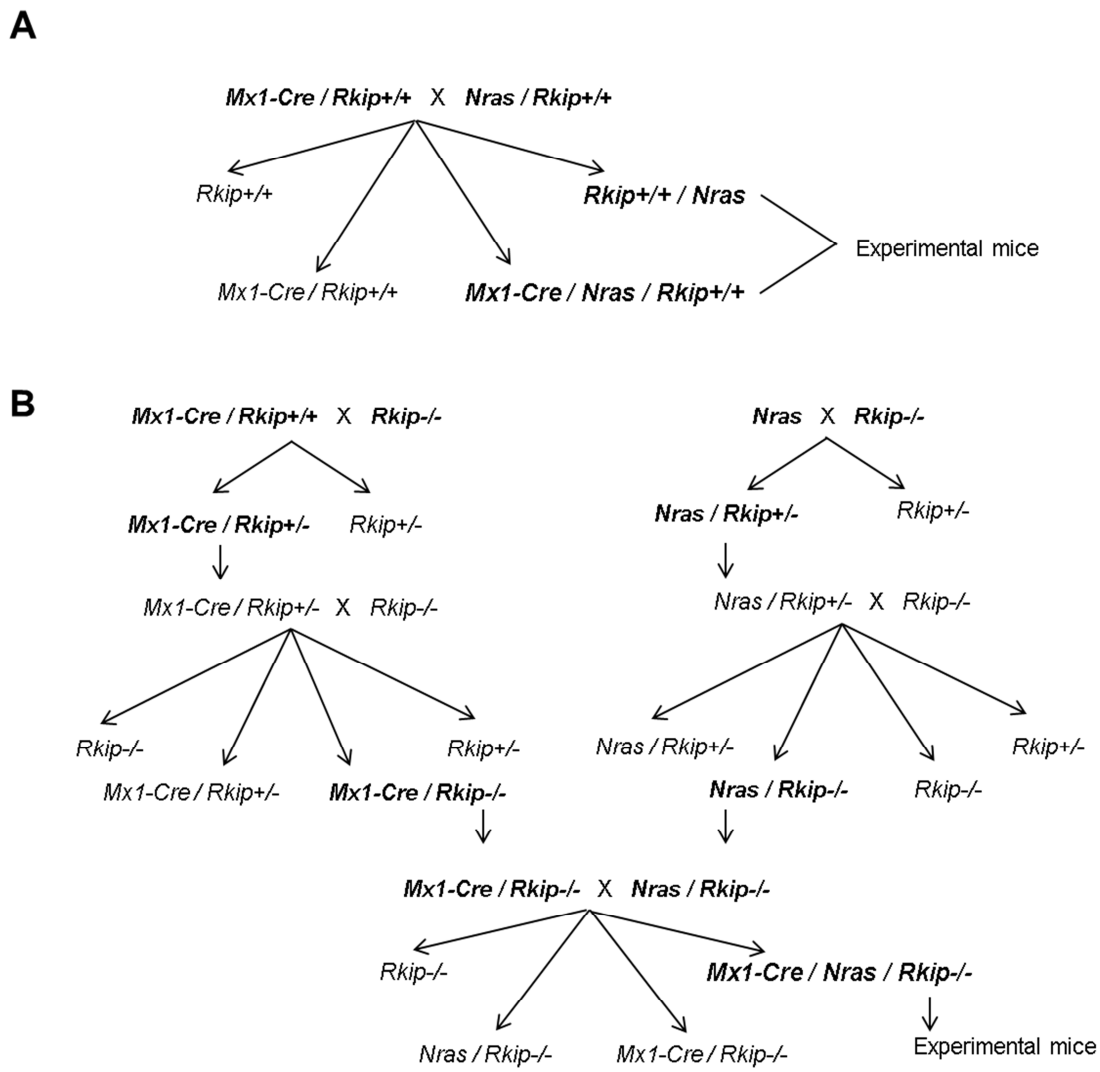

Figure 3. Breeding strategy used to obtain the *Nras*-mutated mice used in this project. (A) Breeding strategy for *Mx1-Cre/Nras/Rkip+/+* and *Nras/Rkip+/+* mice. (B) Breeding procedure for *Mx1-Cre/Nras/Rkip-/-* mice. "*Mx1-Cre*" indicates the presence of heterozygous Mx1-Cre. "*Nras"* indicates the presence of a heterozygous G12D mutation with a stop codon flanked by LoxP sites; wherever *Nras* presence is not indicated, the mouse is wild type for *Nras*.

3.3.2.4. pIpC injections

In order to obtain activation of the *Nras* mutation, *Mx1-Cre/Nras/Rkip-/-* and *Mx1-Cre/Nras/Rkip+/+* mice received intraperitoneal injections of pIpC (Sigma), 250µg/d every alternate day for three times, starting at an age of around 30 days.

3.3.2.5. Genotyping

DNA was extracted from the ear punches or tail tips of the mice using the KAPA Express Extraction Kit (KAPA Biosystems), following the manufacturer's instructions. The extracted DNA was then amplified using PCR. For *Rkip* and *Nras*-mutated mice, HotStarTaq DNA Polymerase kit (Qiagen) was used, while for *Mx1-Cre* mice the GoTaq G2 Hot Start Green Master Mix (Promega) was employed. The program used for this amplification and the different primers used for this reaction are present in Table 4. The PCR products, together with a 100bp GeneRuler DNA ladder (Thermo Fischer) were subsequently loaded onto a 2% agarose (Biozym ME Agarose) gel supplemented with 8µL GelRed Nucleic Acid Stain (Biotium). The DNA was electrophoretically separated for 40min at constant 120V and the gel was then imaged using ChemiDoc imaging system (BIO-RAD; Figure 4).

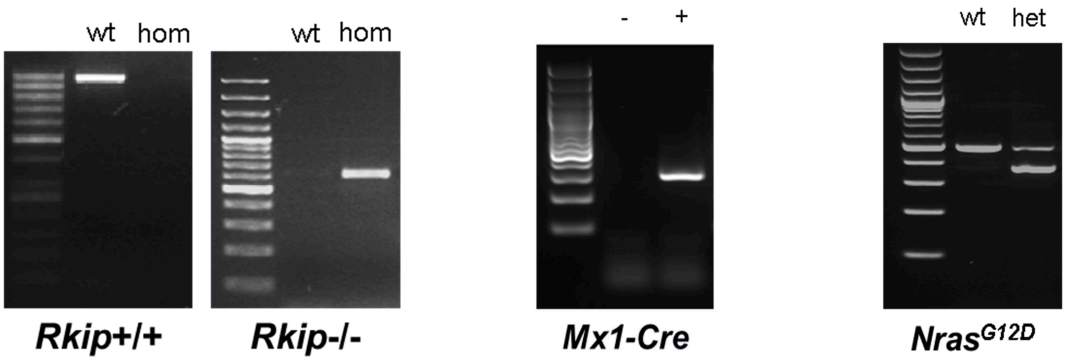

Figure 4. Genotyping results. Representative PCR-gels from genotyping for *Rkip* wild type (*Rkip+/+,* "wt") and *Rkip* deleted (*Rkip-/-,* "hom") mice, *Mx1-Cre* present (-) or absent (+) and *Nras* wild type (wt) as well as *Nras* mice with G12D mutation present in a heterozygous condition ("het"). The figure is adapted from (120) with permission of *Haematologica*.

Thermocycler steps for *Mx1-Cre* PCR			
Step	**Time**	**Temperature**	
Initial denaturation	3 min	95°C	
Denaturation	40 sec	95°C	30 cycles
Annealing	40 sec	62°C	
Extension	40 sec	72°C	
Final extension	10 min	72°C	
Storage	hold	4°C	

Thermocycler steps for *Rkip* PCR			
Rkip	**Time**	**Temperature**	
Initial denaturation	15min	95°C	
Denaturation	1min	94°C	40 cycles
Annealing	1min	68.5°C	
Extension	1min	72°C	
Final extension	10min	72°C	
Storage	hold	4°C	

Thermocycler steps for *Nras* PCR			
Step	**Time**	**Temperature**	
Initial denaturation	15min	95°C	
Denaturation	30sec	94°C	35 cycles
Annealing	1min	69.1°C	
Extension	1min	72°C	
Final extension	10min	72°C	
Storage	hold	4°C	

	Primer sequences		
Gene	**Primer forward**	**Primer reverse**	**Primer mutant**
Mx1-Cre	TCCCCGCAGAACCTGAAGATGTTCG	GCCAGATTACGTATATCCTGGCAGC	
Rkip	GAGCCCTGGCCGGTCTCCCTTGTCCCAAACTTT	CCAAAAGGGTCTTTGAGCACCAGAGGACATCCG	AGACTTCCGTGTCCGGATGATAGATAGCCTCTCC
Nras	AGACGCGGAGACTTGGCGAGC	GCTGGATCGTCAAGGCGCTTTTCC	AGCTAGCCACCATGGCTTGAGTAAGTCTGCA

Table 4. Protocol and primers for PCR for genotyping. Thermocycler steps for *Mx1-Cre*, *Rkip* and *Nras* PCR. Below, the primers used for amplification are listed

3.3.2.6. Sacrificing

For all the experiments that required terminal procedures, mice were anaesthetized using 4% isofluorane (AbbVie) mixed with O_2 (1.5 l/min) and subsequently sacrificed by cervical dislocation.

3.3.3. Analysis of the *Rkip-/-* mouse model

Rkip-/- and *Rkip+/+* animals were electively sacrificed at an age of 3, 6, 9 and 12 months. The PB and BM of these mice were investigated in order to find possible differences in the composition of the PB and in the hematopoietic progenitor compartments in the BM between mice with *Rkip* deletion and control littermates. Flow cytometric analysis was performed as described above (section "3*.1.6.1. Flow cytometry*"). For flow cytometry of PB samples, 20 µl of blood were stained using a myeloid panel comprising 7-AAD, 1 µl FITC-CD11b and 2 µl PE-CD115 (all eBioscience) as well as a lymphoid panel comprising 7-AAD, 1 µl FITC-CD3e, 1 µl PE-Cy7-CD49b (all eBioscience) and 1 µl PE-CD45R/B220 (BD Pharmingen). Cells were then resuspended in 150 µl diluted Pharm Lyse (1X Pharm Lyse, BD Biosciences, diluted with distilled water) to obtain lysis of red blood cells. For flow

cytometric analysis of BM, $2x10^6$ cells were stained with Biotin mouse lineage panel (BD Pharmingen), 1 µl PE-Cy7 Sca-1, 2 µl PE-CD115, 1 µl PE-Cy5-CD135, 3 µl APC-CD117, 1 µl efluor-CD16/32, 1 µl efluor-CD34 (all eBioscience) and 7-AAD (BD Pharmingen) were used to analyze hematopoietic progenitor cell compartments. Cells were resuspended in 150 µl PBS and strained to avoid clumps. In both cases, before measurement, 5 µl of 7-AAD (BD Biosciences) were added to the cell suspension.

3.3.3.1. Preparation of blood

Blood was collected from the living mice from the submandibular vein or, from mice selected for sacrifice, from cardiac puncture. Blood was collected into microvet EDTA tubes (BD Biosciences) and used for complete cell counts (V-sight, Menarini diagnostics), PB smears stained with May-Grünwald Giemsa staining and flow cytometry. For PB smears, 4 µl of blood were smeared onto a slide and air-dried. Then, May-Grünwald Giemsa staining was performed, as indicated above (section "3*.1.1.1. Preparation of peripheral blood and bone marrow patient samples by Ficoll density gradient centrifugation*").

3.3.3.2. Preparation of bone marrow

After sacrifice of the mice, the hind limbs, sternum, hips and spine were collected and cleaned from muscle tissue using sterile wipes and surgical scissors. All the bones were transferred into 1x HBSS (Thermo Fischer) and kept on ice. Subsequently, the bones were thoroughly cleaned under a tissue culture hood and placed in a sterile mortar. HBSS (Gibco), supplemented with 10% FBS (Thermo Fischer Scientific) and 1X Antibiotic-Antimycotic (Thermo Fischer Scientific), was added, the bones were crushed and filtered using a 70 µm cell strainer into a Falcon tube. The tube was then centrifuged at 1500 r.p.m. for five minutes, the supernatant was removed and the cell pellet was resuspended with 1 ml 1X PharmLyse (BD Bioscience; diluted 1:10 with distilled water) to lyse the erythrocytes, incubated at room temperature for two minutes and then centrifuged as previously done. The cell pellet was then resuspended in 1ml complete HBSS and cells were counted using a Casy cell counter (Innovatis) and used for flow cytometric analysis.

3.3.3.3. Differentiation experiment

Two-month-old mice, both *Rkip-/-* and *Rkip+/+*, were used for in-vitro differentiation experiments, four mice for each genotype. 500ng of GM-CSF (Peprotech), diluted in distilled water, were injected intraperitoneally for four days, twice a day, and mice were analyzed on day five. PB and BM were treated as described above (sections "*3.3.3.1. Preparation of blood*" and "*3.3.3.2. Preparation of bone marrow*") and, additionally, PBS was used to perform a peritoneal cavity lavage in order to collect the cells from this area. To check the differentiation in these cells, flow cytometry was performed as described above (section "*3.1.6.1. Flow cytometry*") for BM and PB cells. Regarding the peritoneal cavity cells, all the cells obtained from the lavage were used for flow cytometry. Cells were stained using 1 µl efluor-CD11b (eBiosciences), 1 µl PE-Cy7-Ly6G (eBiosciences), 3 µl APC-CD117 (eBiosciences) and 7-AAD (BD Pharmingen) antibodies. Cell were resuspended in 150 µl PBS additioned with 5 µl 7-AAD (BD Biosciences), for BM and peritoneal cavity cells, or first lysed as described above, for PB cells.

3.3.3.4. Preparation of peritoneal cavity cells

After sacrifice, 5 ml of sterile PBS were injected into the peritoneal cavity of the mice using a syringe. The injected area was massaged to allow the detachment of the cells and the liquid was collected into a Falcon tube. This tube was centrifuged at 1500 r.p.m. for five minutes, the supernatant was removed and a wash with PBS was performed. All the cells were subsequently used for flow cytometric analysis.

3.3.4. Analysis of *Nras*-mutated mice at 180 days after pIpC

Mx1-Cre/Nras/Rkip-/- and *Mx1-Cre/Nras/Rkip+/+* mice were sacrificed at day 180 after the first pIpC injection and *Nras/Rkip+/+* mice were sacrificed at the same age. PB and BM were collected and treated as described before (sections "*3.3.3.1. Preparation of blood*" and "*3.3.3.2. Preparation of bone marrow*"), together with the SP. All these organs were used for flow cytometric analysis, as described above (section "*3.1.6.1. Flow cytometry*") for BM and PB. Regarding the SP, $2x10^6$ cells were used for flow cytometric analysis. Cells were stained using 1 µl efluor-CD11b (eBiosciences), 1 µl PE-Cy7-Ly6G (eBiosciences), 3 µl APC-CD117 (eBiosciences) and 7-AAD (BD Pharmingen) antibodies. BM and SP cells were then resuspended in 150 µl PBS supplemented with 5 µl 7-AAD (BD Biosciences)

and filtered, while PB cells were first lysed, as described above. Moreover, a portion of the SP and the liver were collected in 10% formalin solution (Sigma), subsequently embedded in paraffin, cut in 3-4 µm thick section and subjected to H&E staining, performed as described above (section "*3.3.1.1. Hematoxylin and eosin staining*").

3.3.4.1. Preparation of spleen

The SP was collected after sacrifice of the mice, weighted and measured. After removing one part for paraffin embedding, the remaining SP was transferred into 1x HBSS (Thermo Fischer) and kept on ice. The SP was then mashed and filtered through a 70 µM cell strainer into a Falcon tube, using HBSS (Gibco), supplemented with 10% FBS (Thermo Fischer Scientific) and 1X Antibiotic-Antimycotic (Thermo Fischer Scientific). The tube was then centrifuged at 1500 r.p.m. for five minutes, the supernatant was removed and the cell pellet was resuspended with 1ml complete HBSS. Cells were counted with a Casy cell counter and used for flow cytometry.

3.3.5. Analysis of moribund Nras mice

Mx1-Cre/Nras/Rkip-/- and *Mx1-Cre/Nras/Rkip+/+* mice were constantly observed for signs of disease and taken for experiments when moribund. After the sacrifice, BM, SP, liver, thymus and lymph nodes, as well as tumors and/or other abnormal organs, were collected in formalin and successively embedded in paraffin.

3.3.5.1. Immunohistochemistry for moribund mice

For immunohistochemical analysis of *Mx1-Cre/Nras/Rkip-/-* and *Mx1-Cre/Nras/Rkip+/+* moribund mice, H&E staining was performed on sections from SP, liver, BM (from the sternum, obtained after decalcification), thymus and lymph nodes, as described above in more detail (section "*3.3.1.1. Hematoxylin and eosin staining*"). A grading system was then used to define the presence and the intensity of myeloproliferative disease (MPD), myeloproliferation (MP) and histiocytic sarcoma (HS). In more detail, MPD was defined as either present (+) or absent (-), as defined previously (137). For grading the extension of MP, a slightly adapted scoring system from Lacroix-Triki et al. (138) was used. This considered the average amount of hematopoietic foci per one 100x field in the liver and SP and the results were scored as follows: 0 = absent, + = 1-2 hematopoietic foci, ++ = 3-4 hematopoietic foci and +++ = >4 hematopoietic foci. For HS, we employed a

scoring system that includes both, the number of organs infiltrated and the amount of organ infiltration. As there was no previously established protocol, we routinely analysed BM, SP, liver, lymph nodes and the thymus for the presence of HS (as defined by the Bethesda classification of nonlymphoid hematopoietic neoplasms in mice) (137). Since infiltration of the organs was either very low or very high in all samples studied, we arbitrarily defined as extensive infiltration of an organ the condition in which more than 50% HS infiltration was present. This cut-off was then lowered to >30% when considering the liver, due to a generally lower infiltration rate. Successively, the extension of HS was defined as follows: 0 = no HS in any of the organs, "+" = HS present, but extensive organ infiltration in <3 of the 5 organs studied; "++" = extensive organ infiltration in ≥3 of the 5 organs studied.

3.3.5.2. Survival analysis

Mice conditions were checked twice a day and the death of every mouse, both when happened in cage or by sacrificing due to the conditions of the mice, was annotated. Survival analysis included groups of at least eleven mice.

3.3.6. *Ras*-pathway activation

$CD11b^+$ cells were isolated from the BM of *Rkip-/-* and *Mx1-Cre/Nras/Rkip-/-* mice, as well as from their controls, in order to analyze the activation of the *RAS-MAPK/ERK* signaling pathway. BM cells were obtained as described above (section "*3.3.3.2. Preparation of bone marrow*") using HBSS without the addition of FBS at every isolation step. Cells were then counted using a Casy cell counter and used for subsequent isolation of $CD11b^+$ cells. $CD11b^+$ cells were then used for immunoblot analysis, in order to check the activation of the *RAS*-pathway. For this reason, an immunoblot was performed as described above (section "*3.1.3.2. Immunoblot*"), blotting the membranes with anti-RKIP (Merck Millipore), anti-ERK (Sigma), anti-pERK (Cell Signaling) and anti-Vinculin (Abcam) antibodies.

3.3.6.1. $CD11b^+$ cell isolation

To isolate the $CD11b^+$ cells, anti-CD11b magnetic particles (BD biosciences) were used according to the manufacturer's protocol. This kit allows a direct selection of cells harboring CD11b marker by magnetic separation. The cells were then counted using a Casy cell counter and pellets were made for subsequent immunoblot analysis. In the case of *Mx1-Cre/Nras/Rkip-/-* mice and control

littermates, cells were either treated or not with cytokines before immunoblot. In detail, 10 ng/ml GM-CSF (Peprotech) were added to serum-free HBSS media and the cells were treated for 15 minutes.

3.4. Statistical analysis

Student's *t* test was employed for the statistical analysis of in-vitro and in-vivo experiments. For comparisons between primary samples, the Mann–Whitney–Wilcoxon test was used for continuous variables while the Fisher's Exact Test was employed for dichotomous variables. For the statistical analysis of the microarray experiment, 1-way ANOVA test was performed between THP-1 RKIP KD and control in triplicates. A correction for multiple testing (FDR 5%) was employed and genes with $P<0.05$ as well as a fold change of at least ±1.5 were considered to be significantly de-regulated. The log-rank test was used for survival analysis in mice.

The calculations were performed using SPSS version 22.0 (SPSS Inc.) and Microsoft Excel™. All tests were two-sided and a P value of <0.050 was considered statistically significant.

3.5. Study approval and ethical considerations

This study was reviewed and approved by the institutional review board (24-036 ex 11/12 and 28-481 ex 15/16) and was conducted in accordance with the declaration of Helsinki. Mouse experiments were approved by the Federal Ministry for Science, Research and Economy (GZ: BMWF-66.010/0050-II/3b/2013).

4. Results

The following sections are dedicated to describe the results of this thesis and discuss them. These data were also largely published in Caraffini et al. (119,120).

4.1. RKIP in myeloid sarcoma

4.1.1. Loss of RKIP plays a functional role in leukemic tissue infiltration

RKIP is known to be a metastasis-suppressor in numerous solid cancers (99,105,139) and MS is characterized by the formation of solid tumors composed of myeloid blasts in extramedullary tissues. For this reason, we aimed at investigating the possible involvement of RKIP loss in MS development.

We started by studying the role of RKIP in leukemic tissue infiltration using in-vitro migration and invasion assays. These experiments were designed to assess the migration and invasion potential of THP-1 and U937 cells, two AML cell lines. First, these cells were lentivirally transduced (Figure 5) in order to obtain a stable knockdown (THP-1 RKIP KD and U937 RKIP KD) as well as overexpression (THP-1 RKIP OE and U937 RKIP OE) of RKIP expression.

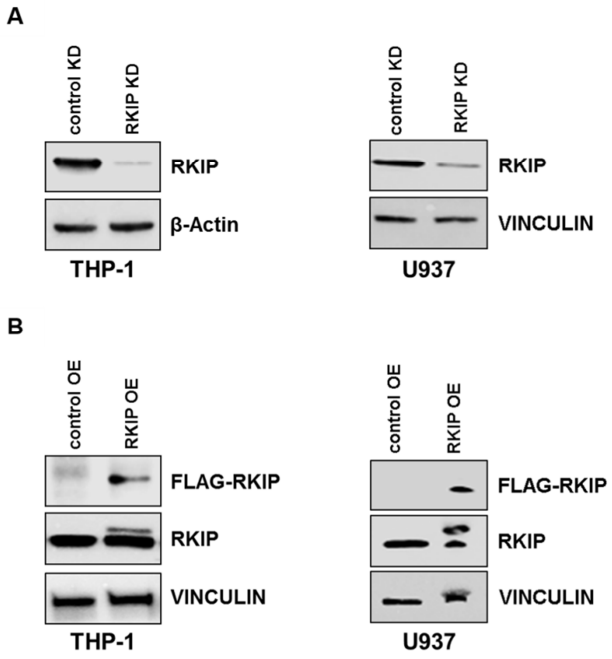

Figure 5. Stable downregulation and overexpression of RKIP in THP-1 and U937 AML cells. Stably transduced THP-1 and U937 AML cell lines were tested by immunoblot to assess the successful knockdown (KD) and overexpression (OE) of RKIP, as

previously described (86). (A) In order to obtain RKIP knockdown, THP-1 and U937 cells were lentivirally transduced with either an empty vector control (control KD) or RKIP shRNA (RKIP KD). (B) For RKIP overexpression, THP-1 and U937 cells were lentivirally transduced with an empty vector control (control OE) or a FLAG-tagged RKIP construct (RKIP OE). The figure is adapted from (119) with permission of *Blood*.

Then, THP-1 and U937 cells with RKIP modulation were employed in migration and invasion assays. On the one hand, we observed, that cells with RKIP KD showed an increased migration (Figure 6A) and invasion (Figure 6B) potential ($P=0.010$ and $P=0.020$ for THP-1 and $P=0.049$ and $P=0.012$ for U937 cells, respectively) as compared to control cells. On the other hand, cells harboring RKIP OE showed the opposite effect, with a decreased migration (Figure 7A) and invasion (Figure 7B) potential ($P=0.004$ and $P=0.004$ for THP-1 and $P=0.042$ and $P=0.019$ for U937 cells, respectively).

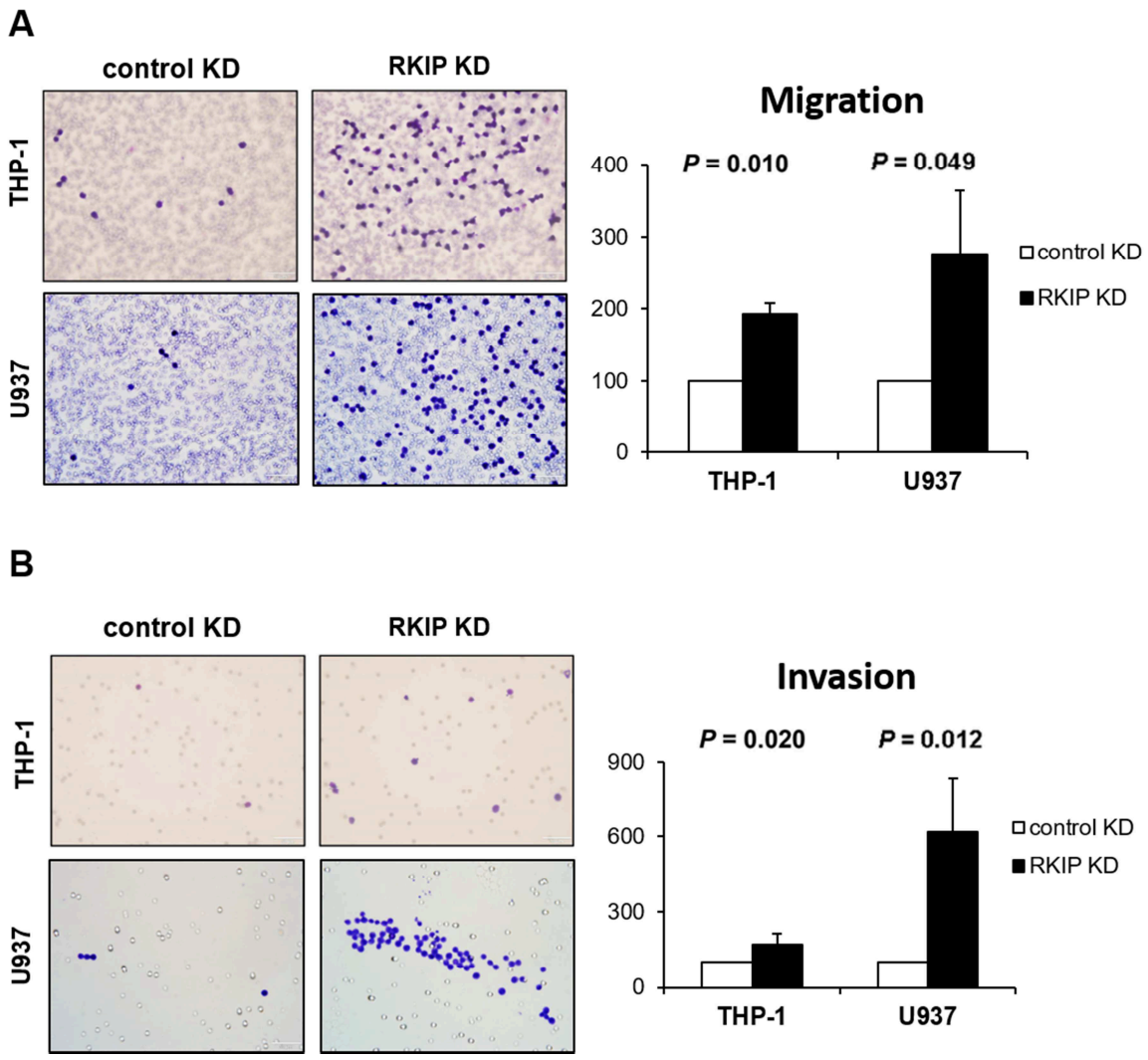

Figure 6. Knockdown of RKIP expression increases the migration and invasion potential of THP-1 and U937 cells. In-vitro migration (A) and invasion (B) experiments were performed employing THP-1 and U937 cells harbouring RKIP KD, obtained by lentiviral transduction. On the left, representative images (40X magnification) of the PET membranes with the Giemsa-stained cells are presented. An inverted microscope was used to count the number of cells on each membrane. Cells transduced with the empty control vectors (indicated as control KD) have been arbitrarily set to a value of 100 and the x-fold change in cells transduced with RKIP shRNA (RKIP KD) was calculated using the ratio "number of cells RKIP KD/number of cells control KD". The graphs on the right side summarize the results of at least three independent experiments. Data are shown as mean values ± S.D. and Student's t-test was used to calculate P-values. The figure is adapted from (119) with permission of *Blood*.

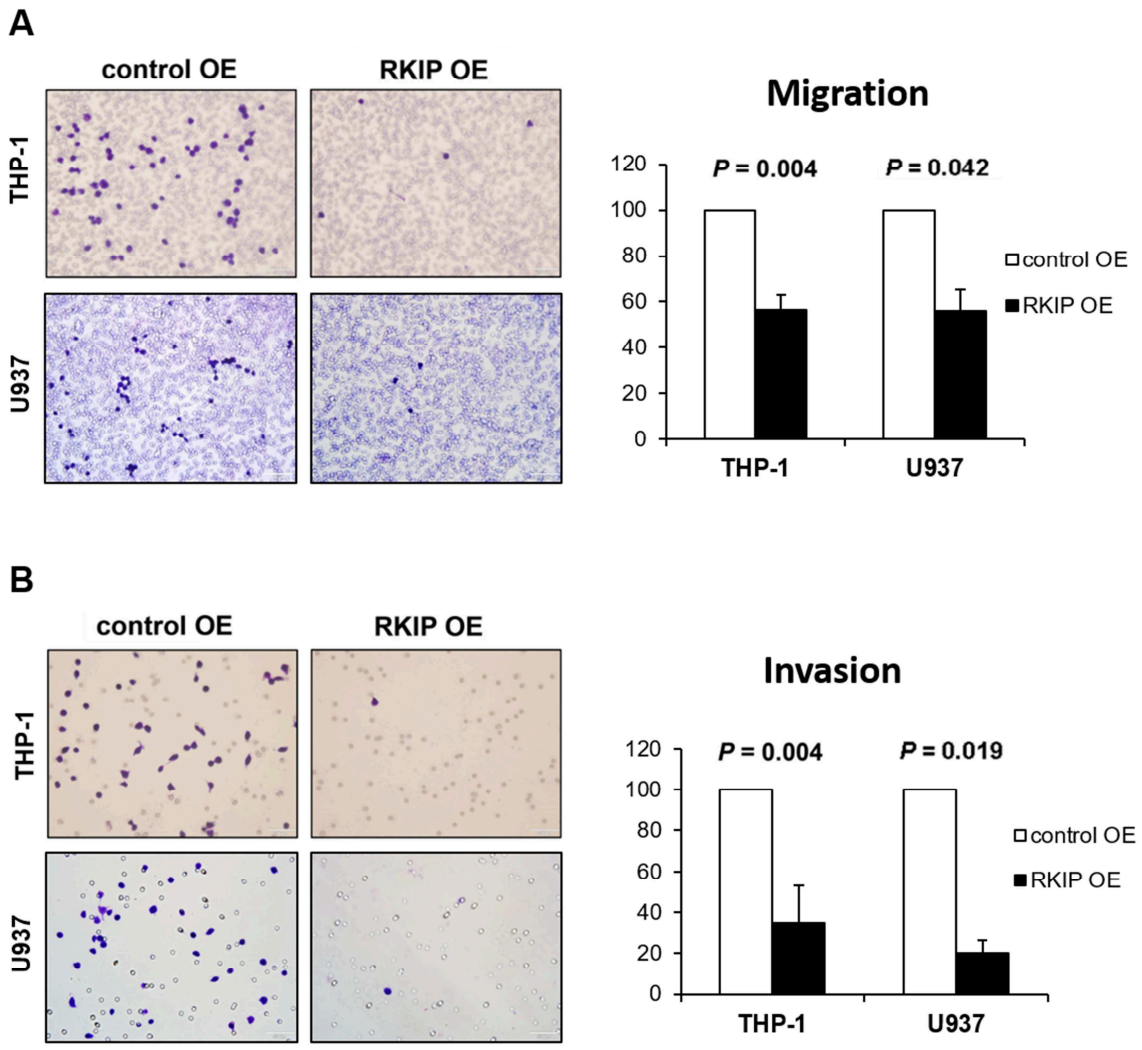

Figure 7. RKIP overexpression reduces the migration and invasion potential of THP-1 and U937 cells. In-vitro migration (A) and invasion (B) experiments were performed employing THP-1 and U937 cells harbouring RKIP OE, obtained by lentiviral transduction. On the left, representative images (40X magnification) of the PET membranes with the Giemsa-stained cells are presented. An inverted microscope was used to count the number of cells on each membrane. Cells transduced with the empty control vectors (indicated as control OE) have been arbitrarily set to a value of 100 and the x-fold change in cells transduced with FLAG-RKIP (RKIP OE) was calculated using the ratio "number of cells RKIP OE/number of cells control OE". The graphs on the right side summarize the results of at least three independent experiments. Data are shown as mean values ± S.D. and Student's t-test was employed to calculate the P-values. The figure is adapted from (119) with permission of *Blood*.

To further confirm these results in an in-vivo setting, the chorioallantoic membrane (CAM) assay was performed. This experiment was used to measure the invasion potential of THP-1 cells together with their ability to form tumor masses in the CAM of chicken embryos. According to the results of the in-vitro experiments, we observed that THP-1 RKIP KD cells infiltrated and formed tumor masses whenever deposited on the CAM. Conversely, THP-1 control cells showed only sparse and occasional infiltration of single cells in the CAM (P<0.001; Figure 8).

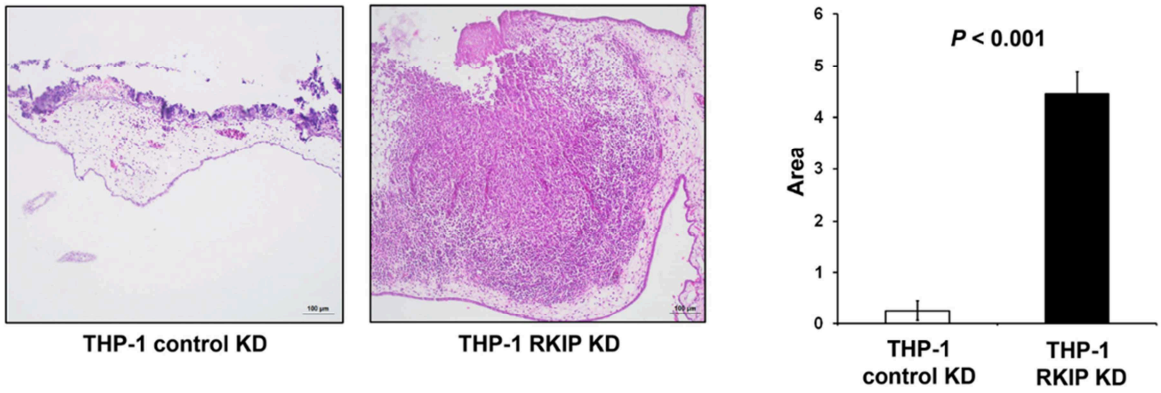

Figure 8. RKIP knockdown favors the formation of tumor masses in a CAM assay. In-vivo CAM assay was performed employing stably transduced THP-1 cells, with (THP-1 RKIP KD) or without (THP-1 control KD) RKIP knockdown. Representative H&E staining of the CAM of chicken embryos are shown. On the left side, a CAM with THP-1 control KD cells is visible, while THP-1 RKIP KD cells were seeded on the CAM shown on the right side. Invasion of the CAM and tumor formation are visible in the THP-1 RKIP KD condition (10X magnification). The graph on the right shows the area of invading cells/tumors as assessed by ImageJ. Data are expressed as mean values ± S.D. and four independent experiments were performed. P-values were calculated using Student's t-test. The figure is reproduced from (119) with permission of *Blood*.

All in all, these results from both in-vitro and in-vivo experiments prove a functional role for RKIP loss in tissue infiltration of leukemic cells, and therefore its potential role in the development of MS.

4.1.2. RKIP loss promotes MS formation via *RAS-MAPK/ERK* pathway-independent effectors

Next, we aimed at elucidating the mechanism, by which RKIP loss contributes to MS formation. RKIP is a negative regulator of the *RAS-MAPK/ERK* pathway and therefore we hypothesized that RKIP loss could cause MS via activation of this signaling cascade. To test this hypothesis, we performed migration experiments employing THP-1 cells with and without RKIP knockdown, with the addition of a MEK inhibitor, U0126. By adding the MEK inhibitor, we expected to be able to rescue the effects of RKIP knockdown on the migration potential of THP-1 cells. However, we noticed that THP-1 RKIP KD cells treated with U0126 retained the same migration potential observed in untreated THP-1 RKIP KD cells (Figure 9A). Therefore, we concluded that the development of MS in AML cases with RKIP loss is mediated via other effectors, which are *RAS-MAPK/ERK* pathway-independent.

In order to discover some of these potential effectors, as well as possible pathways responsible for MS development in absence of RKIP, we performed an mRNA microarray. The same THP-1 cells as used before, both with and without RKIP knockdown, were employed for this experiment. Interestingly, THP-1 RKIP KD cells showed a specific gene expression profile when compared to control cells. By grouping the genes depending on their function, we noticed that the most prominently deregulated ones belonged to networks involved in migration and degradation of connective tissues, as well as in the binding, interaction and engulfment of hematopoietic cells (Figure 9B; Table 5).

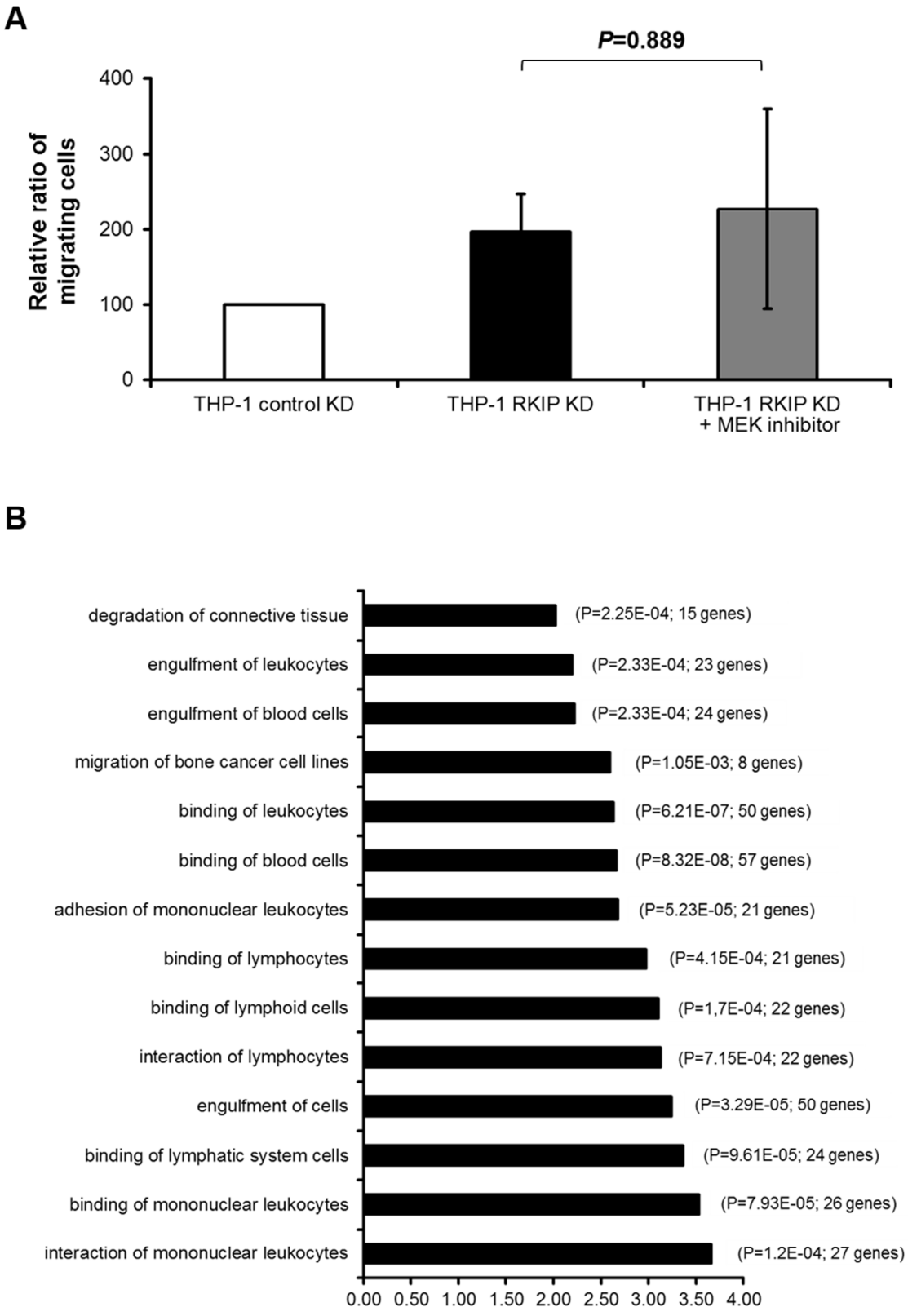

Figure 9. RKIP knockdown in THP-1 cells acts in a *RAS* pathway-independent manner and causes a specific gene expression profile in these cells. (A) Migration experiments were performed using THP-1 control and THP-1 cells harboring RKIP knockdown with the addition of either DMSO or of 10µM of the MEK inhibitor U0126.

Control cells (THP-1 control KD) were arbitrarily set to a value of 100 and the relative increase of migrating cells in the RKIP knockdown conditions (THP-1 RKIP KD) has been calculated using the ratio migrating cells "THP-1 RKIP KD conditions"/migrating cells "THP-1 control KD". The graph summarizes the results of three independent experiments and data are expressed as mean values ± S.D. P-values have been calculated using Student's t-test. (B) Results of the mRNA microarray analysis, which showed a distinct gene expression profile in THP-1 cells harboring knockdown of RKIP. In more detail, THP-1 cells with RKIP knockdown showed a significant activation of genes involved in migration and degradation of connective tissues, as well as in the binding, interaction and engulfment of hematopoietic cells. In the graph, the horizontal axis indicates the z-scores, with higher numbers indicating a more prominent upregulation. The P-values of each group, as well as the number of genes belonging to each group, are also displayed. The Ingenuity Pathway Analysis software was used for this analysis. The figure is reproduced from (119) with permission of *Blood*.

Diseases or Functions Annotation	**Number of genes**	**Genes**
interaction of mononuclear leukocytes	27	*ANXA1, BPI, CALR, CBLB, CCL5, CD48, CXCL10, CXCL8, DEPTOR, FAS, FN1, FUT4, FYB, HGF, IL6R, ITGAX, MSN, MYO1G, PIK3CG, RAP2A, RGS1, RGS16, SELL, TERT, TLR4, TNF, ULBP1*
binding of mononuclear leukocytes	26	*ANXA1, BPI, CALR, CBLB, CCL5, CD48, CXCL10, CXCL8, DEPTOR, FAS, FN1, FUT4, FYB, HGF, IL6R, ITGAX, MSN, MYO1G, PIK3CG, RAP2A, RGS1, SELL, TERT, TLR4, TNF, ULBP1*
binding of lymphatic system cells	24	*ANXA1, CALR, CBLB, CCL5, CD48, CSF2RB, CXCL10, DEPTOR, FAS, FN1, FUT4, FYB, HGF, IL6R, KITLG, MSN, MYO1G, RAP2A, RGS1, SELL, SYK, TLR4, TNF, ULBP1*

engulfment of cells	50	*ANXA1, ANXA3, ATP6V0D1, BICD1, CALR, CCL5, CD48, CD63, CEBPB, CEBPE, CLN3, CR1, CSF2RB, CXCL10, CYBA, DNM1, ELANE, FAS, FCGR1A, FN1, FYN, G6PC3, GAB2, HGF, HSPA5, IL1RL1, ITGAX, KITLG, LIMK1, LRPAP1, MYO1G, NEDD4, P2RX7, PLD1, PRKCD, PRTN3, PYCARD, RAB31, RAB5C, RASA4, SIRPB1, SYK, TLR3, TLR4, TNF, TNFSF10, TRIM21, TUSC2, UCP2, WASF1*
interaction of lymphocytes	22	*ANXA1, CALR, CBLB, CCL5, CD48, CXCL10, DEPTOR, FAS, FN1, FUT4, FYB, HGF, IL6R, MSN, MYO1G, RAP2A, RGS1, RGS16, SELL, TLR4, TNF, ULBP1*
binding of lymphoid cells	22	*ANXA1, CALR, CBLB, CCL5, CD48, CXCL10, DEPTOR, FAS, FN1, FUT4, FYB, HGF, IL6R, MSN, MYO1G, RAP2A, RGS1, SELL, SYK, TLR4, TNF, ULBP1*
binding of lymphocytes	21	*ANXA1, CALR, CBLB, CCL5, CD48, CXCL10, DEPTOR, FAS, FN1, FUT4, FYB, HGF, IL6R, MSN, MYO1G, RAP2A, RGS1, SELL, TLR4, TNF, ULBP1*
adhesion of mononuclear leukocytes	21	*ANXA1, CBLB, CCL5, CD48, CXCL8, DEPTOR, FAS, FN1, FUT4, FYB, HGF, IL6R, ITGAX, MYO1G, PIK3CG, RAP2A, RGS1, SELL, TERT, TLR4, TNF*
binding of blood cells	57	*ANGPT1, ANXA1, BPI, CALR, CBLB, CCL5, CD37, CD48, CD83, CR1, CSF2RB, CTSZ, CXCL10, CXCL8, CYBB, DEPTOR, ELANE, ENTPD1, F5, FAS, FCGR1A, FN1, FUT4, FYB, FYN, GAB2, HGF, IL6R, ITGA2, ITGA6, ITGAX, KITLG, LIMK1, LRPAP1, MSN, MYO1G, NFE2, NFE2L2, P2RX7, PIK3CG, PLCG2, PRKCQ, PRTN3, RAP2A, RGS1, RGS16, SDC4, SELL, SYK, TERT, TLR3, TLR4, TNF, TRAF3IP2, TSLP, ULBP1, VEGFA*
binding of leukocytes	50	*ANGPT1, ANXA1, BPI, CALR, CBLB, CCL5, CD37, CD48, CD83, CR1, CSF2RB, CTSZ, CXCL10, CXCL8, CYBB, DEPTOR, ELANE, ENTPD1, FAS, FCGR1A, FN1, FUT4, FYB, FYN, GAB2, HGF, IL6R, ITGA6, ITGAX, KITLG, MSN, MYO1G, P2RX7, PIK3CG, PRKCQ, PRTN3, RAP2A, RGS1, RGS16, SDC4, SELL, SYK, TERT, TLR3, TLR4, TNF, TRAF3IP2, TSLP, ULBP1, VEGFA*

migration of bone cancer cell lines	8	*FN1, FYN, HGF, IL6R, KITLG, MMP9, PRKCD, VCP*
engulfment of blood cells	24	*ANXA1, CALR, CCL5, CEBPB, CSF2RB, CXCL10, DNM1, FAS, FCGR1A, FYN, G6PC3, GAB2, HGF, IL1RL1, ITGAX, MYO1G, P2RX7, RASA4, SIRPB1, SYK, TLR3, TLR4, TNF, UCP2*
engulfment of leukocytes	23	*ANXA1, CALR, CCL5, CEBPB, CSF2RB, CXCL10, DNM1, FAS, FCGR1A, FYN, G6PC3, GAB2, HGF, IL1RL1, MYO1G, P2RX7, RASA4, SIRPB1, SYK, TLR3, TLR4, TNF, UCP2*
degradation of connective tissue	15	*C5AR1, CXCL8, ELANE, FCGR1A, FGFR1, FN1, IL18, IL1RL1, MTF1, PHC1, PIK3CG, PRKCQ, PRTN3, TLR4, TNF*

Table 5. List of all the genes upregulated in THP-1 cells harboring RKIP knockdown. These genes were obtained by analyzing the mRNA microarray data from THP-1 cells with the Ingenuity Pathway Analysis software and considering genes with an annotated role in a specific disease or function. The table is reproduced from (119) with permission of *Blood*.

4.1.3. Loss of RKIP is of clinical relevance for the development of MS

Having proven that RKIP loss plays a functional role in leukemic tissue infiltration, we decided to investigate the clinical relevance of this finding. For this aim, we analyzed two cohorts of AML patients, in which the presence of MS was assessed either clinically (“cohort I”) or by biopsy (“cohort II”).

The first cohort included 103 AML patients (Figure 10A; Table 6) and for all of them, the status of RKIP expression in the BM had been characterized previously (86). The presence or absence of MS in this cohort was investigated retrospectively by clinical evaluation, as previously described (121,122), and was possible in 58 of the 103 patients. In more detail, we observed presence of MS in 16/58 cases (28%) and, interestingly, samples harboring RKIP loss were significantly enriched in AML with concomitant occurrence of MS (8/16 [50%] vs.

6/42 [14%]; P=0.013; Figure 10B). This result suggests a link between RKIP loss in AML and concomitant development of MS.

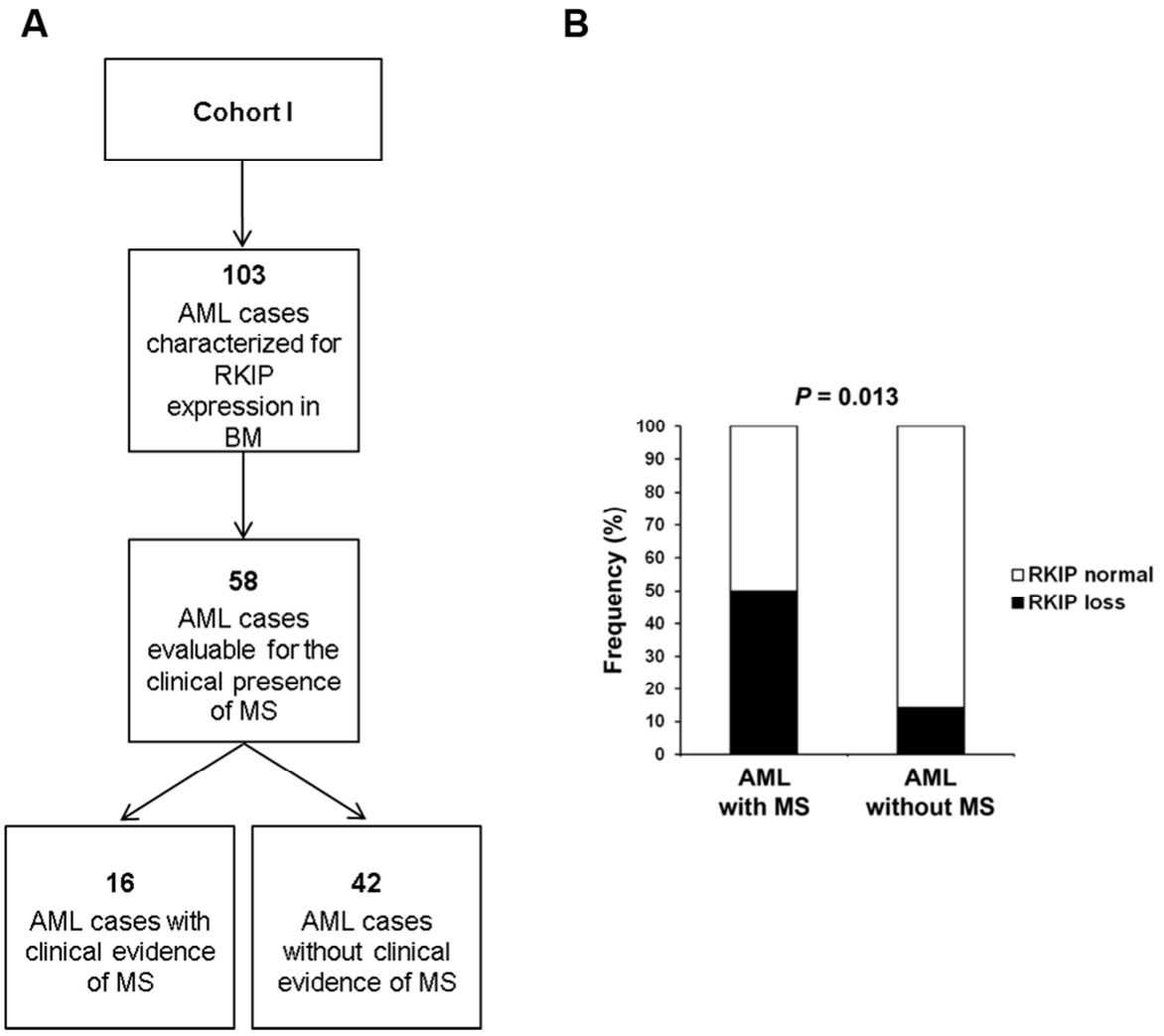

Figure 10. RKIP knockdown is a frequent event in AML patients with concomitant clinical evidence of MS presence. (A) The frequency of RKIP knockdown was studied in "cohort I", which comprised 103 AML patient samples, whose diagnostic BM was investigated before for the RKIP expression status (86). The medical records of these patients were re-analyzed, screening the respective physical examination and radiology results in order to find clinical evidence of MS, as previously described (121,122). Due to lacking of sufficient data at the time of diagnosis, 45 cases were excluded from this retrospective clinical evaluation. The remaining 58 patients were classified as either "AML with MS" or "AML without MS" cases depending on the presence or absence of clinical signs of MS, respectively. (B) The frequency of RKIP loss was then compared between

the two groups of patients, with and without evidence of MS. The graph shows that the frequency of specimens harboring RKIP loss was significantly increased in AML patients with MS as compared to those without clinical evidence of MS. Statistical analysis was performed using Fisher's exact test. The figure is adapted from (119) with permission of *Blood*.

Cohort I										
UPN	**MS site**	**MS diagnosis**	**Concomitant BM infiltration**	**Timepoint of MS occurence during course of AML**	**AML course before MS occurence**	**AML course after MS occurence**	**AML WHO classification**	**AML FAB classification**	**AML karyotype**	**Overall survival from MS diagnosis (months)**
4626	Liver	Clinical evaluation	Yes	Diagnosis	NA	HD chemotherapy and auto-SCT	AML, NOS; Acute monoblastic/ monocytic leukemia	M5	46,XX	146*
5589	Lung/Pleura	Clinical evaluation	Yes	Diagnosis	NA	HD chemotherapy	AML, NOS; Acute monoblastic/ monocytic leukemia	M5	46,XY	17
961	Gingiva; Lymph node	Clinical evaluation	Yes	Diagnosis	NA	HD chemotherapy	AML, NOS; Acute monoblastic/ monocytic leukemia	M5	46,XX	234*
5536	Lymph node	Clinical evaluation	Yes	Diagnosis	NA	HD chemotherapy and auto-SCT	AML with inv(16)(p13.1q22) or t(16;16)(p13.1;q22); CBFB-MYH11	M4Eo	46,XY, inv(16)(p13q22)	76*
4855	Gingiva	Clinical evaluation	Yes	Diagnosis	NA	HD chemotherapy	AML with mutated NPM1	M4	46,XX	136*
3120	Gingiva, Lymph node	Clinical evaluation	Yes	Diagnosis	NA	HD chemotherapy	AML with myelodysplasia-related changes	M5	46,XX, 22ps+	9*
4963	Lung	Clinical evaluation	Yes	Diagnosis	NA	HD chemotherapy and allo-MUD-SCT	AML with inv(16)(p13.1q22) or t(16;16)(p13.1;q22); CBFB-MYH11	M4Eo	46,XY, inv(16)(p13q22)	137*
4323	Skin	Clinical evaluation	Yes	Diagnosis	NA	HD chemotherapy	AML, NOS; Acute monoblastic/ monocytic leukemia	M5	48,XY,+8,+8	150*
1878	Gingiva	Clinical evaluation	Yes	Diagnosis	NA	HD chemotherapy	AML, NOS: AML without differentiation	M1	46,XX	9
5081	Skin; Lymph node	Clinical evaluation	Yes	Diagnosis	NA	HD chemotherapy and allo-sibl-SCT	AML, NOS: AML with minimal differentiation	M0	46,XX	134*
4687	Gingiva, Lymph node	Clinical evaluation	Yes	Diagnosis	NA	HD chemotherapy and allo-UCB-SCT	AML, NOS: AML without differentiation	M1	46,XX	15
2325	Spleen; Lymph node; Kidney	Clinical evaluation	Yes	Diagnosis	NA	BSC	AML, NOS: AML with maturation	M2	NA	0
4379	Skin	Clinical evaluation	Yes	Diagnosis	NA	BSC	AML, NOS: AML with maturation	M2	NA	1
5216	Gingiva	Clinical evaluation	Yes	Diagnosis	NA	HD chemotherapy	t-AML	M2	Complex	2*
4816	Gingiva	Clinical evaluation	Yes	Diagnosis	NA	HD chemotherapy	AML, NOS: AML without differentiation	M1	45,XX,-7	7
4892	Spleen; Lymph node	Clinical evaluation	Yes	Diagnosis	NA	HD chemotherapy and allo-sibl-SCT	AML with mutated NPM1	M4	46,XX	142*

Table 6. Clinical characteristics of the "cohort I" patients. The table depicts the clinical characteristics of the 16 MS patients belonging to "cohort I", in which presence of MS was assessed by clinical evaluation.

For the overall survival column, the presence of an asterisk indicate patients who were still alive at the last contact.

Abbreviations: UPN, Unique patient ID; WHO, World Health Organization; FAB, French-American-British; NA, not applicable; n.d., not done; HD, high-dose; SCT, stem cell transplantation; MUD, matched unrelated donor; sibl, sibling; UCB, umbilical cord blood. The table is reproduced from (119) with permission of *Blood*.

To further corroborate this finding, we employed a second cohort comprising 28 AML patients ("cohort II"), in which the presence of MS was assessed by biopsy

(Figure 11A; Table 7-8). RKIP protein expression was studied by immunohistochemistry in 14 FFPE patient specimens of MS, as well as in their corresponding leukemic BM samples (available for analysis in 6/14 AML patients with MS), and in 14 BM samples from patients without any evidence of MS (Figure 11B). Loss of RKIP protein was observed in seven of the MS patients analyzed (7/14, 50%) while only one of the AML patients without evidence of MS showed RKIP loss (1/14, 7%). Interestingly, we did not observe any difference in RKIP expression between the MS site and the corresponding leukemic BM specimen as well as between diagnostic and relapse material (Figure 11D). These data further support an association between RKIP loss and MS.

When searching for the mechanism behind loss of RKIP in MS, we observed that samples harboring loss of RKIP at protein level also demonstrated decreased levels of *RKIP* mRNA, as assessed by qPCR (P=0.041; Figure 11C). We have previously shown that loss of RKIP in myeloid malignancies is caused by increased expression of miR-23a, which causes the downregulation of *RKIP* mRNA by direct binding (86,117,118). Therefore, this suggests that the same mechanism could be present in MS.

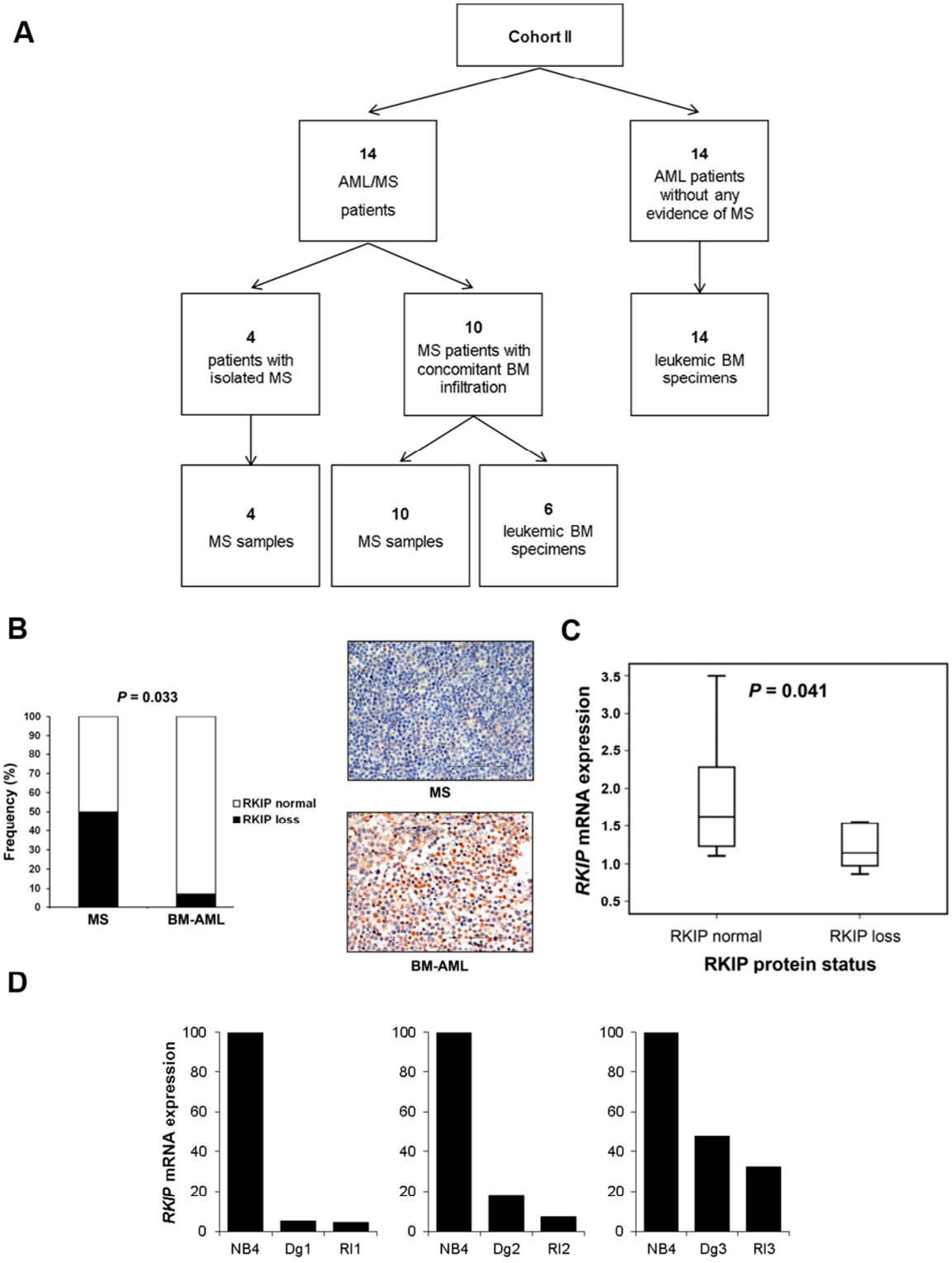

Figure 11. RKIP knockdown is a frequent event in MS, both at protein and mRNA level, and appears stable during the course of the disease. (A) The frequency of RKIP knockdown was also studied in "cohort II", comprising 14 MS patients as well as 14 AML patients without any evidence of MS. In this cohort, independent from "cohort I", MS presence was assessed by biopsy. RKIP expression was assessed both in BM specimens as well as MS samples, as depicted in the flow chart. (B) RKIP status was studied in

FFPE samples by immunohistochemistry. As shown in cohort I, also in these patients the frequency of RKIP loss was significantly increased in the AML patients with MS (MS) as compared to AML specimens without any evidence of MS (BM-AML). Fisher's exact test was used for this statistical analysis. On the right side, representative pictures of immunohistochemistry analysis show loss of RKIP expression in a sample of MS and presence of normal RKIP levels in a BM-AML specimen. (C) Results of qPCR showing that samples harboring RKIP loss at protein level also demonstrate decreased levels of *RKIP* mRNA. The Mann–Whitney–Wilcoxon test was used to calculate statistical significance and NB4 AML cells were used as calibrator. (D) In order to evaluate how stable the loss of RKIP is during the course of AML/MS, we used leukemic BM specimens of three AML samples, which were analyzed by qPCR both at diagnosis (Dg) and relapse (Rl) as previously described (86). These patients were chosen since they had enough material to perform the analysis both at diagnosis and relapse, exhibited decreased *RKIP* expression levels at diagnosis and showed clinical evidence of MS. NB4 AML cells served as calibrator and were arbitrarily set to a value of 100. These cells were chosen as it was previously shown that they exhibit a normal *RKIP* expression (86). Interestingly, in all three cases *RKIP* mRNA expression appeared decreased at both disease stages. This led to the conclusion that loss of RKIP during the course of AML/MS is a stable event. However, a larger cohort with sequentially collected samples will be needed in order to ultimately prove the correctness of this assumption. The figure is adapted from (119) with permission of *Blood*.

	MS cases - cohort II	AML cases - cohort II	P-value
Age at diagnosis (years)	46 (21-93)	57 (28-76)	0.427
AML subtype			0.075
de novo, n=	8/14 (57%)	13/14 (93%)	
Secondary, n=	3/14 (21.5%)	1/14 (7%)	
therapy-related, n=	3/14 (21.5%)	0/14 (0%)	
Sex			0.999
male, n=	9/14 (64%)	9/14 (64%)	
female, n=	5/14 (36%)	5/14 (36%)	
WBC at diagnosis (10^9/L)	12.73 (2.77-64.98)	19.24 (1.13-178.45)	0.874
LDH (U/L)	361 (186-3023)	443 (144-1108)	0.462
Cytogenetic risk group			0.414
Favorable, n=	2/10 (20%)	1/14 (7%)	
Intermediate, n=	7/10 (70%)	9/14 (64%)	
Adverse, n=	1/10 (10%)	4/14 (29%)	

Table 7. Clinical characteristics of the "cohort II" patients. The clinical characteristics of all the 28 patients belonging to "cohort II", including both MS cases and AML cases, are depicted. The table is reproduced from (119) with permission of *Blood*.

Cohort II										
UPN	MS site	MS diagnosis	Concomitant BM infiltration	Timepoint of MS occurence during course of AML	AML course before MS occurence	AML course after MS occurence	AML WHO classification	AML FAB classification	AML karyotype	Overall survival from MS diagnosis (months)
K5167	Lymph node	Biopsy	Yes	Relapse	HD chemotherapy and allo-MUD-SCT	BSC	AML with myelodysplasia-related changes	M0	46, XY	3
K5166	Soft tissue	Biopsy	Yes	Diagnosis	NA	HD chemotherapy and allo-MUD-SCT	AML with myelodysplasia-related changes	M0	47, XY, +8	25
K4963	Lymph node	Biopsy	Yes	Diagnosis	NA	HD chemotherapy and allo-MUD-SCT	t-AML	M4Eo	49, XY,+8,+14,inv(16)(p13q22),+22	11
K4962	Lymph node	Biopsy	Yes	Relapse	HD chemotherapy and auto-SCT	HD chemotherapy and allo-MUD-SCT	AML, NOS; Acute monoblastic/monocytic leukemia	M5	46, XY	32
K4974	Lymph node	Biopsy	Yes	Diagnosis	NA	HD chemotherapy	t-AML	n.d.	Complex	1
K4964	Stomach	Biopsy	Yes	Diagnosis	NA	HD chemotherapy and allo-MUD-SCT	AML, NOS; Acute monoblastic/ monocytic leukemia	M5	46, XY	12
K5168	Parotid gland	Biopsy	No	Relapse	AML Dg without MS; HD chemotherapy and allo-sibl-SCT; Relapse with isolated MS	Radiotherapy	AML with inv(16)(p13.1q22) or t(16;16)(p13.1;q22); CBFB-MYH11	M0	46, XY, inv(16)(p13q22)	5
K4965	Skin	Biopsy	Yes	Diagnosis	NA	HD chemotherapy and allo-MUD	AML with mutated NPM1	M4	46, XY	59*
K4111	Liver	Biopsy	Yes	Diagnosis	NA	HD chemotherapy	AML; NOS: Acute megakaryoblastic leukemia	M7	47,XX,+14	2
K4976	Bone	Biopsy	No	Diagnosis	NA	HD chemotherapy and allo-MUD-SCT	n.d.	M4	n.d.	10
K4112	Skin	Biopsy	Yes	Diagnosis	NA	Decitabine	AML with myelodysplasia-related changes	M4	n.d.	8
K4966	Spleen	Biopsy	Yes	Diagnosis	NA	Decitabine	AML with myelodysplasia-related changes	M5	46, XX	32
K4975	Oral mucosa	Biopsy	No	Diagnosis	NA	Decitabine	t-AML	n.d.	n.d.	67
K4113	Soft tissue	Biopsy	No	Diagnosis	NA	HD chemotherapy and Radiotherapy	n.d.	n.d.	n.d.	19

Table 8. Clinical characteristics of the MS patients in "cohort II". The table depicts the clinical characteristics of the 14 MS patients, belonging to "cohort II".

For the overall survival column, the presence of an asterisk indicate patients who were still alive at the last contact.

Abbreviations: UPN, Unique patient ID; WHO, World Health Organization; FAB, French-American-British; NA, not applicable; n.d., not done; HD, high-dose; SCT, stem cell transplantation; MUD, matched unrelated donor; sibl, sibling. The table is reproduced from (119) with permission of *Blood*.

4.1.4. RKIP loss and *RAS*-signaling mutations co-occur in MS

The patient samples belonging to "cohort II" were further analyzed to understand the molecular landscape of MS in presence of RKIP loss. This analysis was performed via NGS (Figure 12), covering 39 genes frequently mutated in leukemia. NGS was carried out on all the FFPE MS samples showing DNA quality sufficient for this analysis (n=11), as previously described (42). Interestingly, samples harboring RKIP loss showed a higher frequency of *RAS*-signaling mutations. In more detail, five out of six samples (83%) showed one or more of these mutations affecting in particular the RASopathy genes (140), while only two out of five patients with RKIP loss (40%) were affected. Pyrosequencing was used

to validate all *RAS* mutations. Unfortunately, the small sample size of the cohort used precluded a statistical analysis of these results. However, the co-occurrence of *RAS*-signaling mutations and RKIP loss was previously shown in AML and therefore might be of importance also for MS. Moreover, every patient harboring normal levels of RKIP showed at least one mutation in either *NPM1* or *DNMT3A*, while only two out of six samples with RKIP loss did. Mutations affecting these genes are known to induce MS in a *RAS*-signaling independent way (42,141–145). Therefore, this observation strengthens the idea of a synergistic effect in MS development between RKIP loss and *RAS*-signaling mutations.

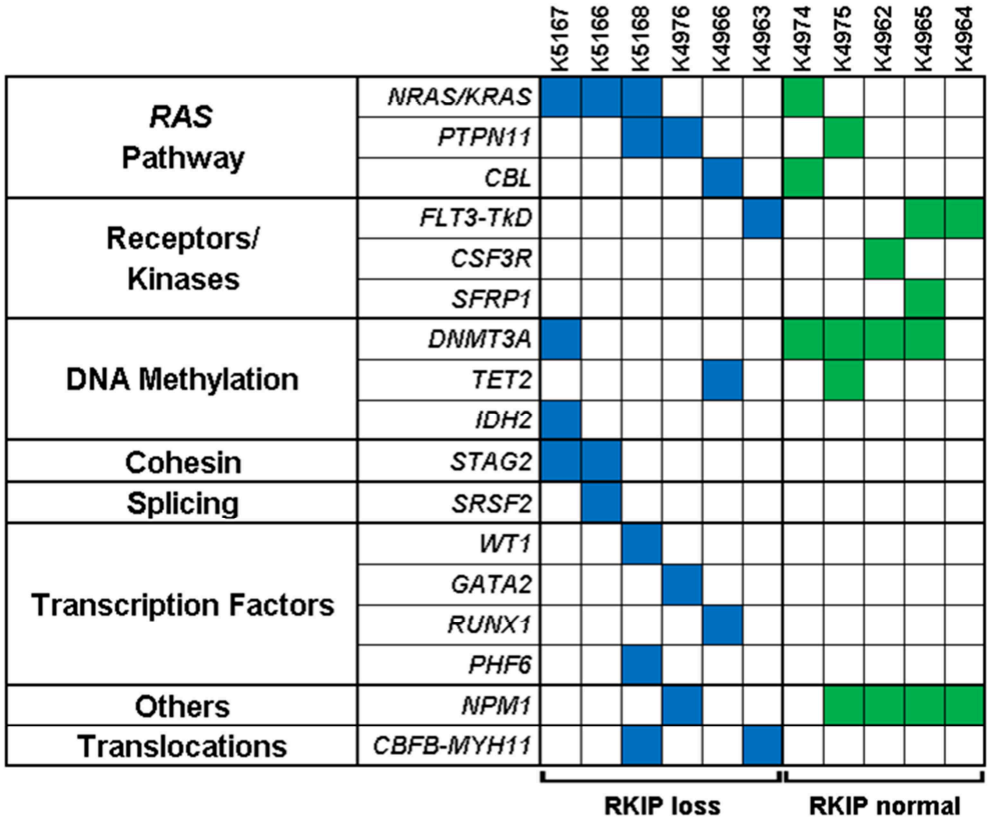

Figure 12. Next-Generation Sequencing of MS patients harboring either RKIP loss of RKIP normal. NGS was performed on all the FFPE MS samples belonging to "cohort II" that had sufficient material for this analysis. Every column refers to one MS patient with "RKIP loss" or "RKIP normal", as defined by the immunochemistry results. NGS was performed using a panel of 39 genes recurrently mutated in myeloid neoplasms, but only those carrying at least one mutation are listed in the figure. The whole list of genes analyzed comprised *CEBPA*, *NPM1*, *FLT3, ASXL1*, *BCOR*, *BRAF*, *CALR*, *CBL*, *CSF3R*,

DDX41, DNMT3a, *ETNK1*, *ETV6*, *EZH2*, *GATA2*, *IDH1*, *IDH2*, *JAK2*, *KIT*, *KRAS*, *MPL*, *NF1*, *NRAS*, *PHF6*, *PTPN11*, *RUNX1*, *SETBP1*, *SF3B1*, *SF3B2*, *SFRP1*, *SRP72*, *SRSF2*, *STAG2*, *STAT3*, *TET2*, *TP53*, *U2AF1*, *WT1* and *ZRSR2*. *FLT3*-ITD has been studied by PCR fragment length analysis as previously described (42). Blue is used to highlight genes mutated in samples with "RKIP loss" while genes mutated in samples defined as "RKIP normal" are highlighted in green. The figure is reproduced from (119) with permission of *Blood*.

4.2. RKIP in chronic myelomonocytic leukemia

4.2.1. Cells belonging to the myeloid lineage show low levels of RKIP expression

RKIP is a negative regulator of the *RAS-MAPK/ERK* pathway. Activating mutations affecting this pathway are known to alter the homeostasis in the differentiation of HSPCs in myeloid or lymphoid cells. For this reason, we hypothesized that RKIP loss could disrupt this equilibrium and favor myelomonocytic lineage commitment of HSPCs.

To verify this hypothesis, we started by studying RKIP levels in myeloid cells, obtained via in-vitro differentiation, from healthy donors and from re-analysis of online datasets. First, we employed HL-60 cells, an undifferentiated AML cell line, which can be forced into myelomonocytic differentiation by adding 1,25-Dihydroxyvitamin D_3 ($1,25D_3$) (146). After treatment with $1,25D_3$, HL-60 cells showed a concomitant decrease of RKIP protein expression, as assessed by immunoblot (P=0.002; Figure 13A). Next, we studied RKIP expression levels in human hematopoiesis employing $CD34^+$ HSPCs from umbilical cord blood specimens (n=3) as well as lymphocytes, monocytes and granulocytes derived from healthy subjects (n=4). In agreement with the results from HL-60 cells, RKIP expression was high in healthy $CD34^+$ HSPCs, while it appeared significantly reduced in cells belonging to the myeloid lineage (monocytes, P=0.001, and granulocytes, P<0.001; Figure 13B). Interestingly, lymphocytes showed RKIP expression levels similar to HSPCs (P=0.244). Due to the restricted amount of cells available from these primary samples, RKIP expression was studied by qPCR as *RKIP* mRNA expression. This was possible as we have previously shown that decreased RKIP protein expression is accompanied by mRNA

downregulation (86,117–119). In order to confirm these findings also in a murine setting, we investigated the GEO database. In more detail, we re-analyzed the microarray data of different hematopoietic cell and progenitor compartments in C57BL/6 mice, which was performed by Konuma et al. (128) (GEO data set GDS3997) and checked *RKIP* mRNA expression levels (Figure 13C). In agreement with our findings in HL-60 cells and hematopoietic cells from healthy donors, also in a murine model *RKIP* mRNA levels appeared high in HSPCs and lymphocytes, while they were significantly lower in cells belonging to the myeloid lineage ($P<0.001$). To better understand the exact stage at which RKIP expression starts decreasing, we analyzed specific HSPCs compartments within GDS3997 as well as in three additional datasets (128–131). Interestingly, we observed that RKIP expression remains high until the granulocyte-macrophage-progenitor (GMP) stage, while decreases during the terminal stages of myelomonocytic differentiation (Figure 13D-G).

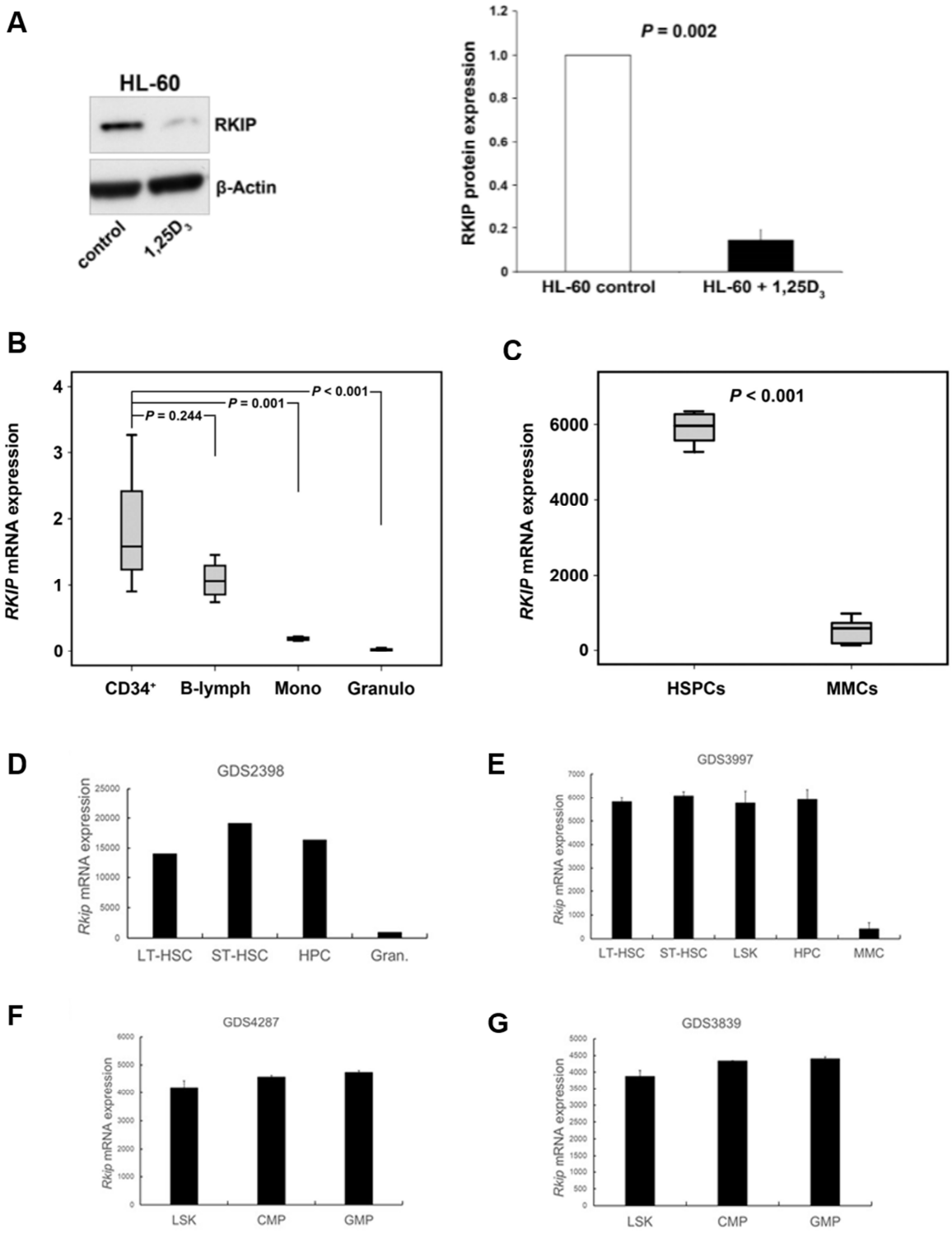

Figure 13. Cells belonging to the myeloid lineage show low levels of RKIP expression, starting after the GMP stage. (A) Immunoblot showing decreased RKIP expression in HL-60 AML cells treated with 1,25D_3. In more detail, the immature cells were treated with 100nM 1,25D_3 for 48 hours in order to induce myeloid differentiation and then tested by immunoblot. The graph shows the mean of three independent experiments ± S.D. Expression values of HL-60 cells treated with 1,25D_3 are given as x-fold expression

of the HL-60 control cells. Student's t-test was used to calculate statistical significance. (B) Box plots showing *RKIP* mRNA expression in different cell compartments of healthy donors. RKIP expression was studied by qPCR in $CD34^+$ HSPCs ($CD34^+$, n=3), lymphocytes (B-lymph, n=4), monocytes (Mono, n=4) and granulocytes (Granulo, n=4). NB4 cells were used as a calibrator and arbitrarily set to a value of 1. The box plots indicate the x-fold RKIP expression levels as compared to NB4 cells. Student's t-test was used to calculate P-values. (C) Results of the *RKIP* mRNA expression from the re-analysis of a previously published murine microarray gene expression profiling dataset (128) made using the Gene Expression Omnibus (https://www.ncbi.nlm.nih.gov/geo/,GEO) database. As observed in the healthy donors, the box plot show that, also in mice, *RKIP* mRNA expression is decreased in differentiated cells belonging to the myeloid lineage (MMCs), including $Gr\text{-}1^+$ neutrophils and $Mac\text{-}1^+$ monocytes/macrophages. The comparison was made with murine HSPCs which included long-term hematopoietic stem cells (lin^-, Sca^+, kit^+, $CD34^-$), short-term hematopoietic stem cells (lin^-, Sca^+, kit^+, $CD34^+$), LSK (lin^-, Sca^+, kit^+) and hematopoietic progenitor cells (lin^-). Statistical significance was calculated using Student's t-test. GEO was also used to download and re-analyze microarray expression data for murine *Rkip* mRNA expression for different compartments. (D) Data from Sung LY et al., GEO accession number GSE5677, GDS2398 (129), show *Rkip* expression in LT-HSC (lin^-, Sca^+, kit^+, $CD34^-$), ST-HSC (lin^-, Sca^+, kit^+, $CD34^+$), HPC (lin^-, Sca^-, kit^+) and granulocytes (Gran.; based on SSC sorting and $Gr1^{high}$). (E) Data regarding *Rkip* expression in LT-HSC (lin^-, Sca^+, kit^+, $CD34^-$), ST-HSC (lin^-, Sca^+, kit^+, $CD34^+$), LSK (lin^-, Sca^+, kit^+), HPC (lin^-) and myelomonocytic cells (MMC, $Gr\text{-}1^+$ neutrophils and $Mac\text{-}1^+$ monocytes/macrophages) were downloaded from Konuma T et al., GEO accession number GSE27787, GDS3997 (128). (F) Data from Moran-Crusio K et al., GEO accession number GSE27816, GDS4287 (130), were downloaded to show *Rkip* expression in LSK (lin^-, Sca^+, kit^+), CMP (lin^-, Sca^-, kit^+, $FcγR^{lo}$, $CD34^+$) and GMP (lin^-, Sca^-, kit^+, $FcγR^+$, $CD34^+$). (G) Data regarding *Rkip* expression in LSK (lin^-, Sca^+, kit^+), CMP (lin^-, Sca^-, kit^+, $FcγR^{lo}$, $CD34^+$) and GMP (lin^-, Sca^-, kit^+, $FcγR^+$, $CD34^+$) were downloaded from Wang Y et al., GEO accession number GSE20377, GDS3839 (131).

Abbreviations: LT-HSC, long-term hematopoietic stem cells; ST-HSC, short-term hematopoietic stem cells; HPC, hematopoietic progenitor cells; MMC, myelomonocytic cells; CMP, common myeloid progenitor; GMP, granulocyte-macrophage progenitor. The figure is adapted from (120) with permission of *Haematologica*.

4.2.2. Knockdown of RKIP expression increases the myeloid lineage differentiation of HSPCs

Having proven that RKIP expression is lower in myeloid cells as compared to HSPCs, we next asked whether this loss of RKIP is functionally relevant for myeloid differentiation. As a first step, we employed human $CD34^+$ HSPCs from umbilical cord blood and performed lentiviral knockdown of RKIP in these cells. The transduced cells were then treated for five days with a cytokine mix, containing GM-CSF/FL/SCF/TNFα (132), in order to induce myelomonocytic differentiation. After the treatment, the extent of myelomonocytic differentiation was measured assessing the expression of the myelomonocytic surface markers CD11b and CD14 (Figure 14). We observed, that myelomonocytic differentiation of HSPCs harboring RKIP knockdown (HSPCs RKIP KD) was significantly increased when compared to control cells (HSPCs control KD; P=0.001 for $CD11b^+$ cells and P=0.002 for $CD11b^+$ $CD14^+$ cells). This result highlights a functional role for RKIP loss in myelomonocytic differentiation of HSPCs. It has to be noted that RKIP KD as a single event, without the cytokine treatment, proved to be insufficient to induce myeloid differentiation.

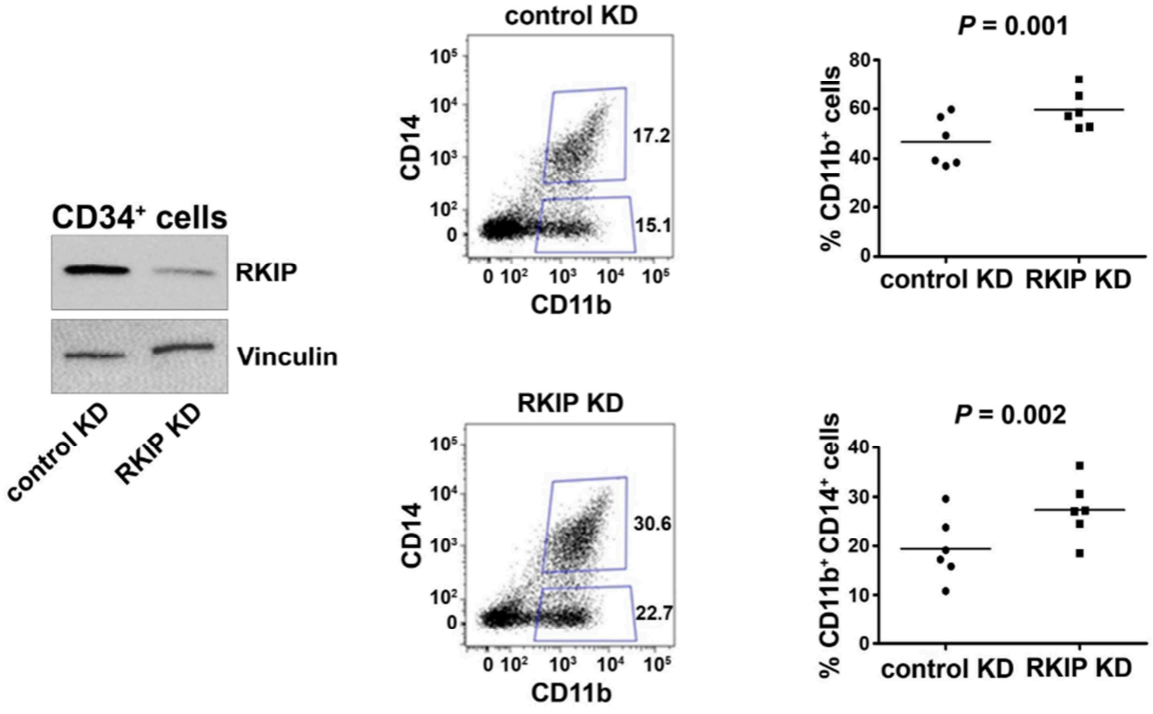

Figure 14. RKIP knockdown in CD34$^+$ human HSPCs increases myelomonocytic differentiation. On the left, the immunoblot shows the successful knockdown of RKIP in CD34$^+$ human HSPCs (RKIP KD) as compared to control cells (control KD). In the middle, representative flow cytometry plots show increased myelomonocytic differentiation, by the increased expression of the myelomonocytic surface markers CD11b and CD14, in CD34$^+$ HSPCs with RKIP KD. Both RKIP KD and control KD cells were treated with a cytokine mix including GM-CSF/FL/SCF/TNFa. On the right, the graphs show the results of the six experiments performed as well as the median. Student´s t-test was employed to calculate statistical significance. The figure is reproduced from (120) with permission of *Haematologica*.

To further corroborate the functional role of RKIP expression levels in myeloid lineage differentiation, we again used the 1,25D_3-based HL-60 differentiation model. HL-60 cells were transduced with either RKIP siRNA (Figure 15A) or overexpression constructs (Figure 15B), treated with 1,25D_3 to induce myeloid differentiation and afterwards the amount of myelomonocytic differentiation was assessed by checking the expression of the CD11c surface marker (147). On the one hand, HL-60 cells harboring RKIP knockdown, additionally treated with 1,25D_3, showed increased expression of CD11c (P=0.009) and therefore an increased myeloid differentiation (Figure 15C). On the other hand, the same treatment caused HL-60 cells with RKIP overexpression to have a decreased potential to differentiate into the myeloid lineage as compared to control cells (P=0.005; Figure 15D). When we tested the effects of RKIP modulation without 1,25D_3 treatment, we did not see a significant difference in the amount of myelomonocytic differentiation when comparing the different cells (P=0.112 for RKIP knockdown and P=0.168 for RKIP overexpression). This indicates that, also in the immature AML cell line HL-60, a modulation of RKIP expression has effects on the myelomonocytic differentiation capacity of these cells treated with 1,25D_3.

Altogether, these results show the functional relevance of RKIP loss in myelomonocytic differentiation.

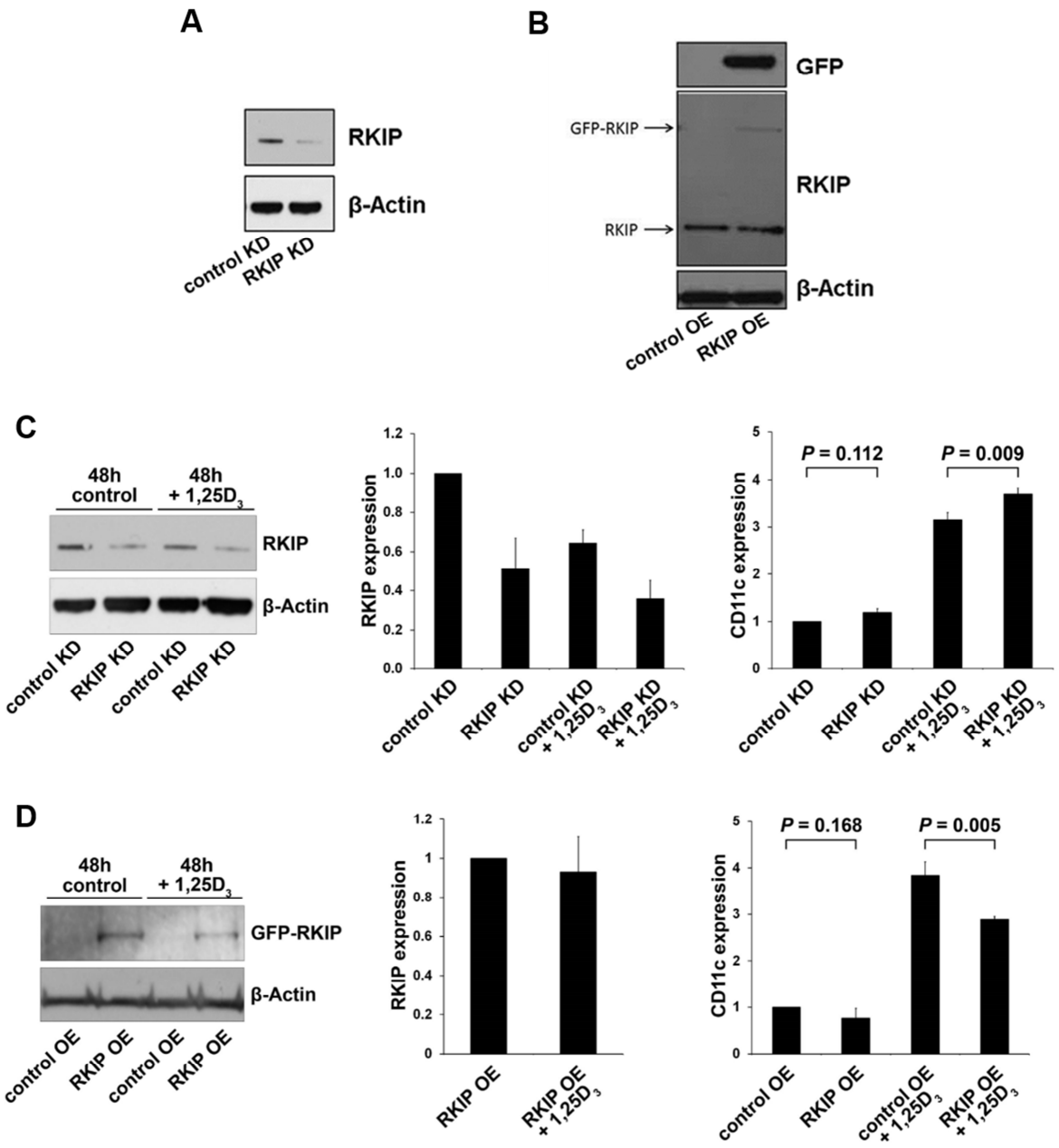

Figure 15. Knockdown of RKIP in HL-60 cells induces increased myelomonocytic differentiation while RKIP overexpression causes the opposite effect. Immunoblot showing the successful knockdown (A) and overexpression (B) of RKIP in HL-60 cells, performed using siRNA and lentiviral overexpression constructs, respectively. After transduction, these cells were treated with 10nM 1,25D_3 for 48 hours and the level of myelomonocytic differentiation was studied considering the expression levels of CD11c by flow cytometry. (C) On the left side, the immunoblot shows the successful knockdown of RKIP (RKIP KD) after 1,25D_3 treatment, while the graph on the right side represents the mean of three independent experiments ± S.D. for CD11c expression. Expression values are calculated as x-fold expression of HL-60 control cells (control KD). Student's t-test was used to calculate statistical significance. (D) On the left side, the immunoblot shows

the successful overexpression of RKIP (RKIP OE) after 1,25D_3 treatment. On the right side, the graph represents the mean of three independent experiments ± S.D. for CD11c expression. Expression values are calculated as x-fold expression of HL-60 control cells (control OE). Statistical significance was evaluated using Student's t-test. The figure is adapted from (120) with permission of *Haematologica*.

4.2.3. Deletion of Rkip in a murine model contributes to the development of a hematopoietic system characterized by myelomonocytic lineage bias

Having shown in-vitro that RKIP loss plays a functional role in myelomonocytic differentiation, we focused on studying its effects in-vivo. For this aim, we used a murine model with a complete deletion of the *Rkip* gene, hereby referred to as *Rkip-/-*. First, we analyzed the hematopoietic system of this mouse model, comparing it to a control murine model (*Rkip+/+*), as well as specific HSPC compartments (Figure 16; Table 9). As already observed in the in-vitro experiments, also in-vivo RKIP loss as a single event failed at increasing the amount of myelomonocytic cells in the various compartment analyzed at every time point. Together with the in-vitro data, these results suggest that RKIP modulates the sensitivity to extracellular inducers of differentiation and therefore RKIP loss alone is insufficient to produce an effect. For this reason, we injected intraperitoneally *Rkip-/-*, as well as *Rkip+/+* mice, with GM-CSF, in order to challenge their hematopoietic system (Figure 17A). After the GM-CSF treatment, *Rkip-/-* mice showed an increased percentage of myelomonocytic cells in BM, peritoneal cavity and PB when compared to control littermates, as assessed by analysis of PB smears as well as by flow cytometry using the markers CD11b and Ly6G (Figure 17B-C).

These results indicate that loss of RKIP increases the GM-CSF-induced myelomonocytic lineage commitment and differentiation of HSPCs.

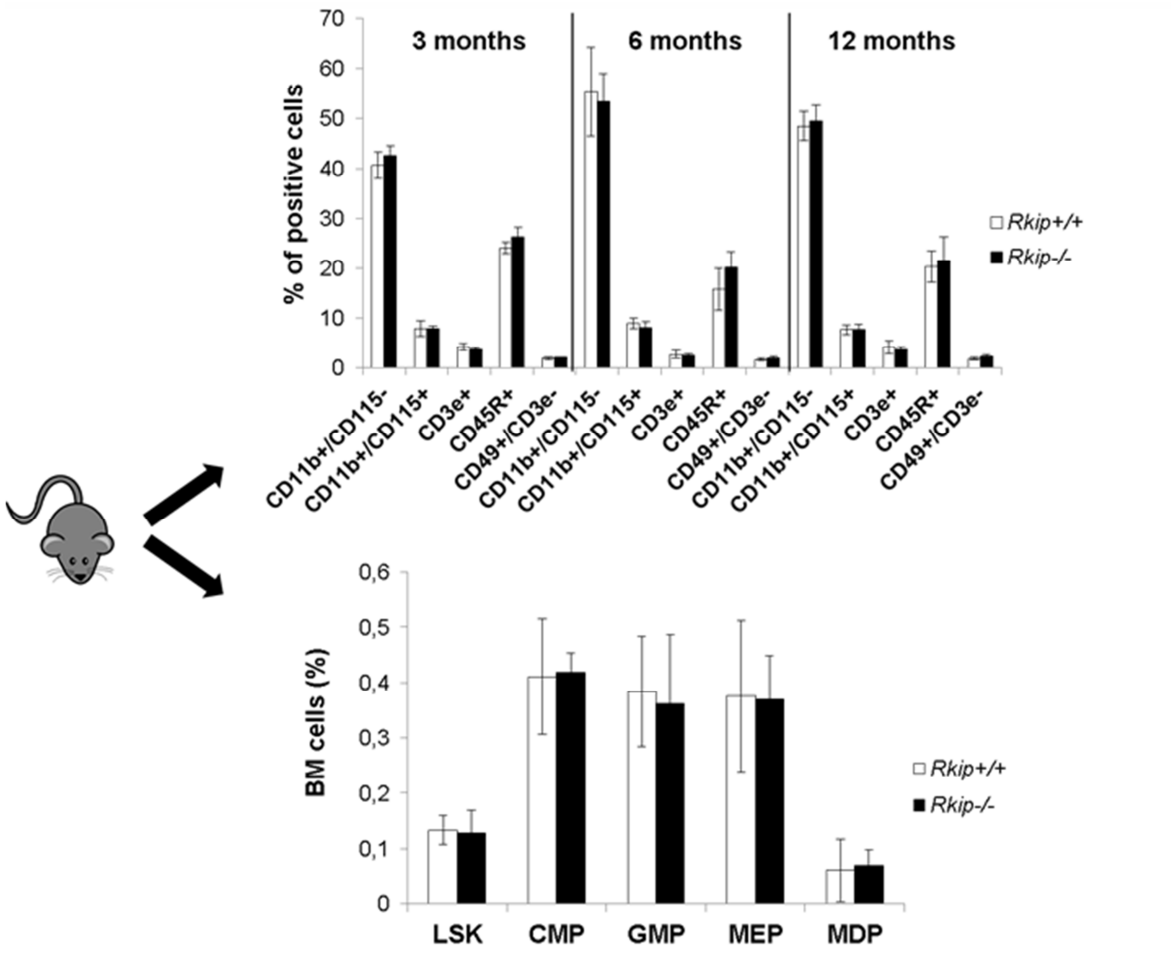

Figure 16. Characterization of the murine model with *Rkip* deletion. *Rkip*-/- mice, as well as control littermates, were sacrificed when 3-, 6- and 12-month-old. As visible in the upper graph, no significant differences were observed in the composition of leukocytes in PB when comparing *Rkip*-/- with *Rkip*+/+ mice. The same result was obtained when comparing hematopoietic progenitor compartments in BM, as seen in the graph below. Both graphs denote the average of at least four independent experiments ± S.D. and Student´s t-test was employed to study statistical significance.

Abbreviations: LSK (lin^-, Sca^+, kit^+); CMP (common myeloid progenitor, lin^-, Sca^-, kit^+, $FcγR^{lo}$, $CD34^+$); GMP (granulocyte macrophage progenitor, lin^-, Sca^-, kit^+, $FcγR^+$, $CD34^+$); MDP (macrophage dendritic cell progenitor, lin^-, Sca^-, kit^+, $CD115^+$, $CD135^+$); MEP (megakaryocyte erythrocyte progenitor, lin^-, Sca^-, kit^+, $FcγR^{lo}$, $CD34^-$). The figure is reproduced from (120) with permission of *Haematologica*.

		WBC (10^3/µl) [median]	Hb (g/dl) [median]	Hct (%) [median]	PLT (10^3/µl) [median]
3 months	***Rkip+/+***	4.36-12.02 [7.49] n=10	14.1-16.4 [14.8] n=10	43.4-49.9 [45.0] n=10	469.0-979.0 [634.5] n=10
	Rkip-/-	6.88-11.58 [10.35] n=9	13.1-16.1 [15] n=9	19.8-49.5 [45.8] n=9	211.0-665.0 [485.0] n=9
		P = 0.182	*P* = 0.604	*P* = 0.720	*P* = 0.095
6 months	***Rkip+/+***	4.59-13.81 [9.06] n=10	13.1-16.4 [15.3] n=10	43.8-56.0 [51.9] n=10	716.0-1214.0 [880.5] n=10
	Rkip-/-	8.28-19.46 [11.78] n=9	13.4-17.0 [15.2] n=9	46.2-59.1 [53.7] n=9	605.0-1126.0 [926.0] n=9
		P = 0.079	*P* = 0.780	*P* = 0.356	*P* = 0.780
9 months	***Rkip+/+***	3.58-12.03 [9.11] n=10	14.4-16.8 [15.5] n=10	42.8-50.3 [47.8] n=10	378.0-1599.0 [864.5] n=10
	Rkip-/-	7.24-15.71 [9.56] n=9	13.0-16.2 [14.9] n=9	42.9-51.1 [48.3] n=9	436.0-1268.0 [798.0] n=9
		P = 0.447	*P* = 0.079	*P* = 0.720	*P* = 0.604
12 months	***Rkip+/+***	4.78-12.2 [6.17] n=8	14.0-15.6 [14.4] n=8	31.6-47.7 [43.0] n=8	588.0-940.0 [787.0] n=8
	Rkip-/-	6.16-14.11 [10.36] n=9	12.5-17.1 [14.6] n=9	38.6-49.7 [44.4] n=9	409.0-1984.0 [926.0] n=9
		P = 0.068	*P* = 0.633	*P* = 0.146	*P* = 0.034

Table 9. Blood counts in *Rkip* mice. Results of the blood count performed in *Rkip-/-* mice as well as in control mice (*Rkip+/+*) at 3, 6, 9 and 12 months of age. The table depicts ranges, the respective medians are shown in square brackets. Student´s t-test was employed for calculating P-values.

WBC, white blood cells; Hb, hemoglobin; Hct, hematocrit; PLT, platelets. The table is reproduced from (120) with permission of *Haematologica*.

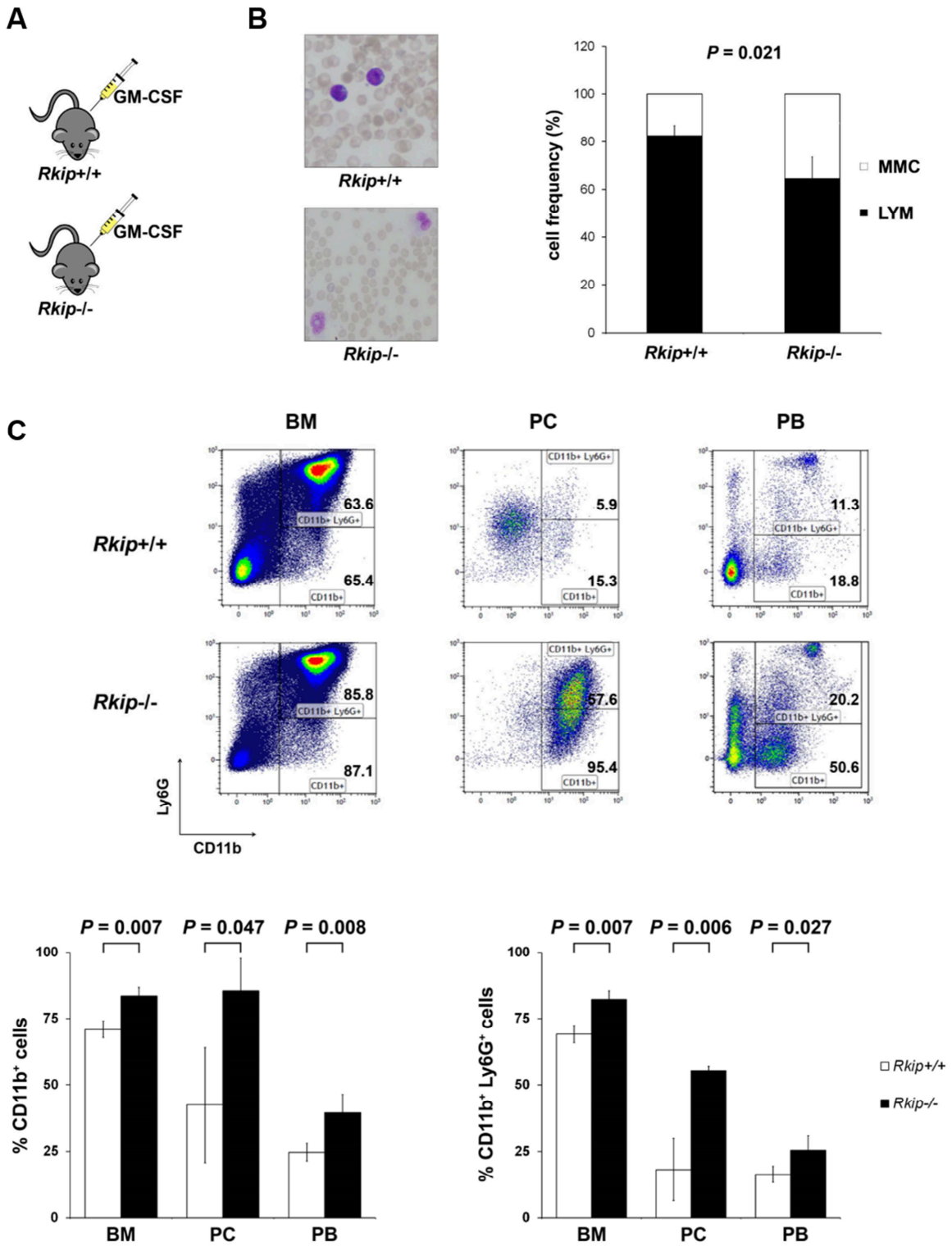

Figure 17. Deletion of *Rkip* in a murine model causes increased myeloid lineage commitment. (A) In order to assess the effects of GM-CSF treatment in a murine in-vivo model, four mice with *Rkip* knockout *(Rkip*-/-), as well as four control littermates (*Rkip*+/+) were injected intraperitoneally with GM-CSF as stated in the Materials and Methods section. (B) *Rkip*-/- mice showed an increased percentage of myelomonocytic cells (MMC) in the PB, as assessed by cytological analysis of blood smears from these animals. On

the left, a representative picture of PB smears is presented. The graph on the right side shows the average ± S.D., lymphoid cells are referred to as LYM. Student's t-test was employed to calculate statistical significance. (C) *Rkip*-/- animals also showed an increased percentage of $CD11b^+$ and $CD11b^+$ $Ly6G^+$ cells in the BM, peritoneal cavity (PC) and PB, as seen in the representative flow cytometric plots. The graphs denote the average ± S.D P-values were calculated using Student's t-test. The figure is reproduced from (120) with permission of *Haematologica*.

4.2.4. Deletion of Rkip in *Ras*-mutated mice aggravates myeloproliferation as well as the development of myelomonocytic MPD

With all the experiments performed, we could show that RKIP loss is functionally involved in increasing myelomonocytic lineage commitment both in-vitro and in-vivo. Since this is known to be a pre-phase step for myeloid leukemogenesis, we next aimed at identifying the role of RKIP loss in this process. Interestingly, our mouse model harboring a complete deletion of Rkip, *Rkip-/-*, did not develop myeloid neoplasias. This is in accordance with our functional assays, which show that RKIP loss acts as an amplifier of the activated GM-CSF/*RAS* signaling rather than having an effect as a single event. Therefore, we crossed our *Rkip* mouse model with *Nras*-mutated animals, to study the effects of *Rkip* loss on the development of *Ras*-mutated malignancies. This was done because, on the one hand, it was previously shown that RKIP loss and *RAS* mutations frequently co-occur in AML (86,117,119) and, on the other hand, because it was observed that RKIP loss potentiates the oncogenic effects of *RAS*-signaling mutations in-vitro (86,117).

In this study, we compared *Mx1-Cre/Nras*/*Rkip*-/- mice with *Nras/Rkip+/+* and *Mx1-Cre/Nras/Rkip+/+* littermates. Mice were electively sacrificed at an age of 180 days after the first pIpC injection, for mice presenting *Mx1-Cre*, and a comparable age for mice without. It has to be noted that *Nras*-mutated mice on a pure C57BL/6 background are known to develop MP, which preferentially affects the myelomonocytic lineage. However, it was previously shown that these mice ultimately succumb to HS, while only randomly developing full blown MPD (90). In our study, *Mx1-Cre/Nras*/*Rkip*-/- mice showed aggravated myeloproliferation when compared to *Nras*/*Rkip*+/+ as well as when compared to *Mx1-Cre/Nras*/*Rkip*+/+ animals. In particular, mice with *Rkip* knockout showed splenomegaly (Figure

18A), increased percentage of myeloid cells in PB, BM and SP, as assessed by increased percentage of cells with the myelomonocytic markers CD11b and Ly6G (Figure 18B), and increased myeloid infiltration of SP and liver, as seen by immunohistochemistry (Figure 18C). Interestingly, as previously shown by Li and colleagues (90), HS was detected in all the *Nras*-mutated animals analyzed. However, its presence was mitigated in the *Mx1-Cre/Nras*/*Rkip*-/- mice. Moreover, only *Mx1-Cre/Nras*/*Rkip*-/- mice showed a full-blown MPD, as indicated by leukocytosis in the PB (Figure 19A-B; Table 10) (137). We did not observe transformation into AML in any of the mice model employed, as assessed by flow cytometric and morphologic evaluation of PB, BM and SP.

Despite the aggravated MPD development in the *Nras*-mutated mice with *Rkip* deletion, the median survival between *Mx1-Cre/Nras*/*Rkip*-/- and *Mx1-Cre/Nras*/*Rkip*+/+ animals was similar (P=0.339; Figure 19C). We therefore proceeded to analyze moribund mice by histopathologic examination. *Mx1-Cre/Nras*/*Rkip*+/+ mice showed extensive HS development while *Mx1-Cre/Nras*/*Rkip*-/- animals exhibited a mitigated HS phenotype but an increased occurrence of MP and MPD (Figure 20; Table 11). Altogether, our data demonstrate that loss of RKIP contributes to aggravating the development of myeloproliferation and MPD in a murine model harboring *Nras* mutation.

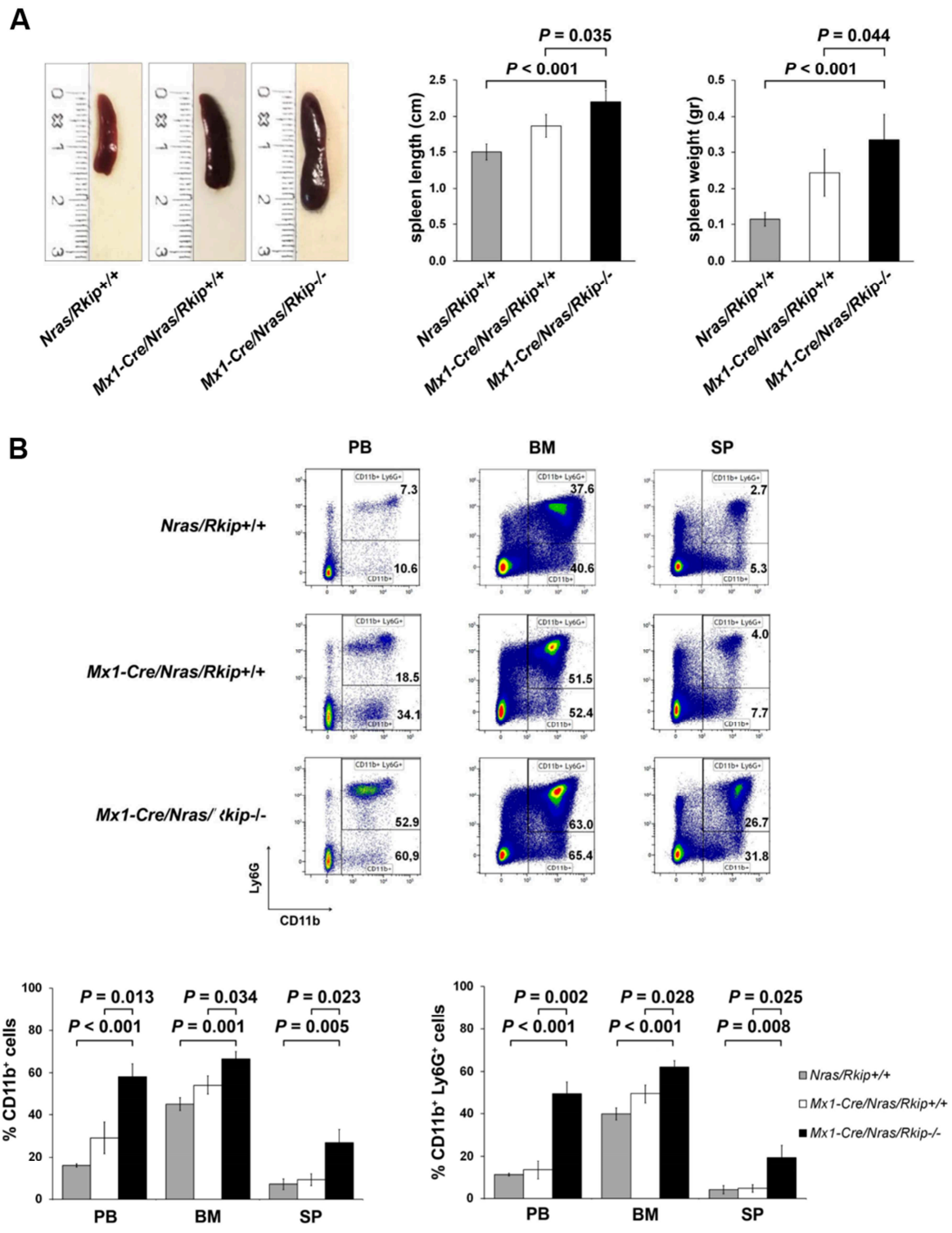
A
P = 0.035
P < 0.001
P = 0.044
P < 0.001
spleen length (cm)
spleen weight (gr)
Nras/Rkip+/+
Mx1-Cre/Nras/Rkip+/+
Mx1-Cre/Nras/Rkip-/-
B
PB
BM
SP
Nras/Rkip+/+
Mx1-Cre/Nras/Rkip+/+
Mx1-Cre/Nras/Rkip-/-
7.3
10.6
37.6
40.6
2.7
5.3
18.5
34.1
51.5
52.4
4.0
7.7
52.9
60,9
63.0
65.4
26.7
31.8
Ly6G
CD11b
P = 0.013
P < 0.001
P = 0.034
P = 0.001
P = 0.023
P = 0.005
% CD11b+ cells
P = 0.002
P < 0.001
P = 0.028
P < 0.001
P = 0.025
P = 0.008
% CD11b+ Ly6G+ cells
Nras/Rkip+/+
Mx1-Cre/Nras/Rkip+/+
Mx1-Cre/Nras/Rkip-/-

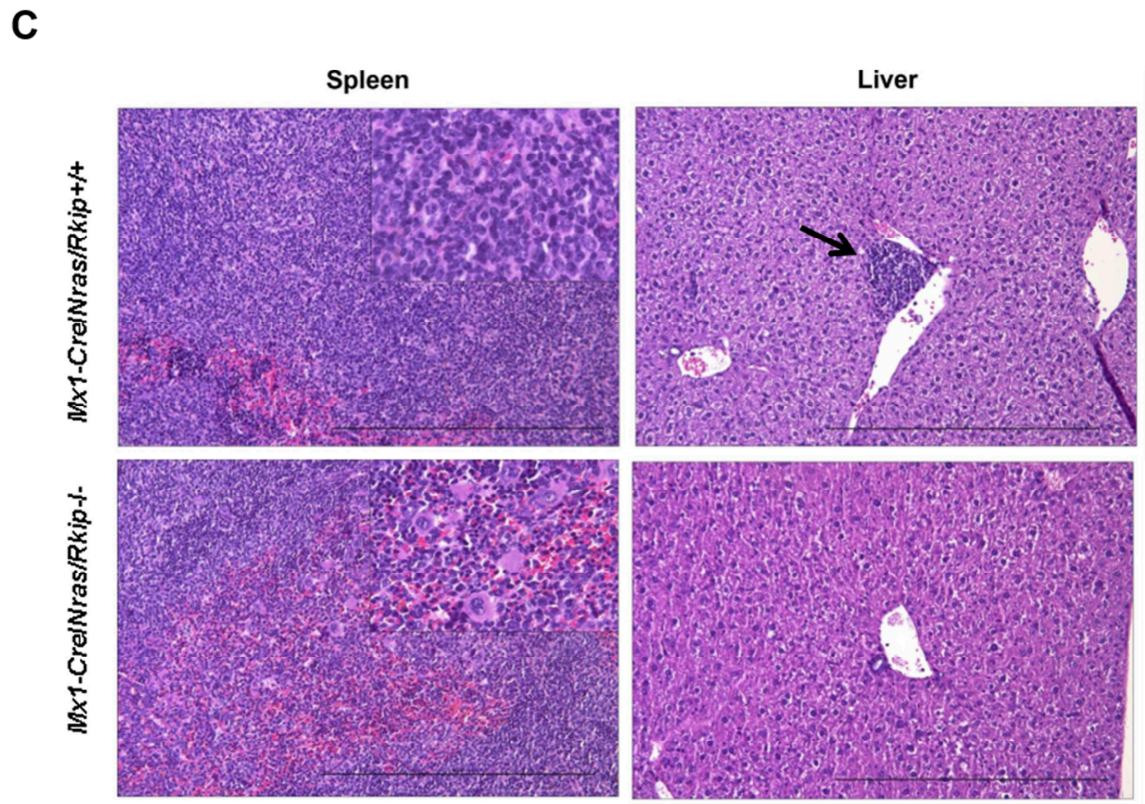

Figure 18. Knockout of *Rkip* in *Nras*-mutated mice aggravates MP and MPD while mitigating HS development. *Mx1-Cre/Nras/Rkip*-/- mice (n=3) and control mice (*Mx1-Cre/Nras/Rkip*+/+; n=3) were electively sacrificed at an age of six months after the first pIpC injection, while *Nras/Rkip*+/+ mice were killed at a comparable age. Different organs of these mice were analyzed and compared. (A) Animals harboring Rkip knockout show splenomegaly, as visible in the representative images of the SP from the indicated genotyping. The bar graphs on the right side show the SP lengths and weights, respectively. The graphs depict the average ± S.D. and Student´s t-test was used to calculate statistical significance. (B) Representative flow cytometric plots show that *Mx1-Cre/Nras/Rkip*-/- mice have an increased percentage of $CD11b^+$ and $CD11b^+$ $Ly6G^+$ myelomonocytic cells in PB, BM and SP when compared to *Mx1-Cre/Nras/Rkip*+/+ animals as well as when compared to *Nras/Rkip*+/+ littermates. The graphs show the average ± S.D. and for calculating statistical significance the Student´s t-test was employed. (C) Representative sections of SP and liver, stained with H&E staining, of the mouse genotypes as indicated in the picture when sacrificed 6 months after the first pIpC injection. On the one hand, as observed in the flow cytometric analysis, mice with *Rkip* knockout showed increased MP, as visible in the SP (bottom left and insert bottom left, showing the presence of multiple megakaryocytes), as compared to the control littermates with *Rkip* normal (SP top left, and insert top left showing almost exclusively HS). On the other hand, *Mx1-Cre/Nras/Rkip+/+* mice showed infiltration by HS, as visible in the liver

(top right, arrow), while in mice with *Rkip* knockout the formation of HS was mitigated (bottom right, no infiltrate). The black bar indicates a length of 500 µm. The figure is adapted from (120) with permission of *Haematologica*.

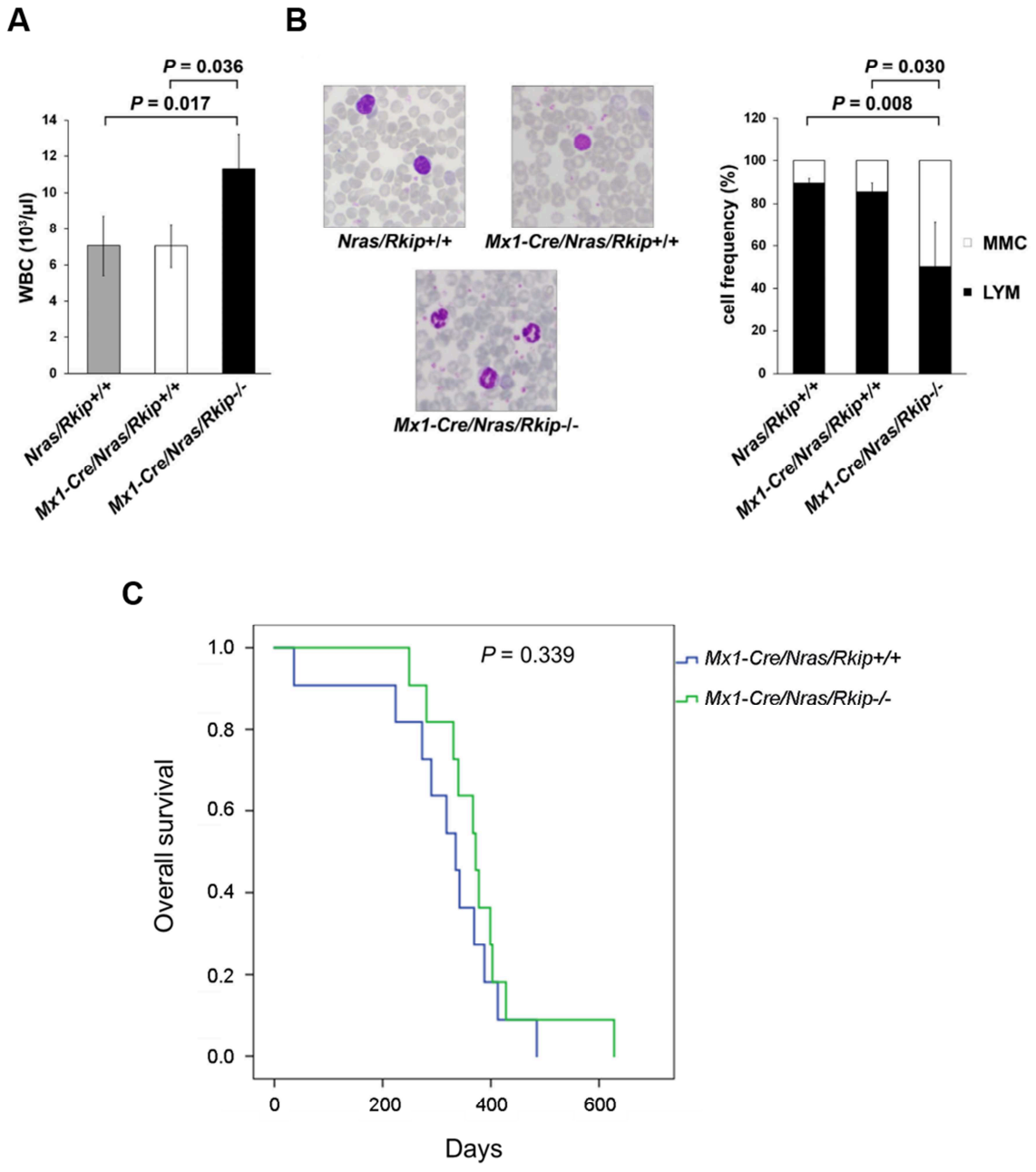

Figure 19. *Rkip* knockout in an *Nras*-mutated murine model causes leukocytosis, increased activation of the *RAS* pathway but no difference in survival. (A) The blood of *Mx1-Cre/Nras/Rkip*-/- mice shows an increase in the number of white blood cells (WBC) when compared to *Mx1-Cre/Nras/Rkip*+/+ as well as *Nras/Rkip*+/+ animals in PB counts. (B) This leukocytosis in *Mx1-Cre/Nras/Rkip*-/- mice derives from an increased number of

myelomonocytic cells (MMC) in the blood of these animals, as visible in the representative PB smear on the left side as well as the correspondent graph on the right side and in the flow cytometric analyses shown in Figure 18. The graphs indicate the average ± S.D. and P-values were calculated using Student´s t-test. (C) No significant difference was observed in the survival rate of *Mx1-Cre/Nras/Rkip*-/- (n=11) when compared to control littermates (*Mx1-Cre/Nras/Rkip*+/+, n=11). A log-rank test was employed to calculate statistical significance. The figure is adapted from (120) with permission of *Haematologica*.

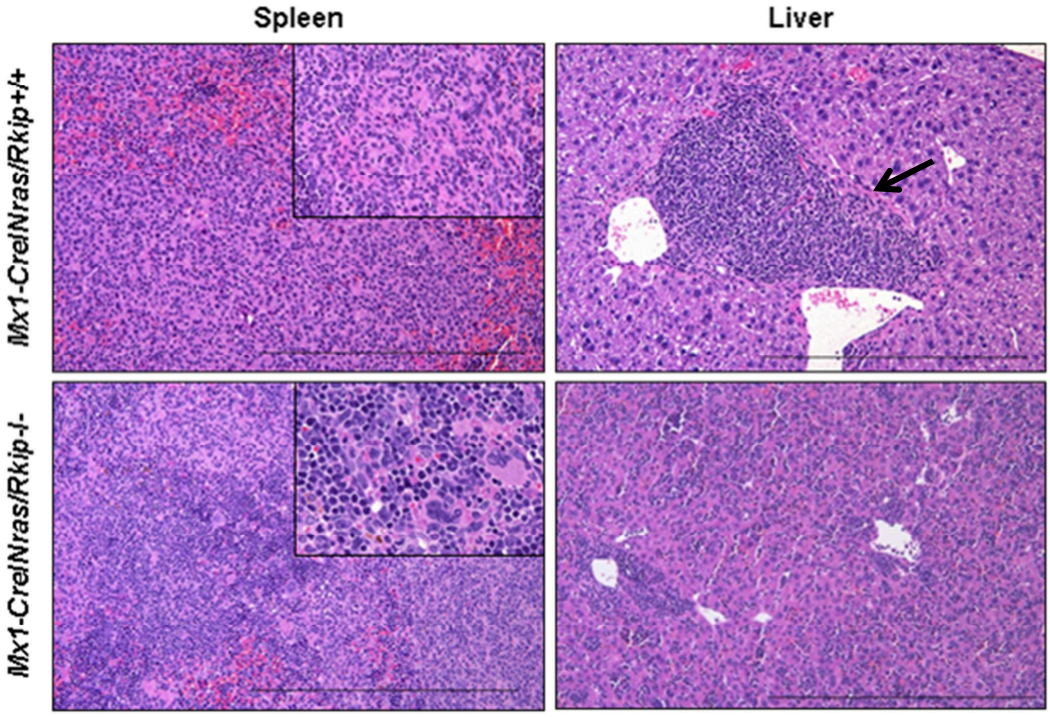

Figure 20. Increased myeloproliferation in *Nras*-mutated mice with additional *Rkip* knockout corresponds with a reduced histiocytic sarcoma development. *Mx1-Cre/Nras/Rkip-/-* mice as well as control littermates (*Mx1-Cre/Nras/Rkip+/+*) were sacrificed when moribund. Here are depicted representative H&E stained sections of SP and liver from both genotypes. As previously observed in mice sacrificed 6 months after the first pIpC injection, on the one hand *Rkip* knockout caused increased MP in the *Nras*-mutated mice (as visible in the SP, bottom left, as well as in the insert, showing multiple megakaryocytes) when compared to the *Mx1-Cre/Nras/Rkip+/+* mice (SP and insert, top left, where almost exclusively HS is visible). On the other hand, the formation of HS appeared mitigated in the mice with *Rkip* deletion, as visible in the liver (bottom right, only small infiltrates present) compared to the liver from control mice, showing an extensive

infiltration by HS (top right, arrow). The black bar indicates a distance of 500 µm. The figure is reproduced from (120) with permission of *Haematologica*.

	WBC (10^3/µl) [median]	Hb (g/dl) [median]	Hct (%) [median]	PLT (10^3/µl) [median]
Nras/Rkip+/+	4.60-9.70 [6.80] n=5	9.20-15.50 [15.20] n=5	30.50-49.20 [48.50] n=5	454.00-1952.00 [1214.00] n=5
Mx1-Cre/Nras/Rkip+/+	5.80-8.65 [6.70] n=3	6.80-12.60 [11.90] n=3	24.90-41.50 [38.80] n=3	99.00-1106.00 [865.00] n=3
Mx1-Cre/Nras/Rkip-/-	9.78-14.57 [10.42] n=4	13.60-19.40 [14.00] n=4	39.30-60.00 [39.85] n=4	289.00-1368.00 [948.00] n=4
Nras/Rkip+/+ **vs** ***Mx1-Cre/Nras/Rkip-/-***	*P* = 0.017	*P* = 0.961	*P* = 0.532	*P* = 0.449
Mx1-Cre/Nras/Rkip+/+ **vs** ***Mx1-Cre/Nras/Rkip-/-***	*P* = 0.036	*P* = 0.248	*P* = 0.085	*P* = 0.622

Table 10. Blood counts of *Nras*-mutated mice. Results of the blood counts performed at 180 days after the first pIpC injection in *Nras/Rkip*+/+, *Mx1-Cre/Nras/Rkip*+/+ as well as *Mx1-Cre/Nras/Rkip*-/- mice. The table shows ranges, respective medians are presented in square brackets. P-values were calculated using the Student´s t-test.

WBC, white blood cells; Hb, hemoglobin; Hct, hematocrit; PLT, platelets. The table is reproduced from (120) with permission of *Haematologica*.

Genotype	Mouse ID	WBC (10^3/µl)	Hb (g/dl)	Hct (%)	PLT (10^3/µl)	HS	MP	MPD
Mx1-Cre/Nras/Rkip+/+	**#1121**	7.90	15.70	48.60	1421.00	++	+	-
Mx1-Cre/Nras/Rkip+/+	**#1249**	28.40	12.00	40.00	2029.00	++	++	+
Mx1-Cre/Nras/Rkip+/+	**#1301**	6.20	15.10	48.60	1329.00	++	+	-
Mx1-Cre/Nras/Rkip+/+	**#1455**	5.40	14.40	47.50	1170.00	+	++	-
Mx1-Cre/Nras/Rkip-/-	**#1139**	84.30	8.20	26.90	321.00	+	+++	+
Mx1-Cre/Nras/Rkip-/-	**#1176**	11.30	11.60	37.40	837.00	++	++	+
Mx1-Cre/Nras/Rkip-/-	**#1134**	80.10	14.30	45.50	124.00	+	+++	+
Mx1-Cre/Nras/Rkip-/-	**#1278**	28.60	14.50	46.70	1788.00	+	+++	+
Mx1-Cre/Nras/Rkip-/-	**#1434**	15.20	14.80	45.60	1120.00	+	++	+
Mx1-Cre/Nras/Rkip-/-	**#1263**	23.30	14.00	44.00	1481.00	++	+++	+
Mx1-Cre/Nras/Rkip-/-	**#1342**	23.40	12.20	37.70	1454.00	+	+++	+

Table 11. Blood count from moribund mice. *Mx1-Cre/Nras/Rkip*+/+ and *Mx1-Cre/Nras/Rkip*-/- mice were sacrificed when moribund. The table shows the results of the

blood counts from these animals (abbreviations: WBC, white blood cells; Hb, hemoglobin; Hct, hematocrit; PLT, platelets). Moreover, the organs from these mice were analyzed as described in the Materials and Methods section and presence and severity of HS, MP and MPD, respectively, are shown. The table is reproduced from (120) with permission of *Haematologica*.

4.2.5. RKIP loss causes increased activation of the *RAS-MAPK/ERK* pathway

Since RKIP is a negative regulator of the *RAS-MAPK/ERK* pathway, we tested whether the knockdown of RKIP could enhance this signaling pathway in HSPCs. To do this, we evaluated the phosphorylation of ERK (pERK) in HSPCs with knockdown of RKIP (RKIP KD) as well as in control HPSCs (control KD). Interestingly, HSPCs harboring RKIP knockdown showed increased pERK levels as compared to control (Figure 21A), suggesting that the aggravation of myeloid differentiation induced by RKIP loss might be mediated by the activation of the *RAS-MAPK/ERK* signaling pathway. Moreover, we wanted to test also in HL-60 cells, whether knockdown of RKIP expression correlated with an increased activation of the *RAS-MAPK/ERK* signaling pathway. For this reason, we studied the expression levels of pERK in HL-60 cells lentivirally transduced to have RKIP downregulation as well as in control HL-60 cells (Figure 21B). As observed in healthy $CD34^+$ HSPCs, the knockdown of RKIP increased pERK levels, thereby confirming a role for RKIP as a regulator of the *RAS-MAPK/ERK* signaling. According to in-vitro experiments, deletion of *Rkip* caused increased pERK levels also in murine models. This was observed in $CD11b^+$ cells isolated from *Rkip-/-* mice, indicating an enhanced activation of the *RAS-MAPK/ERK* pathway in these animals (Figure 21C). The same result was obtained in *Nras*-mutated mice, both in absence and presence of GM-CSF stimulation. In detail, we observed an increase of pERK levels in *Mx1-Cre/Nras/Rkip-/-* mice without the addition of cytokines (Figure 21D). When the $CD11b^+$ cells were treated with GM-CSF (Figure 21E), *Rkip* deletion increased ERK phosphorylation under these conditions as well. Al together, these data indicate RKIP loss as an aberration which causes activation of the *RAS-MAPK/ERK* pathway.

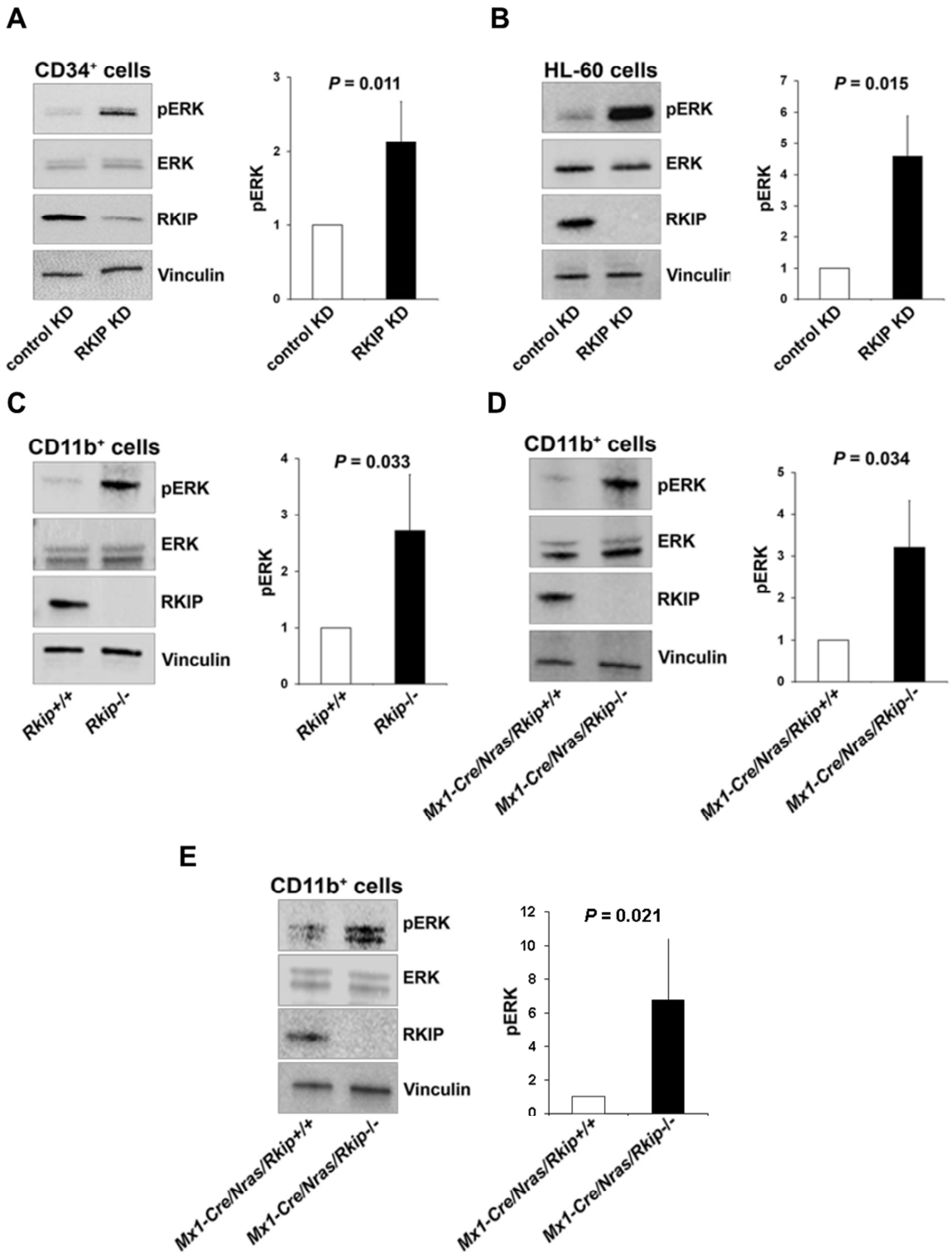

Figure 21. Loss of RKIP expression causes activation of the *RAS-MAPK/ERK* signaling pathway. Lentiviral knockdown of RKIP (RKIP KD) in CD34$^+$ human HSPCs (A) and HL-60 AML cells (B) increased also the *RAS-MAPK/ERK* signaling, as measured by increased phosphorylation of ERK (pERK). (C) Also in a murine model, knockout of *Rkip*

increased the activation of the *RAS-MAPK/ERK* signaling pathway. For this analysis, $CD11b^+$ cells isolated from the BM of *Rkip-/-* and control mice (*Rkip+/+*) were used. *Rkip* knockout caused increased activation of the *RAS*-MAPK/ERK signaling pathway also in $CD11b^+$ cells isolated from *Nras*-mutated mice, both in absence (D) and in presence (E) of GM-CSF stimulation. The $CD11b^+$ cells were isolated in absence of FBS and, in the case of figure E, stimulated with 10 ng/ml GM-CSF in serum-free HBSS media for 15 minutes. For the mice experiments, n=3 mice for each genotype were employed. For all the figures, a representative immunoblot is displayed on the left side, while the graph on the right side shows the mean of three independent experiments ± S.D. pERK intensity is given as x-fold change to the control KD cells or to the control mice harboring normal *Rkip* expression. Statistical significance calculated employing Student's t-test. The figure is adapted from (120) with permission of *Haematologica*.

4.2.6. Loss of RKIP is frequently detected in primary CMML patient samples and often co-occurs with mutations affecting the *RAS*-signaling pathway

Lastly, we decided to investigate the clinical relevance of these findings. Increased myeloid lineage commitment and *RAS*-signaling aberrations are typical manifestations of the pathogenesis of CMML. Since loss of RKIP increases both, myeloid differentiation and *RAS*-pathway activation, we aimed at investigating the role of RKIP loss in CMML. For this reason, we analyzed a cohort comprising 41 primary CMML patient specimens, whose clinical characteristics as well as treatment regimens are described in Table 12. Expression of RKIP was studied by means of immunoblot, as previously described (86,119), and a loss of RKIP was observed in 12/41 CMML specimens (29.3%; Figure 22A-B). Interestingly, RKIP loss was observed not only at protein level, but also at mRNA level ($P<0.001$), as assessed by qPCR (Figure 22C). It has been previously shown in AML that RKIP loss is caused by increased expression of miR-23a which causes the decay of *RKIP* mRNA via binding to its 3'-UTR (118,119). Our results indicate that the same mechanism might be present also in CMML.

Moreover, we observed that a loss of RKIP in patient samples correlated with an increased percentage of myelomonocytic cells (MMC; monocytes and granulocytes) in the PB (86% vs 76%, $P=0.030$; Table 12), indicating a more pronounced myelomonocytic phenotype in these patients. This result is in

agreement with our functional experiments as well as with previous findings in AML (86).

It is important to observe that OS was similar when comparing patients with and without loss of RKIP (P=0.913; Figure 22D). However, it has to be noted that the small sample size of the cohort analyzed precluded an analysis performed after grouping the patients depending on the treatment they received.

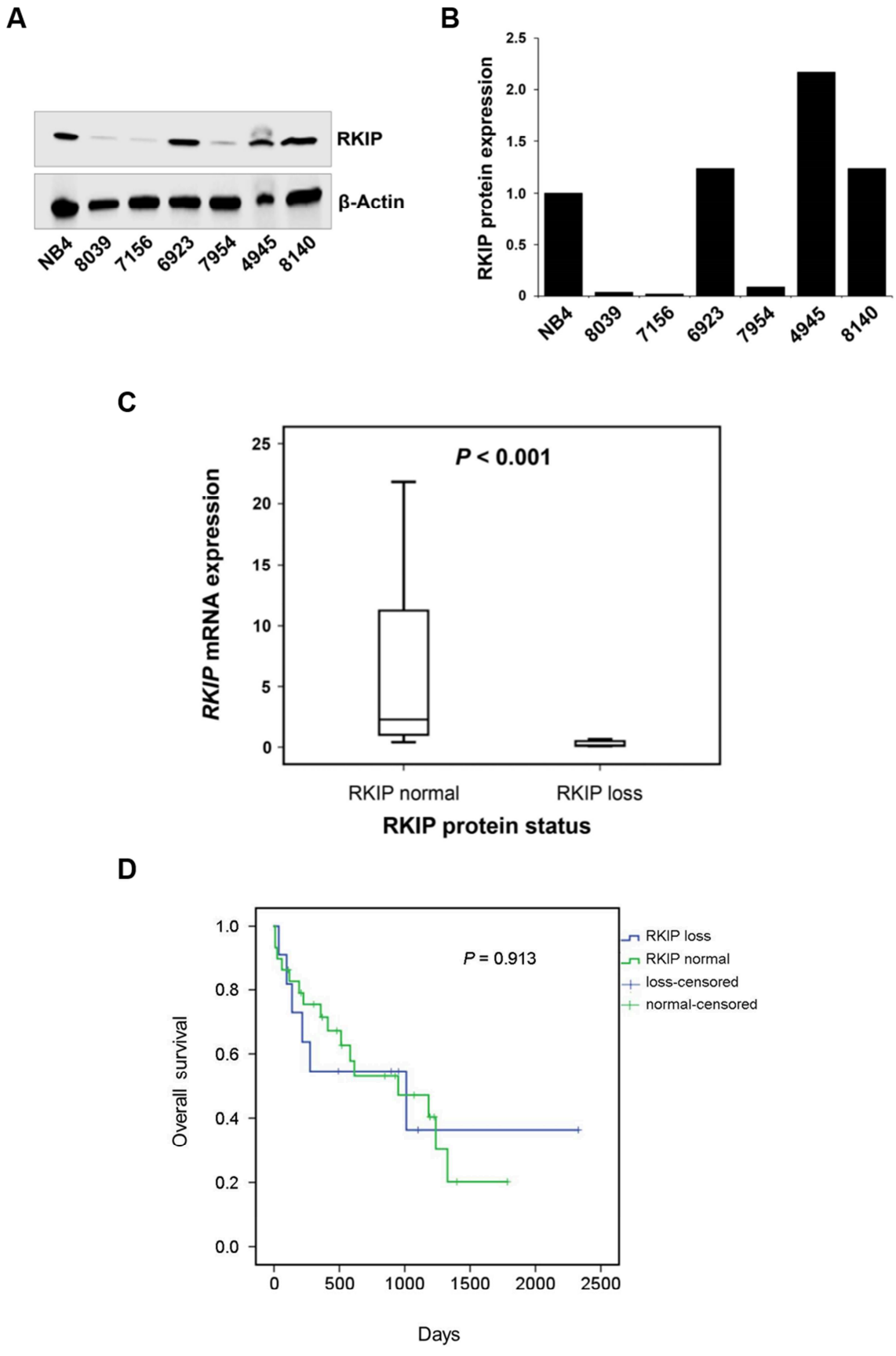
A
RKIP
β-Actin
NB4
8039
7156
6923
7954
4945
8140
B
RKIP protein expression
2.5
2.0
1.5
1.0
0.5
0
NB4
8039
7156
6923
7954
4945
8140
C
P < 0.001
RKIP mRNA expression
25
20
15
10
5
0
RKIP normal
RKIP loss
RKIP protein status
D
P = 0.913
Overall survival
1.0
0.8
0.6
0.4
0.2
0.0
0
500
1000
1500
2000
2500
Days
RKIP loss
RKIP normal
loss-censored
normal-censored

Figure 22. Loss of RKIP expression, both at protein and mRNA level, is a frequent event in CMML patients but does not affect their survival. (A) Loss of RKIP protein expression, defined as previously described (86), was observed in 12/41 (29.3%) primary CMML patient samples. The representative immunoblot depicts RKIP protein loss in patients 8039, 7156 and 7954. (B) The graph shows the x-fold change of RKIP protein expression in the CMML patients as compared with NB4 cells. NB4 AML cells were chosen as a calibrator due to their physiologic RKIP expression levels (86) and their RKIP expression was arbitrarily set to 1. (C) *RKIP* mRNA levels were calculated by qPCR and the box plots show the results in CMML patients considered either having RKIP normal or RKIP loss at the protein level, depending on the immunoblot results. NB4 AML cells were used as a calibrator and the Wilcoxon-Mann–Whitney test was used to calculate statistical significance. (D) Overall survival, calculated using a log-rank test, did not show any significant difference between CMML patients with RKIP loss (n=12) and those with RKIP normal (n=29). The figure is adapted from (120) with permission of *Haematologica*.

	total	RKIP loss	RKIP normal	p-value
n	41/41 (100%)	12/41 (29%)	29/41 (71%)	
Age at diagnosis (y)	69 (54-85)	72 (60-85)	67 (54-84)	0.180
Sex				0.734
male (n)	23/41 (56%)	6/12 (50%)	17/29 (59%)	
female (n)	18/41 (44%)	6/12 (50%)	12/29 (41%)	
MMC (%)	79 (27-96)	86 (80-91)	76 (27-96)	0.030
AML transformation (n)	23/41 (56%)	8/12 (66%)	15/29 (52%)	0.497
Karyotype				0.458
normal (n)	22/27 (81%)	6/6 (100%)	16/21 (76%)	
-7 (n)	1/27 (4%)	0/6 (0%)	1/21 (5%)	
+8 (n)	3/27 (11%)	0/6 (0%)	3/21 (14%)	
complex	1/27 (4%)	0/6 (0%)	1/21 (5%)	
Therapy				0.471
BSC	22/37 (60%)	5/10 (50%)	17/27 (63%)	
HMA	12/37 (32%)	5/10 (50%)	7/27 (26%)	
low-dose AraC	2/37 (5%)	0/10 (0%)	2/27 (7%)	
Allo-SCT	1/37 (3%)	0/10 (0%)	1/27 (4%)	

Table 12. Clinical characteristic of the CMML primary patient samples. The clinical characteristics of all the 41 primary CMML patient samples studied are depicted. For “age at diagnosis” and myelomonocytic cells (MMC), the median with the ranges in parentheses are shown in the table. For calculating statistical significance, Wilcoxon-

Mann-Whitney test was used for all continuous variables and Fisher´s exact test was employed for all dichotomous variables.

Abbreviations: BSC, best supportive care; HMA, hypomethylating agents; AraC, cytarabine; Allo-SCT, allogeneic stem cell transplantation. The table is reproduced from (120) with permission of *Haematologica*.

In order to analyze the molecular landscape associated with CMML patients harboring RKIP loss, 39 genes recurrently mutated in myeloid neoplasias were investigated using NGS (Figure 23; Table 13). This analysis could be performed in 37/41 patient specimens and we observed a total number of 186 mutations affecting 37/37 (100%) of the patients, out of which 33/37 showed more than one mutation and a median of four variants per sample (ranging from 1 to 32). The genes which appeared to be most frequently affected were *TET2* (75.7%), *SRSF2* (46.0%), *CBL* (24.3%), and *ASXL1* (24.3%). 13/37 (35.1%) CMML patients showed one or more mutations in NRAS or KRAS and this high frequency resulted even increased when we considered mutations affecting all the genes in the *RAS*-signaling group (29/37, 78.4%; including *NRAS, KRAS, CBL, PTPN11, FLT3, CSF3R, KIT, JAK2, and NF1*). Interestingly, 11/12 (91.7%) of the patients harboring RKIP loss exhibited one or more mutations affecting the genes belonging to the *RAS*-signaling pathway. As previously published for AML, these results show, that RKIP loss and *RAS* mutations co-occur in myeloid neoplasms too. Interestingly, mutations affecting the *RAS*-signaling pathway were present also in 72% (18/25) of the patients with RKIP normal. This suggests that not only RKIP, but also other second genetic hits, can interact with mutations of the *RAS*-signaling pathway, causing myeloid leukemogenesis.

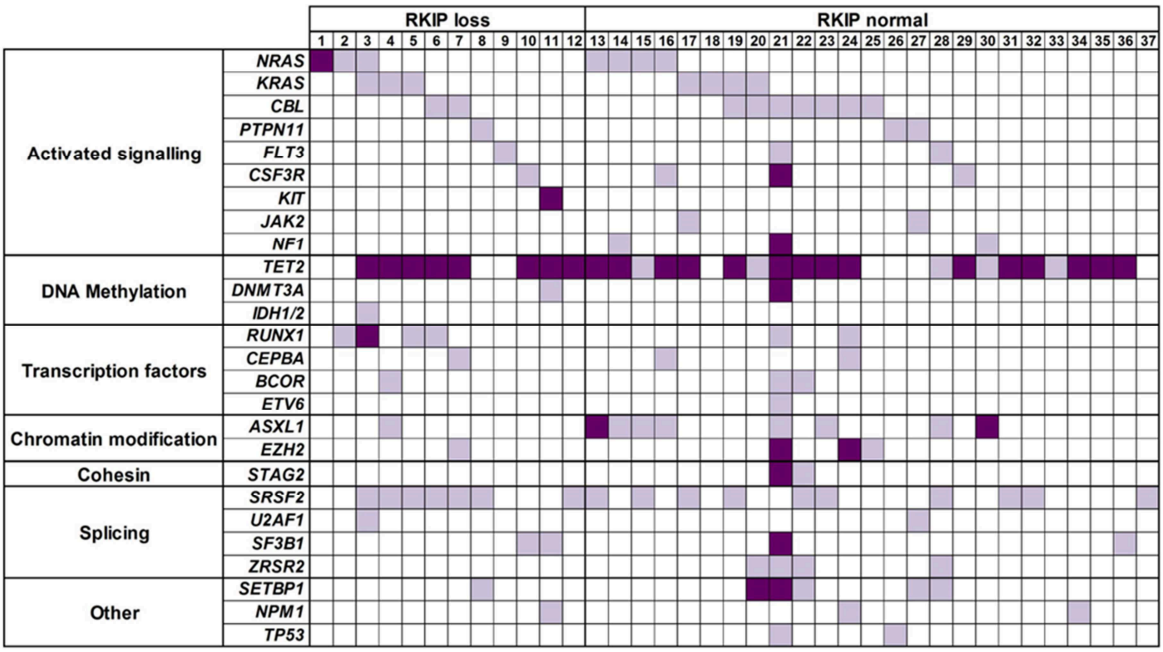

Figure 23. CMML patients with RKIP loss show a high frequency of mutation affecting the *RAS*-signaling pathway. NGS was employed to screen for mutations affecting 39 genes recurrently mutated in myeloid neoplasias, as previously described (42). Only genes carrying at least one mutation are shown in the figure. The heatmap depicts the number and distribution of the mutations observed in every CMML patient with sufficient material to perform this analysis (n=37). Every column indicates one CMML patient, belonging to the group "RKIP loss" or "RKIP normal" depending on the immunoblot results. The presence of one mutation is indicated with light purple while dark purple indicates the presence of more than one mutation. The figure is reproduced from (120) with permission of *Haematologica*.

Patient	Gene	Nucleotide change	Amino acid change
#1	*NRAS*	c.G35A	p.G12D
#2	*NRAS*	c.G35A	p.G12D
#3	*NRAS*	c.G35A	p.G12D
	KRAS	c.G34A	p.G12S
#4	*KRAS*	c.G35T	p.G12V
#5	*KRAS*	c.C176G	p.A59G
#13	*NRAS*	c.G38A	p.G13D
#14	*NRAS*	c.G38A	p.G13D
#15	*NRAS*	c.G35A	p.G12D
#16	*NRAS*	c.G34A	p.G12S
#17	*KRAS*	c.A182G	p.Q61R
#18	*KRAS*	c.G35C	p.G12A
#19	*KRAS*	c.G57T	p.L19F
#20	*KRAS*	c.G34A	p.G12S

Table 13. Details about the RAS mutations in the CMML patients. The details of all the *RAS* mutations found in the CMML primary patient samples by NGS are depicted. The first column ("patient") refers to the CMML patients in Figure 23, classified as either "RKIP loss" or "RKIP normal". The table is reproduced from (120) with permission of *Haematologica*.

5. Discussion

In this thesis work, we aimed at investigating the role of RKIP in myeloid malignancies. Previous research from our group, performed employing AML patient specimens and cell lines, showed that loss of RKIP is functionally relevant for leukemogenesis in AML (86,116,117). Following this finding, we tried to extend our knowledge about RKIP loss in the development of myeloid malignancies. In particular, we investigated its involvement in the development of MS and CMML.

5.1. Loss of the metastasis-suppressor RKIP contributes to the development of MS

The role of RKIP as a metastasis-suppressor is well-established in various solid cancers (99,105,139). Since MS is a subtype of AML, in which myeloid cells invade extramedullary tissues and form solid tumor masses, we aimed at investigating a possible role of RKIP loss in MS.

For our aim, we employed two AML cell lines - THP-1 and U937 - and performed lentiviral knockdown of RKIP expression. These cells were then used for in-vitro migration and invasion experiments, in order to test the effects of RKIP on these phenomena. In both cell lines, knockdown of RKIP resulted in an enhanced migration and invasion potential. Migration and invasion experiments were performed also employing THP-1 and U937 cells harbouring RKIP overexpression. Conversely to what we obtained with RKIP knockdown, overexpression of RKIP reduced the migration and invasion potential of AML cells. These results indicate that modulation of RKIP plays a role in the infiltration of myeloid cells in an in-vitro setting. Our findings are in agreement with previous studies performed in solid tumors, in which RKIP inhibited the migration and invasion potential of various cancer cell lines as well (106,108,148–150). It has to be noted that, even if we could significantly reduce endogenous RKIP expression, we did not achieve a complete knockout. Therefore, the results obtained in the cell lines with RKIP knockdown might be partly inhibited by the residual RKIP expression. Future experiments, employing for example the CRISPR-Cas9 methodology, could help in achieving a complete knockout of RKIP and, therefore, a more reliable in-vitro model. To further evaluate the role of RKIP loss in-vivo, we employed the CAM assay. This experiment is performed using chicken embryos, and is a well-

established system to study the infiltration of cells as well as the formation of tumor masses (151). Moreover, the use of this animal model presents numerous advantages. Chicken embryos develop in only four weeks, can be maintained easily and are relatively inexpensive. Most importantly for our study, this model is easily accessible for experimental manipulation and imaging. CAM experiments were performed employing THP-1 cells with stable RKIP knockdown. As previously observed in-vitro, RKIP loss also caused infiltration of leukemic cells as well as formation of a solid tumor mass in-vivo. On the contrary, control cells failed at invading the CAM. Since the invasion potential observed in control cells appeared to be already extremely low, we refrained from repeating this experiment employing THP-1 cells with RKIP overexpression. The CAM assay had been employed previously to study RKIP effects in-vivo in solid tumors. For example, Martinho and colleagues performed this experiment using glioma and cervical cancer cells (149,150). In agreement with our results, they could observe an increase in the size of the tumors formed by cells with RKIP knockdown, but their results were not significant when compared to control cells. The cause of this difference might be technical, since we used Matrigel for our experiments, or tumor-specific. Our results are also in agreement with other studies, where different solid tumor cell lines were tested in murine xenograft models (106,108,148). Also in this context, knockdown of RKIP favoured the invasion of tumor cells and the formation of metastasis. All together, these results evidence, that loss of RKIP expression is indeed involved in enabling the tissue infiltration of leukemic cells on the one hand, and in subsequent formation of solid tumor masses on the other hand, indicating a possible role of RKIP loss in MS development.

Next, we investigated the pathway, through which RKIP loss acts in MS development. Since RKIP is a negative regulator of the *RAS-MAPK/ERK* pathway, we hypothesized that the aberrant activation of this signaling cascade following RKIP loss could cause MS. Moreover, the *RAS-MAPK/ERK* pathway is altered in around 30% of cancers and has been reported to play a role in metastasis formation, as well as in invasiveness in-vitro (110,152). In order to test this hypothesis, we employed a MEK inhibitor. This substance blocks the *RAS*-signaling pathway and, therefore, mimes the presence of RKIP, even when RKIP

expression is knocked down. However, the use of a MEK inhibitor failed to reverse the effects of RKIP loss. In detail, cells with RKIP knockdown, either treated or not with the MEK inhibitor, retained the same migration potential. This indicates that the role of RKIP loss in MS probably acts through other, *RAS-MAPK/ERK*-independent pathways.

In order to discover possible pathways and genes responsible for MS development in the absence of RKIP expression, we performed an mRNA microarray in THP-1 cells with RKIP knockdown. When comparing the results to THP-1 cells with normal RKIP expression, we observed a large number of deregulated genes. By grouping them depending on their function, we noticed, that most of the deregulated genes belonged to networks involved in degradation of connective tissues and migration, as well as in the interaction, binding and engulfment of hematopoietic cells. All these processes are pivotal for the migration of leukemic cells, invasion of extra-hematopoietic areas and the formation of solid tumor masses, as it happens in MS. Therefore, future studies, investigating prominently deregulated genes belonging to these groups, will help in better understanding possible pathways, through which RKIP loss acts in development of MS. Studies performed in breast cancer delineated one such possible pathway, the RKIP-Myc-LIN28-let-7 signaling cascade, through which RKIP inhibits metastasis in this specific tumor (153–157). In more detail, RKIP inhibits MAPK, which causes suppression of Myc activation. This results in suppression of LIN28 and in a consequent increase of microRNA let-7. Therefore, RKIP plays a role as a metastasis-suppressor by positively regulating let-7 expression and causing decreased expression of targets of let-7, which control genes fundamental for metastasis formation, like *MMP1*, *OPN* and *CXCR4*. Even if this signaling cascade might be breast cancer specific, studies focusing on the components of this pathway might help in elucidating a mechanism for RKIP-mediated tissue infiltration of leukemic cells in MS as well.

Having proven a functional role for RKIP loss in MS development, both in-vitro and in-vivo, we wanted to focus on the clinical implications of this finding. With this aim, we started by investigating RKIP levels in MS/AML patient samples. In more detail, two cohorts were employed: one in which MS was detected by clinical evaluation and one in which it was detected by biopsy. In both cases, RKIP loss was more

frequent in MS patients as compared to AML patients without extramedullary involvement. It was previously shown by our group, that loss of RKIP is a frequent event in AML patients (86). We could now show, that this is also true for the AML subtype of MS. It has to be noted, that in our previous study in AML patients, we did not distinguish between AML patients harbouring MS and AML patients without, as we did in this study. Therefore, the frequency of RKIP loss in AML might be influenced by the presence of patients with concomitant MS. Of note, in some of the MS patients, it was possible to study RKIP expression not only in the MS site, but also in the corresponding leukemic BM. Interestingly, in all of these patients, RKIP levels were comparable between MS site and BM. This result excludes a geographical clonal heterogeneity during MS formation in respect to RKIP expression. Generally, in solid tumors, RKIP levels are often decreased in the primary tumor site, as compared to benign tissue, and even lower if not absent in the metastatic site. The presence of low levels of RKIP expression in the primary tumor can even indicate the presence of metastasis (106,110,148). Since we could observe RKIP loss in both, BM and MS site, our study also suggests, that RKIP expression levels could be used as a potential biomarker. RKIP expression could be easily detected in the BM of AML patients and, in presence of lower RKIP levels, point out patients who already developed MS or who are at risk to do so in the future. Unfortunately, the small sample size of the cohorts used for this study did not allow us to investigate if MS in general, and in particular its RKIP expression status, could be of prognostic relevance for AML. However, we had previously shown that RKIP loss seems to be a favourable prognostic factor in AML (86). Therefore, this could also be true for MS patients, where the frequency of RKIP loss is even increased when compared to AML patients without any sign of MS. To confirm this hypothesis, the analysis of larger and preferentially prospective cohorts will be needed. Of note, these data are in disagreement with data from many solid cancers, where the absence of RKIP indicates a worse prognosis (109,158). This discrepancy might be caused by the differences between solid cancers and liquid cancers, in particular regarding mutational, epigenetic and microenvironmental status (109). This highlights the importance of taking into account the specific tumor type, when the effects of RKIP expression on the clinical outcome are studied.

In order to obtain an overview of the mutational landscape that accompanies RKIP loss in MS, we performed NGS in all the samples, in which RKIP loss was detected by biopsy. In particular, NGS was performed using a panel covering 39 genes, which are frequently mutated in myeloid neoplasias (42). The small samples size was again a limitation of our study, precluding the possibility of performing a statistical analysis. However, we observed that mutations in the *RAS* signaling pathway, and in particular in the RASopathy genes, affected 5/6 MS patients with RKIP loss, while being present in only 2/5 patients with RKIP normal. Considering that a functional synergism between mutant *RAS* and RKIP loss was observed in AML without MS previously (86), these data suggest, that mutant *RAS* and RKIP loss cooperate in MS development as well. Most interestingly, mutations affecting *NPM1* and *DNMT3A* were observed almost exclusively in patients with normal RKIP levels. Aberrations affecting *NPM1* and *DNMT3A* are frequently observed in MS and are known to induce MS formation, both in-vitro and in-vivo, in a *RAS*-independent way (42,141–145). This strengthens our hypothesis of a synergism between RKIP loss and *RAS* mutations in MS even more.

It is important to observe that the MS patient samples analyzed showed loss of RKIP not only at protein level but also at mRNA level. This is in accordance with previous studies, which have shown a decreased expression of RKIP in solid tumors both at mRNA and protein levels (159,160). It was previously shown by our group, that in AML, RKIP loss is caused by miR23a, which induces downregulation of *RKIP* mRNA (118,119). Therefore, this suggests that the same mechanism might be the one responsible for RKIP loss in MS. Future studies, assessing the levels of miR23a in MS patients as well as a possible role for this microRNA in MS, will be required to test this hypothesis.

5.2. RKIP loss promotes myeloid differentiation and aggravates the development of CMML

5.2.1. RKIP in myelomonocytic differentiation

Differentiation of HSPCs into myeloid and lymphoid hematopoietic cells is a tightly regulated process, with various genetic programs in place, which maintain this system in homeostasis. However, genetic aberrations can skew hematopoiesis in one direction and therefore cause the development of malignancies. For example,

mutations affecting the *RAS*-signaling pathway cause hypersensitivity to extracellular growth factors, like GM-CSF, causing an increase of myeloid lineage commitment (161–163). Since RKIP is a negative regulator of the *RAS-MAPK/ERK* pathway, we hypothesized that RKIP loss could be a factor involved in myelomonocytic differentiation.

When studying different hematopoietic cells, both in human and murine systems, we observed that RKIP levels were significantly lower in cells belonging to the myeloid lineage, when compared to HSPCs and lymphoid cells. This is in agreement with previous results from our group, where we also observed, that HSPCs show normal RKIP levels when compared to AML cell lines and patient samples (86). Here we could confirm once more this finding and compare the other hematopoietic cells to $CD34^+$ HSPCs. A reduction in RKIP levels starts after the GMP stage, as observed in a murine setting (128–131). This might indicate that reduced RKIP expression has a role in this step and is functionally involved in myeloid differentiation. Therefore, we modulated RKIP expression in both, healthy HSPCs and undifferentiated HL-60 AML cells. In both cases, we could show that knockdown of RKIP could increase the myeloid differentiation in these cells. Moreover, RKIP knockdown caused increased activation of the *RAS-MAPK/ERK* pathway in HSPCs and HL-60 cells. This is in accordance with previous studies, which have shown that activation of the MEK/ERK signaling cascade in HSPCs promotes myeloid differentiation and is necessary for $1,25D_3$-induced myelomonocytic differentiation of HL-60 cells (164,165). However, our results seems to be in disagreement with the work of Schuierer and colleagues (166). In their research, they showed that increase of RKIP expression is functionally involved in the differentiation of monocytes into macrophages and dendritic cells. Even if they observed minimal *RKIP* mRNA levels in monocytes, which are in accordance with our results, they showed that the subsequent step of differentiation of monocytes requires an induction of RKIP. In our work, we did not study this step of differentiation. Instead, we focused on the early stages of HSPCs differentiating into the myeloid lineage. This might be the cause of this discrepancy. Moreover, Schuierer and colleagues showed in their work, that RKIP induces differentiation of monocytes through the NF-kB pathway, while the role of RKIP loss in inducing myeloid differentiation in HSPCs seems to act via the *RAS*-

MAPK/ERK pathway. Interestingly, when they overexpressed RKIP in THP-1 cells, they observed an increase in CD11c surface expression. This appears opposite to what we observed in HL-60 cells, in which overexpression of RKIP caused a decreased percentage of $CD11c^+$ cells after treatment with $1,25D_3$. However, HL-60 is a more immature AML cell line as compared to THP-1 cells, and this might be the cause for the difference between the results from Schuierer and coworkers and our group. RKIP might act differently, through different pathways, depending on the hematopoietic differentiation stage we are considering.

The functional role of RKIP loss in myeloid differentiation could be corroborated also in in-vivo studies. For these, we employed a mouse model with a complete knockout of the *Rkip* gene. These mice display a normal life expectancy and, most importantly, do not develop neoplasias (167,168). When this murine model was treated with GM-CSF, *Rkip* knockout caused hyperactivation of the *RAS*-pathway and, consequently, increased myelomonocytic differentiation of HSPCs. It has to be noted, that loss of RKIP as a single event was not able to increase myelomonocytic differentiation. When comparing mice with *Rkip* knockout and *Rkip* normal, we did not observe significant differences in the composition of the various hematopoietic compartments. In fact, RKIP loss could induce increased myeloid differentiation when a second factor was present, for example the GM-CSF treatment in *Rkip* mice. Therefore, we concluded that in the myelomonocytic differentiation of HSPCs, RKIP loss acts as an amplifier of GM-CSF signaling and does not induce the differentiation process on its own. Moreover, this highlights the importance of the physiologic and pathologic regulation of *RAS*- and GM-CSF-signaling for hematopoiesis. This is in accordance with previously published data, which show a similar mechanism for other aberrations affecting the *RAS*-signaling pathway (169–171). In general, molecules causing inhibition of the *RAS*-signaling pathway, for example *Akt* and *Cot1*, appear downregulated in HL-60 cells differentiated using $1,25D_3$. After knockdown of *Akt* or *Cot1* in HL-60 cells, in presence of $1,25D_3$, there is an increased myeloid differentiation, while the opposite is observed when these molecules are overexpressed. These results are in agreement with the mechanism proposed for RKIP in myeloid differentiation. On the contrary, molecules that activate the *RAS* pathway, for example KSR, show exactly the opposite result. As observed for RKIP, in absence of $1,25D_3$

stimulation, the downregulation or overexpression of these effectors is not sufficient to produce significant differences in myeloid differentiation.

Increased levels of myeloid differentiation have previously been proposed as an essential pre-phase step for the development of myeloid neoplasms (172). Moreover, RKIP loss is known to play a role in myeloid leukemogenesis, as suggested in previous studies (86,117–119). Most important, in these studies loss of RKIP correlated with myelomonocytic AML phenotypes (86). Therefore, in our work we wanted to confirm that loss of RKIP expression plays a role in the development of myeloid neoplasias. For this aim, we used a mouse model with an inducible *Nras* mutation, which allowed us to study the effects of *Rkip* loss in a model harboring *Ras*-mutated malignancies. We chose to investigate this model because, on the one hand, it was previously shown that RKIP loss and *RAS* mutations frequently co-occur in AML (86,117,119). On the other hand, because it was observed that RKIP loss potentiates the oncogenic effects of *RAS*-signaling mutations in-vitro (86,117). For our study, we employed C57BL/6 mice with an $Nras^{G12D}$ inducible mutation, which are known to develop MP preferentially affecting the myelomonocytic lineage (90). When these mice showed concomitant *Rkip* knockout, the MP was significantly aggravated. Moreover, only *Mx1-Cre/Nras/Rkip-/-* mice showed a full-blown MPD, as evidenced by PB leukocytosis when compared to the control group. Interestingly, there was no significant difference when comparing the survival of *Nras*-mutated mice with or without *Rkip* knockout. It has to be noted, however, that the *Mx1-Cre/Nras* model used in this study is known to only randomly develop full blown MPD and that these mice frequently die of HS (90). With our work, we could demonstrate that *Nras*-mutated mice with concomitant *Rkip* knockout had reduced occurrence of HS, but therefore an aggravation of MPD. In order to better define the role of *Rkip* loss on the survival of these mice in the context of *Ras*-driven leukemogenesis, it will be necessary to conduct a study employing a mouse model without the predisposition to develop HS. For example, using an *Mx1-Cre/Nras* model on a C57BL6/129Sv F1 background, which has been reported to develop MPD at six months after pIpC induction (90), or BM transplantation (173).

Activation of the *RAS*/*MAPK-ERK* pathway was studied also in these mouse models, both in absence and presence of GM-CSF stimulation. As previously

observed, knockout of *Rkip* induced hyper-activation of the *RAS*-signaling pathway. This is in agreement with the study from Kunimoto and colleagues, in which mice double mutant for *Nras* and *Tet2,* showed increased levels of pERK, with and without GM-CSF treatment, as compared to single mutant mice, indicating a synergistic function of these events in MAPK/ERK activation (94). With these experiments, we could therefore conclude that RKIP loss acts as an amplifier of pathologic *RAS*-signaling, aggravating the myelomonocytic MPD in the *Nras*-mutated mice and enhancing the activity of the *RAS-MAPK/ERK* pathway.

5.2.2. RKIP in CMML

In order to understand the clinical role of RKIP loss in myeloid malignancies, we performed an analysis of primary patient samples. In more detail, we chose to analyze RKIP in CMML, a malignancy characterized by increased myelomonocytic proliferation and the frequent occurrence of *RAS*-signaling mutations (55). Based on our functional in-vitro and in-vivo results, we therefore reasoned that RKIP loss could play a role in this entity.

First, we analyzed 41 primary CMML patient samples and we observed RKIP loss to be a frequent event in CMML specimens, being present in around 30% of them. It has to be noted that loss of RKIP expression was observed not only at protein level, but also at mRNA level. It was shown in previous studies from our group, that loss of RKIP in AML is caused by overexpression of miR23a, which causes the decay of *RKIP* mRNA (118,119). The results from our work pinpoint that the same mechanism might be at the base of RKIP loss in CMML as well.

Next, we performed NGS on the CMML patient samples, using a panel of genes frequently mutated in myeloid malignancies (42). Considering both, patients with RKIP loss and with RKIP normal, the most frequently affected genes were *TET2* (75.7%), *SRSF2* (46.0%), *CBL* (24.3%), and *ASXL1* (24.3%), which is in accordance with previous studies (68,174). Interestingly, almost all the patients showing RKIP loss had one or more mutations affecting the *RAS*-signaling pathway. This indicates that RKIP loss frequently co-occurs with *RAS*-signaling mutations in CMML samples. This finding further corroborates the functional in-vivo data showing a functional synergism between these events in myeloid leukemogenesis. These results are also in agreement with previously published data from our group, demonstrating a functional synergism and a clinical

correlation between loss of RKIP expression and the presence of *RAS*-signaling mutations in different subtypes of AML (86,117,119). Interestingly, also many of the CMML patients with RKIP normal showed one or more mutations affecting the *RAS* pathway. This suggests that RKIP loss is not the only second genetic hit that interacts with *RAS*-signaling mutations in myeloid leukemogenesis. Some of these interactions have been previously shown for various genetic aberrations. For example, aberrant expression of members of the dual specificity phosphatase (*DUSP*) and *SPROUTY* (*Spry*) families aggravated *RAS*-driven leukemogenesis. The same has been shown for mutations in *ASXL1* and *TET2* (94–97). These data highlight the complexity of *RAS*-signaling in human leukemias and how its role in myeloid malignancies cannot be explained without taking into account other factors.

Interestingly, we did not observe any significant difference in the survival of CMML patients when comparing them depending on their RKIP expression status. It has to be noted, that this result is limited by the fact that all the patients analyzed were treated differently, ranging from best supportive care to high-dose chemotherapy. It was previously shown in AML, that loss of RKIP is a favorable prognostic factor, which is the opposite of what has been observed for RKIP expression in solid tumors (86). This might be true also for CMML patients, but further studies will be needed to confirm this hypothesis. In particular, analyses focusing on subgroups with uniformly treated patients would be necessary, but were precluded in this study by the small sample size of the cohort analyzed.

Finally, our results seem to be important also for the development of future targeted treatment approaches for myeloid neoplasias, particularly for those targeting the *RAS-MAPK/ERK* cascade. This is important, as the success rates of these agents are disappointing so far. Although they often show promising results when tested in preclinical models, they had a disappointing efficacy in clinical trials of myeloid neoplasias. One example are MEK-inhibitor drugs, which caused a significant reduction of *Ras*-driven MPD, when tested in murine models, but failed at showing the same effects when used in clinical trials for myeloid malignancies (175). We now observed that aberrant expression of *RAS*-signaling regulator proteins can influence both, the signaling and the leukemogenic effects of *RAS* mutations. However, this also means, that the sensitivity to *RAS-MAPK/ERK*

inhibition in *RAS*-mutated patients will be variable, depending on the secondary genetic aberrations present. This has shown to be the case in *Nras*-mutated mice, where it was observed that co-occurrence of lower *Spry2* expression levels and *Tet2* deletion increase the sensitivity to MEK inhibitors (94). From a therapeutic perspective, this means that a more detailed knowledge of the mutational and non-mutational profile of every patient, could help to identify those cases, which show a true dependence on MAPK/ERK signaling and would therefore be the best candidates for a specific MAPK/ERK inhibition. Future studies will be needed to test this hypothesis.

6. Conclusion

The data from this thesis highlight new roles for RKIP in MNs and opens the way to future uses of RKIP as a target for MNs-specific therapies.

In detail, we could show that loss of the metastasis-suppressor RKIP is functionally involved in tissue invasion of leukemic blasts as well as in the development of MS. This makes RKIP an interesting target for future therapies for MS. Moreover, we demonstrated that RKIP loss is a frequent event in MS, which can be detected also in the bone marrow of patients. This indicates that the occurrence of RKIP loss can be used as a biomarker in AML patients to detect the presence of additional extramedullary manifestations.

We could also establish RKIP as a new player in *RAS*-driven myeloid leukemogenesis. Moreover, RKIP could also be important for the development of MNs-specific targeted-therapies. In particular, loss of RKIP could be also used to identify a group of patients who would benefit from a therapeutic approach targeting the *RAS-MAPK/ERK* pathway.

7. Bibliography

1. Fröhling S, Scholl C, Gilliland DG, Levine RL. Genetics of myeloid malignancies: Pathogenetic and clinical implications. J Clin Oncol. 2005;23(26):6285–95.
2. Zebisch A, Cerroni L, Beham-Schmid C, Sill H. Therapy-related leukemia cutis: Case study of an aggressive disorder. Ann Hematol. 2003;82(11):705–7.
3. Arber DA, Orazi A, Hasserjian R, Thiele J, Borowitz MJ, Le Beau MM, et al. The 2016 revision to the World Health Organization classification of myeloid neoplasms and acute leukemia. Vol. 127, Blood. 2016. p. 2391–405.
4. Dohner, Estey E, Grimwade D, Amadori S, Appelbaum FR, Ebert BL, Fenaux P, et al. Diagnosis and management of AML in adults: 2017 ELN recommendations. Blood. 2017;129(4):424–48.
5. Deschler B, Lübbert M. Acute myeloid leukemia: Epidemiology and etiology. Vol. 107, Cancer. 2006. p. 2099–107.
6. Szotkowski T, Rohon P, Zapletalova J, Sicova K, Hubacek J, Indrak K. Secondary acute myeloid leukemia - a single center experience. Neoplasma. 2010;57(2):170–8.
7. Sill H, Olipitz W, Zebisch A, Schulz E, Wölfler A. Therapy-related myeloid neoplasms: Pathobiology and clinical characteristics. Vol. 162, British Journal of Pharmacology. 2011. p. 792–805.
8. Bennett JM, Catovsky D, Daniel M -T, Flandrin G, Galton DAG, Gralnick HR, et al. Proposals for the Classification of the Acute Leukaemias French-American-British (FAB) Co-operative Group. Br J Haematol. 1976 Aug;33(4):451–8.
9. De Kouchkovsky I, Abdul-Hay M. 'Acute myeloid leukemia: A comprehensive review and 2016 update.' Blood Cancer J. 2016;6(7).
10. Vardiman JW, Harris NL, Brunning RD. The World Health Organization (WHO) classification of the myeloid neoplasms. Vol. 100, Blood. 2002. p. 2292–302.
11. Almond LM, Charalampakis M, Ford SJ, Gourevitch D, Desai A. Myeloid Sarcoma: Presentation, Diagnosis, and Treatment. Clin Lymphoma, Myeloma Leuk. 2017;17(5):263–7.

12. Campidelli C, Agostinelli C, Stitson R, Pileri SA. Myeloid sarcoma: Extramedullary manifestation of myeloid disorders. In: American Journal of Clinical Pathology. 2009. p. 426–37.
13. Neiman RS, Barcos M, Berard C, Bonner H, Mann R, Rydell RE, et al. Granulocytic sarcoma: A clinicopathologic study of 61 biopsied cases. Cancer. 1981 Sep 15;48(6):1426–37.
14. Kawamoto K, Miyoshi H, Yoshida N, Takizawa J, Sone H, Ohshima K. Clinicopathological, cytogenetic, and prognostic analysis of 131 myeloid sarcoma patients. Am J Surg Pathol. 2016 Nov;40(11):1473–83.
15. Messager M, Amielh D, Chevallier C, Mariette C. Isolated granulocytic sarcoma of the pancreas: A tricky diagnostic for primary pancreatic extramedullary acute myeloid leukemia. World J Surg Oncol. 2012 Jan 16;10(1):13.
16. Wilson CS, Medeiros LJ. Extramedullary manifestations of myeloid neoplasms. Am J Clin Pathol. 2015;144(2):219–39.
17. Magdy M, Abdel Karim N, Eldessouki I, Gaber O, Rahouma M, Ghareeb M. Myeloid Sarcoma. Oncol Res Treat. 2019;42(4):219–24.
18. Bekkenk MW, Jansen PM, Meijer CJLM, Willemze R. CD56+ hematological neoplasms presenting in the skin: A retrospective analysis of 23 new cases and 130 cases from the literature. Ann Oncol. 2004;15(7):1097–108.
19. Yamauchi K, Yasuda M. Comparison in treatments of nonleukemic granulocytic sarcoma: Report of two cases and a review of 72 cases in the literature. Cancer. 2002;94(6):1739–46.
20. Stölzel F, Röllig C, Radke J, Mohr B, Platzbecker U, Bornhäuser M, et al. 18F-FDG-PET/CT for detection of extramedullary acute myeloid leukemia. Haematologica. 2011;96(10):1552–6.
21. Fergun Yilmaz A, Saydam G, Sahin F, Baran Y. Granulocytic sarcoma: a systematic review. Am J Blood Res. 2013;3(4):265–70.
22. Pileri SA, Ascani S, Cox MC, Campidelli C, Bacci F, Piccioli M, et al. Myeloid sarcoma: Clinico-pathologic, phenotypic and cytogenetic analysis of 92 adult patients. Leukemia. 2007;21(2):340–50.
23. Traweek ST, Arber DA, Rappaport H, Brynes RK. Extramedullary myeloid cell tumors: An immunohistochemical and morphologic study of 28 cases. Am J Surg Pathol. 1993 Oct;17(10):1011–9.

24. Meis JM, Butler JJ, Osborne BM, Manning JT. Granulocytic sarcoma in nonleukemic patients. Cancer. 1986 Dec 15;58(12):2697–709.
25. Antic D, Elezovic I, Milic N, Suvajdzic N, Vidovic A, Perunicic M, et al. Is there a “gold” standard treatment for patients with isolated myeloid sarcoma? Biomed Pharmacother. 2013 Feb;67(1):72–7.
26. Lan TY, Lin DT, Tien HF, Yang R Sen, Chen CY, Wu K. Prognostic factors of treatment outcomes in patients with granulocytic sarcoma. Acta Haematol. 2009;122(4):238–46.
27. Cerrano M, Itzykson R. New Treatment Options for Acute Myeloid Leukemia in 2019. Curr Oncol Rep. 2019;21(2).
28. Döhner H, Weisdorf DJ, Bloomfield CD. Acute Myeloid Leukemia. N Engl J Med. 2015;373:1136–52.
29. Döhner H, Estey EH, Amadori S, Appelbaum FR, Büchner T, Burnett AK, et al. Diagnosis and management of acute myeloid leukemia in adults: recommendations from an international expert panel, on behalf of the European LeukemiaNet. Vol. 115, Blood. 2010. p. 453–74.
30. Orozco JJ, Appelbaum FR. Unfavorable, complex, and monosomal karyotypes: the most challenging forms of acute myeloid leukemia. Oncology (Williston Park). 2012;26(8):706–12.
31. Burnett A, Wetzler M, Löwenberg B. Therapeutic advances in acute myeloid leukemia. J Clin Oncol. 2011;29(5):487–94.
32. Ferrara F, Schiffer CA. Acute myeloid leukaemia in adults. In: The Lancet. 2013. p. 484–95.
33. Stone RM, Mandrekar SJ, Sanford BL, Laumann K, Geyer S, Bloomfield CD, et al. Midostaurin plus Chemotherapy for Acute Myeloid Leukemia with a FLT3 Mutation HHS Public Access. N Engl J Med. 2017;377(5):454–64.
34. Lambert J, Pautas C, Terré C, Raffoux E, Turlure P, Caillot D, et al. Gemtuzumab ozogamicin for de novo acute myeloid leukemia: Final efficacy and safety updates from the open-label, phase III ALFA-0701 trial. Haematologica. 2019;104(1):113–9.
35. Dusenbery KE, Howells WB, Arthur DC, Alonzo T, Lee JW, Kobrinsky N, et al. Extramedullary leukemia in children with newly diagnosed acute myeloid leukemia: A report from the Children’s Cancer Group. J Pediatr Hematol Oncol. 2003;25(10):760–8.

36. Tsimberidou AM, Kantarjian HM, Wen S, Keating MJ, O'Brien S, Brandt M, et al. Myeloid Sarcoma Is Associated with Superior Event-Free Survival and Overall Survival Compared with Acute Myeloid Leukemia. Cancer. 2008;113(6):1370–8.
37. Movassaghian M, Brunner AM, Blonquist TM, Sadrzadeh H, Bhatia A, Perry AM, et al. Presentation and outcomes among patients with isolated myeloid sarcoma: A Surveillance, Epidemiology, and End Results database analysis. Leuk Lymphoma. 2015 Jun 3;56(6):1698–703.
38. Paydas S, Zorludemir S, Ergin M. Granulocytic sarcoma: 32 cases and review of the literature. Leuk Lymphoma. 2006;47(12):2527–41.
39. Byrd JC, Weiss RB, Arthur DC, Lawrence D, Baer MR, Davey F, et al. Extramedullary leukemia adversely affects hematologic complete remission rate and overall survival in patients with t(8;21)(q22;q22): Results from Cancer and Leukemia Group B 8461. J Clin Oncol. 1997 Feb 21;15(2):466–75.
40. Tsimberidou AM, Kantarjian HM, Estey E, Cortes JE, Verstovsek S, Faderl S, et al. Outcome in patients with nonleukemic granulocytic sarcoma treated with chemotherapy with or without radiotherapy. Leukemia. 2003;17(6):1100–3.
41. Mirza MK, Sukhanova M, Stölzel F, Onel K, Larson RA, Stock W, et al. Genomic Aberrations in Myeloid Sarcoma without Blood or Bone Marrow Involvement: Characterization of Formalin-Fixed Paraffin-Embedded Samples by Chromosomal Microarrays. Leuk Res. 2014;38(9):1091–6.
42. Kashofer K, Gornicec M, Lind K, Caraffini V, Schauer S, Beham-Schmid C, et al. Detection of prognostically relevant mutations and translocations in myeloid sarcoma by next generation sequencing. Leuk Lymphoma. 2018;59(2):501–4.
43. The Cancer Genome Atlas Research Network. Genomic and Epigenomic Landscapes of Adult De Novo Acute Myeloid Leukemia. N Engl J Med. 2013;368(22):2059–74.
44. Papaemmanuil E, Gerstung M, Bullinger L, Gaidzik VI, Paschka P, Roberts ND, et al. Genomic Classification and Prognosis in Acute Myeloid Leukemia. N Engl J Med. 2016;374(23):2209–21.
45. Steensma DP, Bejar R, Jaiswal S, Lindsley RC, Sekeres MA, Hasserjian

RP, et al. Clonal hematopoiesis of indeterminate potential and its distinction from myelodysplastic syndromes. Vol. 126, Blood. 2015. p. 9–16.

46. Jaiswal S, Fontanillas P, Flannick J, Manning A, Grauman P V, Mar BG, et al. Age-related clonal hematopoiesis associated with adverse outcomes. N Engl J Med. 2014;371(26):2488–98.
47. Genovese G, Kähler AK, Handsaker RE, Lindberg J, Rose SA, Bakhoum SF, et al. Clonal Hematopoiesis and Blood-Cancer Risk Inferred from Blood DNA Sequence. N Engl J Med. 2014;371(26):2477–87.
48. Abdel-Wahab O, Levine RL. Mutations in epigenetic modifiers in the pathogenesis and therapy of acute myeloid leukemia. Blood. 2013;121(18):3563–72.
49. Corces-Zimmerman MR, Hong W-J, Weissman IL, Medeiros BC, Majeti R. Preleukemic mutations in human acute myeloid leukemia affect epigenetic regulators and persist in remission. Proc Natl Acad Sci. 2014;111(7):2548–53.
50. Jan M, Majeti R. Clonal evolution of acute leukemia genomes. Oncogene. 2013;32(2):135–40.
51. Bakst RL, Tallman MS, Douer D, Yahalom J. How I treat extramedullary acute myeloid leukemia. Vol. 118, Blood. 2011. p. 3785–93.
52. Ohanian M, Huang RSP, Yakoushina T V, Estrov Z, Juneja H, Chen L, et al. Isolated Mesenteric CD20-Positive Myeloid Sarcoma. Clin Lymphoma Myeloma Leuk. 2014;14(6):e217–20.
53. Álvarez P, Navascués CA, Ordieres C, Pipa M, Vega IF, Granero P, et al. Granulocytic sarcoma of the small bowel, greater omentum and peritoneum associated with a CBF/MYH11 fusion and inv(16) (p13q22): A case report. Int Arch Med. 2011;4(1):3.
54. Zhang XH, Zhang R, Li Y. Granulocytic sarcoma of abdomen in acute myeloid leukemia patient with inv(16) and t(6;17) abnormal chromosome: Case report and review of literature. Leuk Res. 2010;34(7):958–61.
55. Patnaik MM, Tefferi A. Cytogenetic and molecular abnormalities in chronic myelomonocytic leukemia. Vol. 6, Blood Cancer Journal. Nature Publishing Group; 2016. p. e393.
56. Vardiman JW, Thiele J, Arber DA, Brunning RD, Borowitz MJ, Porwit A, et al. The 2008 revision of the World Health Organization (WHO) classification

of myeloid neoplasms and acute leukemia: Rationale and important changes. Vol. 114, Blood. 2009. p. 937–51.

57. Loghavi S, Khoury JD. Recent Updates on Chronic Myelomonocytic Leukemia. Vol. 13, Current Hematologic Malignancy Reports. 2018. p. 446–54.
58. Patnaik MM, Parikh SA, Hanson CA, Tefferi A. Chronic myelomonocytic leukaemia: A concise clinical and pathophysiological review. Br J Haematol. 2014;165(3):273–86.
59. Rollison DE, Howlader N, Smith MT, Strom SS, Merritt WD, Ries LA, et al. Epidemiology of myelodysplastic syndromes and chronic myeloproliferative disorders in the United States, 2001-2004, using data from the NAACCR and SEER programs. Blood. 2008;112(1):45–52.
60. Patnaik MM, Tefferi A. Chronic myelomonocytic leukemia: 2016 update on diagnosis, risk stratification, and management. Am J Hematol. 2016;91(6):631–42.
61. Mahmood S, Cooper A, Ireland R, Pocock C. Leukaemia cutis with chronic myelomonocytic leukaemia. Br J Haematol. 2009;147(4):413–413.
62. Germing U, Strupp C, Knipp S, Kuendgen A, Giagounidis A, Hildebrandt B, et al. Chronic myelomonocytic leukemia in the light of the WHO proposals. Haematologica. 2007;92(7):974–7.
63. Such E, Cervera J, Costa D, Solé F, Vallespí T, Luño E, et al. Cytogenetic risk stratification in chronic myelomonocytic leukemia. Haematologica. 2011;96(3):375–83.
64. Such E, Germing U, Malcovati L, Cervera J, Kuendgen A, Della Porta MG, et al. Development and validation of a prognostic scoring system for patients with chronic myelomonocytic leukemia. Blood. 2013;121(15):3005–15.
65. Patnaik MM, Itzykson R, Lasho TL, Kosmider O, Finke CM, Hanson CA, et al. ASXL1 and SETBP1 mutations and their prognostic contribution in chronic myelomonocytic leukemia: A two-center study of 466 patients. Leukemia. 2014;28(11):2206–12.
66. Itzykson R, Kosmider O, Renneville A, Gelsi-Boyer V, Meggendorfer M, Morabito M, et al. Prognostic score including gene mutations in chronic myelomonocytic leukemia. J Clin Oncol. 2013 Jul 1;31(19):2428–36.
67. Onida F, Barosi G, Leone G, Malcovati L, Morra E, Santini V, et al.

Management recommendations for chronic myelomonocytic leukemia: Consensus statements from the SIE, SIES, GITMO groups. Haematologica. 2013;98(9):1344–52.

68. Patnaik MM, Tefferi A. Chronic myelomonocytic leukemia: 2018 update on diagnosis, risk stratification and management. Am J Hematol. 2018;93(6):824–40.
69. Cheng H, Kirtani VG, Gergis U. Current status of allogeneic HST for chronic myelomonocytic leukemia. Bone Marrow Transplant. 2012;47(4):535–41.
70. Kröger N, Zabelina T, Guardiola P, Runde V, Sierra J, Van Biezen A, et al. Allogeneic stem cell transplantation of adult chronic myelomonocytic leukaemia. A report on behalf of the chronic leukaemia working party of the European Group for Blood and Marrow Transplantation (EBMT). Br J Haematol. 2002;118(1):67–73.
71. Costa R, Abdulhaq H, Haq B, Shadduck RK, Latsko J, Zenati M, et al. Activity of azacitidine in chronic myelomonocytic leukemia. Cancer. 2011;117(12):2690–6.
72. Benton CB, Nazha A, Pemmaraju N, Garcia-Manero G. Chronic myelomonocytic leukemia: Forefront of the field in 2015. Vol. 95, Critical Reviews in Oncology/Hematology. NIH Public Access; 2015. p. 222–42.
73. Wattel E, Guerci A, Hecquet B, Economopoulos T, Copplestone A, Resegotti L, et al. A randomized trial of hydroxyuea (HY) versus VP16 in advanced adult chronic myelomonocytic leukemia. Blood. 1996;88(7):2480–7.
74. Kerridge I, Spencer A, Azzi A, Seldon M. Response to erythropoietin in chronic myelomonocytic leukaemia. Intern Med J. 2001;31(6):371–2.
75. Itzykson R, Solary E. An evolutionary perspective on chronic myelomonocytic leukemia. Vol. 27, Leukemia. 2013. p. 1441–50.
76. Ricci C, Fermo E, Corti S, Molteni M, Faricciotti A, Cortelezzi A, et al. RAS mutations contribute to evolution of chronic myelomonocytic leukemia to the proliferative variant. Clin Cancer Res. 2010;16(8):2246–56.
77. Padron E, Painter JS, Kunigal S, Mailloux AW, McGraw K, McDaniel JM, et al. GM-CSF–dependent pSTAT5 sensitivity is a feature with therapeutic potential in chronic myelomonocytic leukemia. Blood. 2013;121(25):5068–77.

78. Beaupre DM, Kurzrock R. RAS and Leukemia : From Basic Mechanisms to Gene-Directed Therapy. J Clin Oncol. 1999;17(3):1071–9.
79. Zebisch A, Czernilofsky A, Keri G, Smigelskaite J, Sill H, Troppmair J. Signaling Through RAS-RAF-MEK-ERK: from Basics to Bedside. Curr Med Chem. 2007 Feb 1;14(5):601–23.
80. Downward J. Targeting RAS signalling pathways in cancer therapy. Vol. 3, Nature Reviews Cancer. 2003. p. 11–22.
81. Chung E, Kondo M. Role of Ras/Raf/MEK/ERK signaling in physiological hematopoiesis and leukemia development. Vol. 49, Immunologic Research. 2011. p. 248–68.
82. Steelman LS, Franklin RA, Abrams SL, Chappell W, Kempf CR, Bäsecke J, et al. Roles of the Ras/Raf/MEK/ERK pathway in leukemia therapy. Vol. 25, Leukemia. 2011. p. 1080–94.
83. Steelman LS, Pohnert SC, Shelton JG, Franklin RA, Bertrand FE, McCubrey JA. JAK/STAT, Raf/MEK/ERK, PI3K/Akt and BCR-ABL in cell cycle progression and leukemogenesis. Vol. 18, Leukemia. 2004. p. 189–218.
84. Scheffzek K, Ahmadian MR, Kabsch W, Wiesmüller L, Lautwein A, Schmitz F, et al. The Ras-RasGAP Complex : Structural Basis for GTPase Its in Activation and Oncogenic Ras Mutants. Science (80-). 1997;277(5324):333–8.
85. Frese KK, Tuveson DA. Maximizing mouse cancer models. Vol. 7, Nature Reviews Cancer. 2007. p. 645–58.
86. Zebisch A, Wölfler A, Fried I, Wolf O, Lind K, Bodner C, et al. Frequent loss of RAF kinase inhibitor protein expression in acute myeloid leukemia. Leukemia. 2012;26(8):1842–9.
87. Bolouri H, Farrar JE, Triche T, Ries RE, Lim EL, Alonzo TA, et al. The molecular landscape of pediatric acute myeloid leukemia reveals recurrent structural alterations and age-specific mutational interactions. Nat Med. 2018;24(1):103–12.
88. Wandler A, Shannon K. Mechanistic and preclinical insights from mouse models of hematologic cancer characterized by hyperactive ras. Cold Spring Harb Perspect Med. 2018 Apr;8(4):a031526.
89. Braun BS, Tuveson DA, Kong N, Le DT, Kogan SC, Rozmus J, et al. Somatic activation of oncogenic Kras in hematopoietic cells initiates a

rapidly fatal myeloproliferative disorder. Proc Natl Acad Sci. 2004;101(2):597–602.

90. Li Q, Haigis KM, McDaniel A, Harding-Theobald E, Kogan SC, Akagi K, et al. Hematopoiesis and leukemogenesis in mice expressing oncogenic NrasG12D from the endogenous locus. Blood. 2011;117(6):2022–32.
91. Chan IT, Kutok JL, Williams IR, Cohen S, Kelly L, Shigematsu H, et al. Conditional expression of oncogenic K-ras from its endogenous promoter induces a myeloproliferative disease. J Clin Invest. 2004;113(4):528–38.
92. Akutagawa J, Huang TQ, Epstein I, Chang T, Quirindongo-Crespo M, Cottonham CL, et al. Targeting the PI3K/Akt pathway in murine MDS/MPN driven by hyperactive Ras. Leukemia. 2016;30(6):1335–43.
93. Lyubynska N, Gorman MF, Lauchle JO, Hong WX, Akutagawa JK, Shannon K, et al. A MEK Inhibitor Abrogates Myeloproliferative Disease in Kras Mutant Mice Natalya. Sci Transl Med. 2012;3(76).
94. Kunimoto H, Meydan C, Nazir A, Whitfield J, Shank K, Rapaport F, et al. Cooperative Epigenetic Remodeling by TET2 Loss and NRAS Mutation Drives Myeloid Transformation and MEK Inhibitor Sensitivity. Cancer Cell. 2018;33:1–16.
95. Abdel-Wahab O, Adli M, LaFave LM, Gao J, Hricik T, Shih AH, et al. ASXL1 Mutations Promote Myeloid Transformation through Loss of PRC2-Mediated Gene Repression. Cancer Cell. 2012;22(2):180–93.
96. Geiger O, Hatzl S, Kashofer K, Hoefler G, Wölfler A, Sill H, et al. Deletion of SPRY4 is a frequent event in secondary acute myeloid leukemia. Ann Hematol. 2015;94(11):1923–4.
97. Zhao Z, Chen CC, Rillahan CD, Shen R, Kitzing T, Mcnerney ME, et al. Cooperative loss of RAS feedback regulation drives myeloid leukemogenesis. Nat Genet. 2015;47(5):539–43.
98. Yoon S, Seger R. The extracellular signal-regulated kinase: Multiple substrates regulate diverse cellular functions. Vol. 24, Growth Factors. 2006. p. 21–44.
99. Al-Mulla F, Bitar MS, Taqi Z, Yeung KC. RKIP: Much more than Raf Kinase inhibitory protein. J Cell Physiol. 2013;228(8):1688–702.
100. Bernier I, Jollés P. Purification and characterization of a basic 23 kDa cytosolic protein from bovine brain. Biochim Biophys Acta (BBA)/Protein

Struct Mol. 1984 Oct 23;790(2):174–81.

101. Escara-Wilke J, Yeung K, Keller ET. Raf kinase inhibitor protein (RKIP) in cancer. Cancer Metastasis Rev. 2012;31(3–4):615–20.
102. Yeung K, Seitz T, Li S, Janosch P, McFerran B, Kaiser C, et al. Suppression of Raf-1 kinase activity and MAP kinase signalling by RKIP. Nature. 1999;401(6749):173–7.
103. Yeung KC, Rose DW, Dhillon AS, Yaros D, Gustafsson M, Chatterjee D, et al. Raf Kinase Inhibitor Protein Interacts with NF-kB-Inducing Kinase and TAK1 and Inhibits NF-kB Activation. Mol Cell Biol. 2001;21(21):7207–17.
104. Lorenz K, Lohse MJ, Quitterer U. Protein kinase C switches the Raf kinase inhibitor from Raf-1 to GRK-2. Nature. 2003 Dec 4;426(6966):574–9.
105. Lamiman K, Keller JM, Mizokami A, Zhang J, Keller ET. Survey of Raf kinase inhibitor protein (RKIP) in multiple cancer types. Crit Rev Oncog. 2014;19(6):455–68.
106. Fu Z, Smith PC, Zhang L, Rubin MA, Dunn RL, Yao Z, et al. Effects of Raf Kinase Inhibitor Protein Expression on Suppression of Prostate Cancer Metastasis. JNCI J Natl Cancer Inst. 2003;95(12):878–89.
107. Granovsky AE, Rosner MR. Raf kinase inhibitory protein: A signal transduction modulator and metastasis suppressor. Vol. 18, Cell Research. 2008. p. 452–7.
108. Dangi-Garimella S, Yun J, Eves EM, Newman M, Erkeland SJ, Hammond SM, et al. Raf kinase inhibitory protein suppresses a metastasis signalling cascade involving LIN28 and let-7. EMBO J. 2009;28(4):347–58.
109. Yesilkanal AE, Rosner MR. Targeting raf kinase inhibitory protein regulation and function. Vol. 10, Cancers. 2018.
110. Hagan S, Al-Mulla F, Mallon E, Oien K, Ferrier R, Gusterson B, et al. Reduction of Raf-1 kinase inhibitor protein expression correlates with breast cancer metastasis. Clin Cancer Res. 2005;11(20):7392–7.
111. Park S, Yeung ML, Beach S, Shields JM, Yeung KC. RKIP downregulates B-Raf kinase activity in melanoma cancer cells. Oncogene. 2005;24(21):3535–40.
112. Al-Mulla F, Hagan S, Behbehani AI, Bitar MS, George SS, Going JJ, et al. Raf kinase inhibitor protein expression in a survival analysis of colorectal cancer patients. J Clin Oncol. 2006;24(36):5672–9.

113. Lee HC, Tian B, Sedivy JM, Wands JR, Kim M. Loss of Raf Kinase Inhibitor Protein Promotes Cell Proliferation and Migration of Human Hepatoma Cells. Gastroenterology. 2006;131(4):1208–17.
114. Chatterjee D, Bai Y, Wang Z, Beach S, Mott S, Roy R, et al. RKIP Sensitizes Prostate and Breast Cancer Cells to Drug-induced Apoptosis. J Biol Chem. 2004;279(17):17515–23.
115. Woods Ignatoski KM, Grewal NK, Markwart SM, Vellaichamy A, Chinnaiyan AM, Yeung K, et al. Loss of Raf Kinase Inhibitory Protein Induces Radioresistance in Prostate Cancer. Int J Radiat Oncol Biol Phys. 2008;72(1):153–60.
116. Zebisch A, Staber PB, Delavar A, Bodner C, Hiden K, Fischereder K, et al. Two Transforming C-RAF Germ-Line Mutations Identified in Patients with Therapy-Related Acute Myeloid Leukemia. Cancer Res. 2006;66(7):3401–8.
117. Zebisch A, Haller M, Hiden K, Goebel T, Hoefler G, Troppmair J, et al. Loss of RAF kinase inhibitor protein is a somatic event in the pathogenesis of therapy-related acute myeloid leukemias with C-RAF germline mutations. Leukemia. 2009;23(6):1049–53.
118. Hatzl S, Geiger O, Kuepper MK, Caraffini V, Seime T, Furlan T, et al. Increased expression of miR-23a mediates a loss of expression in the RAF kinase inhibitor protein RKIP. Cancer Res. 2016;76(12):3644–54.
119. Caraffini V, Perfler B, Berg JL, Uhl B, Schauer S, Kashofer K, et al. Loss of RKIP is a frequent event in myeloid sarcoma and promotes leukemic tissue infiltration. Vol. 131, Blood. 2018. p. 826–30.
120. Caraffini V, Geiger O, Rosenberger A, Hatzl S, Perfler B, Berg JL, et al. Loss of RAF kinase inhibitor protein is involved in myelomonocytic differentiation and aggravates RAS-driven myeloid leukemogenesis. Haematologica. 2019;haematol.2018.209650.
121. Ganzel C, Manola J, Douer D, Rowe JM, Fernandez HF, Paietta EM, et al. Extramedullary disease in adult acute myeloid leukemia is common but lacks independent significance: Analysis of patients in ECOG-ACRIN cancer research group trials, 1980-2008. J Clin Oncol. 2016;34(29):3544–53.
122. Langer C, Marcucci G, Holland KB, Radmacher MD, Maharry K, Paschka P, et al. Prognostic importance of MN1 transcript levels, and biologic insights from MN1-associated gene and microRNA expression signatures in

cytogenetically normal acute myeloid leukemia: A cancer and leukemia group B study. J Clin Oncol. 2009;27(19):3198–204.

123. Taschner S, Koesters C, Platzer B, Jö A, Ellmeier W, Benesch T, et al. Down-regulation of RXRα expression is essential for neutrophil development from granulocyte-monocyte progenitor. Blood. 2007;109(3):971–9.
124. Chatterjee D, Sabo E, Tavares R, Resnick MB. Inverse association between Raf Kinase Inhibitory Protein and signal transducers and activators of transcription 3 expression in gastric adenocarcinoma patients: implications for clinical outcome. Clin Cancer Res. 2008;14(13):2994–3001.
125. Schneider CA, Rasband WS, Eliceiri KW. NIH Image to ImageJ: 25 years of image analysis. Vol. 9, Nature Methods. 2012. p. 671–5.
126. Lal R, Lind K, Heitzer E, Ulz P, Aubell K, Kashofer K, et al. Somatic TP53 mutations characterize preleukemic stem cells in acute myeloid leukemia. Vol. 129, Blood. 2017. p. 2587–91.
127. Gaksch L, Kashofer K, Heitzer E, Quehenberger F, Daga S, Hofer S, et al. Residual disease detection using targeted parallel sequencing predicts relapse in cytogenetically normal acute myeloid leukemia. Am J Hematol. 2018 Jan;93(1):23–30.
128. Konuma T, Nakamura S, Miyagi S, Negishi M, Chiba T, Oguro H, et al. Forced expression of the histone demethylase Fbxl10 maintains self-renewing hematopoietic stem cells. Exp Hematol. 2011;39(6):697–709.
129. Sung LY, Gao S, Shen H, Yu H, Song Y, Smith SL, et al. Differentiated cells are more efficient than adult stem cells for cloning by somatic cell nuclear transfer. Nat Genet. 2006 Nov 1;38(11):1323–8.
130. Moran-Crusio K, Reavie L, Shih A, Abdel-Wahab O, Ndiaye-Lobry D, Lobry C, et al. Tet2 Loss Leads to Increased Hematopoietic Stem Cell Self-Renewal and Myeloid Transformation. Cancer Cell. 2011;20(1):11–24.
131. Wang Y, Krivtsov A V, Sinha AU, North TE, Goessling W, Feng Z, et al. The wnt/β-catenin pathway is required for the development of leukemia stem cells in AML. Science. 2010;327(5973):1650–3.
132. Caux C, Massacrier C, Dubois B, Valladeau J, Dezutter-Dambuyant C, Durand I, et al. Respective involvement of TGF-β and IL-4 in the development of Langerhans cells and non-Langerhans dendritic cells from CD34+progenitors. Journal of Leukocyte Biology. 1999. p. 781–91.

133. Krones E, Eller K, Pollheimer MJ, Racedo S, Kirsch AH, Frauscher B, et al. NorUrsodeoxycholic acid ameliorates cholemic nephropathy in bile duct ligated mice. J Hepatol. 2017;67(1):110–9.
134. Deryugina EI, Quigley JP. Chapter 2 Chick Embryo Chorioallantoic Membrane Models to Quantify Angiogenesis Induced by Inflammatory and Tumor Cells or Purified Effector Molecules. Vol. 444, Methods in Enzymology. 2008. p. 21–41.
135. Stanford WL, Cohn JB, Cordes SP. Gene-trap mutagenesis: Past, present and beyond. Vol. 2, Nature Reviews Genetics. 2001. p. 756–68.
136. Haigis KM, Kendall KR, Wang Y, Cheung A, Haigis MC, Glickman JN, et al. Differential effects of oncogenic K-Ras and N-Ras on proliferation, differentiation and tumor progression in the colon. Nat Genet. 2008;40(5):600–8.
137. Kogan SC, Ward JM, Anver MR, Berman JJ, Brayton C, Cardiff RD, et al. Bethesda Proposals for Classification of Non-lymphoid Hematopoietic Neoplasms in Mice; supplemental material. Blood. 2002;100(1):238–46.
138. Lacroix-Triki M, Lacoste-Collin L, Jozan S, Charlet JP, Caratero C, Courtade M. Histiocytic sarcoma in C57BL/6J female mice is associated with liver hematopoiesis: Review of 41 cases. Vol. 31, Toxicologic Pathology. 2003. p. 304–9.
139. Escara-Wilke J, Keller JM, Ignatoski KMW, Dai J, Shelley G, Mizokami A, et al. Raf kinase inhibitor protein (RKIP) deficiency decreases latency of tumorigenesis and increases metastasis in a murine genetic model of prostate cancer. Prostate. 2015;75(3):292–302.
140. Geissler K, Jäger E, Barna A, Alendar T, Ljubuncic E, Sliwa T, et al. Chronic myelomonocytic leukemia patients with RAS pathway mutations show high in vitro myeloid colony formation in the absence of exogenous growth factors. Vol. 30, Leukemia. 2016. p. 2280–1.
141. Ohanian M, Faderl S, Ravandi F, Pemmaraju N, Garcia-Manero G, Cortes J, et al. Is acute myeloid leukemia a liquid tumor? Int J Cancer. 2013;133(3):534–43.
142. Li Z, Stölzel F, Onel K, Sukhanova M, Mirza MK, Yap KL, et al. Next-generation sequencing reveals clinically actionable molecular markers in myeloid sarcoma. Leukemia. 2015;29(10):2113–6.

143. Xian J, Shao H, Chen X, Zhang S, Quan J, Zou Q, et al. Nucleophosmin mutants promote adhesion, migration and invasion of human leukemia THP-1 cells through MMPs up-regulation via Ras/ERK MAPK signaling. Int J Biol Sci. 2016;12(2):144–55.
144. Xu J, Zhang W, Yan X-J, Lin X-Q, Li W, Mi J-Q, et al. DNMT3A mutation leads to leukemic extramedullary infiltration mediated by TWIST1. J Hematol Oncol. 2016;1–12.
145. Pastoret C, Houot R, Llamas-Gutierrez F, Boulland M-L, Marchand T, Tas P, et al. Detection of clonal heterogeneity and targetable mutations in myeloid sarcoma by high-throughput sequencing. Leuk Lymphoma. 2017 Apr 3;58(4):1008–12.
146. White SL, Belov L, Barber N, Hodgkin PD, Christopherson RI. Immunophenotypic changes induced on human HL60 leukaemia cells by 1α,25-dihydroxyvitamin D3and 12-O-tetradecanoyl phorbol-13-acetate. Leuk Res. 2005;29(10):1141–51.
147. Kim K, Seoh JY, Cho SJ. Phenotypic and Functional Analysis of HL-60 Cells Used in Opsonophagocytic-Killing Assay for Streptococcus pneumoniae. J Korean Med Sci. 2015;30:145–50.
148. Keller ET, Fu Z, Yeung K, Brennan M. Raf kinase inhibitor protein: A prostate cancer metastasis suppressor gene. Vol. 207, Cancer Letters. 2004. p. 131–7.
149. Martinho O, Granja S, Jaraquemada T, Caeiro C, Miranda-Gonçalves V, Honavar M, et al. Downregulation of RKIP is associated with poor outcome and malignant progression in gliomas. PLoS One. 2012;7(1).
150. Martinho O, Pinto F, Granja S, Miranda-Gonçalves V, Moreira MAR, Ribeiro LFJ, et al. RKIP Inhibition in Cervical Cancer Is Associated with Higher Tumor Aggressive Behavior and Resistance to Cisplatin Therapy. PLoS One. 2013;8(3).
151. Nowak-Sliwinska P, Segura T, Iruela-Arispe ML. The chicken chorioallantoic membrane model in biology, medicine and bioengineering. Angiogenesis. 2014;17(4):779–804.
152. Reddy KB, Nabha SM, Atanaskova N. Role of MAP kinase in tumor progression and invasion. Vol. 22, Cancer and Metastasis Reviews. 2003. p. 395–403.

153. Ma L, Teruya-Feldstein J, Weinberg RA. Tumour invasion and metastasis initiated by microRNA-10b in breast cancer. Nature. 2007;449(7163):682–8.
154. Tavazoie SF, Alarcón C, Oskarsson T, Padua D, Wang Q, Bos PD, et al. Endogenous human microRNAs that suppress breast cancer metastasis. Nature. 2008;451(7175):147–52.
155. Yun J, Frankenberger CA, Kuo W-L, Boelens MC, Eves EM, Cheng N, et al. Signalling pathway for RKIP and Let-7 regulates and predicts metastatic breast cancer. EMBO J. 2011;30:4500–14.
156. Minn AJ, Bevilacqua E, Yun J, Rosner MR. Identification of novel metastasis suppressor signaling pathways for breast cancer. Vol. 11, Cell Cycle. 2012. p. 2452–7.
157. Yesilkanal AE, Rosner MR. Raf kinase inhibitory protein (RKIP) as a metastasis suppressor: regulation of signaling networks in cancer. Crit Rev Oncog. 2014 Jan;19(6):447–54.
158. Minoo P, Zlobec I, Baker K, Tornillo L, Terracciano L, Jass JR, et al. Loss of raf-1 kinase inhibitor protein expression is associated with tumor progression and metastasis in colorectal cancer. Am J Clin Pathol. 2007;127(5):820–7.
159. Schuierer MM, Bataille F, Weiss TS, Hellerbrand C, Bosserhoff AK. Raf kinase inhibitor protein is downregulated in hepatocellular carcinoma. Oncol Rep. 2006;16(3):451–6.
160. Li HZ, Wang Y, Gao Y, Shao J, Zhao XL, Deng WM, et al. Effects of Raf Kinase Inhibitor Protein Expression on Metastasis and Progression of Human Epithelial Ovarian Cancer. Mol Cancer Res. 2008;6(6):917–28.
161. Fatrai S, Van Gosliga D, Han L, Daenen SMGJ, Vellenga E, Schuringa JJ. KRASG12V enhances proliferation and initiates myelomonocytic differentiation in human stem/progenitor cells via intrinsic and extrinsic pathways. J Biol Chem. 2011;286(8):6061–70.
162. Van Meter MEM, Díaz-Flores E, Archard JA, Passegué E, Irish JM, Kotecha N, et al. K-RasG12D expression induces hyperproliferation and aberrant signaling in primary hematopoietic stem/progenitor cells. Blood. 2007;109(9):3945–52.
163. Wang X, Studzinski GP. Activation of extracellular signal-regulated kinases (ERKs) defines the first phase of 1,25-dihydroxyvitamin d3-induced differentiation of HL60 cells. J Cell Biochem. 2001;80(4):471–82.

164. Miranda MB, Johnson DE. Signal transduction pathways that contribute to myeloid differentiation. Vol. 21, Leukemia. 2007. p. 1363–77.
165. Johnson DE. Src family kinases and the MEK/ERK pathway in the regulation of myeloid differentiation and myeloid leukemogenesis. Adv Enzyme Regul. 2008;48(1):98–112.
166. Schuierer MM, Heilmeier U, Boettcher A, Ugocsai P, Bosserhoff AK, Schmitz G, et al. Induction of Raf kinase inhibitor protein contributes to macrophage differentiation. Biochem Biophys Res Commun. 2006;342(4):1083–7.
167. Theroux S, Pereira M, Casten KS, Burwelld RD YK. Raf kinase inhibitory protein knockout mice: expression in the brain and olfaction deficit. Brain Res Bull. 2007;71(6):559–67.
168. Moffit JS, Boekelheide K, Sedivy JM, Klysik J. Mice lacking raf kinase inhibitor protein-1 (RKIP-1) have altered sperm capacitation and reduced reproduction rates with a normal response to testicular injury. J Androl. 2007;28(6):883–90.
169. Wang X, Studzinski GP. Kinase Suppressor of RAS (KSR) Amplifies the Differentiation Signal Provided by Low Concentrations 1,25-Dihydroxyvitamin D3. J Cell Physiol. 2004;198(3):333–42.
170. Wang J, Zhao Y, Kauss MA, Spindel S, Lian H. Akt regulates vitamin D3-induced leukemia cell functional differentiation via Raf/MEK/ERK MAPK signaling. Eur J Cell Biol. 2009;88(2):103–15.
171. Wang X, Studzinski GP. Oncoprotein Cot1 represses kinase suppressors of Ras1/2 and 1,25-dihydroxyvitamin D3-induced differentiation of human acute myeloid leukemia cells. J Cell Physiol. 2011;226(5):1232–40.
172. Mason CC, Khorashad JS, Tantravahi SK, Kelley TW, Zabriskie MS, Yan D, et al. Age-related mutations and chronic myelomonocytic leukemia. Leukemia. 2016;30(4):906–13.
173. Wang J, Liu Y, Li Z, Du J, Ryu MJ, Taylor PR, et al. Endogenous oncogenic NRAS mutation promotes aberrant GM-CSF signaling in granulocytic/monocytic precursors in a murine model of chronic myelomonocytic leukemia. Blood. 2010;116(26):5991–6002.
174. Yoshimi A, Balasis ME, Vedder A, Feldman K, Ma Y, Zhang H, et al. Robust patient-derived xenografts of MDS/MPN overlap syndromes capture the

unique characteristics of CMML and JMML. Blood. 2017;130(4):397–407.
175. Smith CC, Shah NP. The role of kinase inhibitors in the treatment of patients with acute myeloid leukemia. Am Soc Clin Oncol Educ Book. 2013;313–8.